Engineering Cell Free Protein Synthesis and Synthetic Cells

Razia Chowdhry

Exeter College

University of Oxford

A thesis submitted for the degree of

Doctor of Philosophy

Trinity 2023

Abstract

Mimicking the structure and function of natural cells, synthetic cells hold significant potential in various applications. These synthetic cells, which come in numerous forms, are developed from different materials, including lipids and proteins, as well as synthetic materials such as polymers. The method of producing synthetic cells depends largely on their intended use and the materials used in their formation. Expression of genes within a synthetic cell can allow its usage in many fields to either study minimal cellular behaviour and function or use them as cargo holding vehicles for controlled delivery to target sites.

This thesis focuses on the production of lipid-based synthetic cells using a cell-free protein expression system and a DNA template. The primary objective of this study was to generate synthetic cells capable of producing a target protein, which can be released in a controlled manner upon the application of heat. Heat is a promising stimulus for future applications in SCs due to its thermal control to allow precise manipulation, biocompatibility, non-invasiveness, versatility, scalability, and integration with existing technologies.

To produce the SCs, we initially optimized the inverted-emulsion method to create giant unilamellar vesicles. These vesicles successfully encapsulated the cell-free protein expression system, enabling the production of a fluorescent protein or a reporter enzyme. However, incorporating heat-sensitive lipids into the synthetic cells using this approach proved unsuccessful. Consequently, we pursued an alternative strategy to produce SCs known as the freeze-dried empty liposomes (FDEL) method. Through optimization, this method enabled us to incorporate thermosensitive materials such as DPPC, lysolipids, and PEG into the SCs at specific compositions, facilitating controlled release upon heating.

Furthermore, we investigate a genetic engineering method to enhance the protein yield in the E. coli cell-free protein expression system, PURExpress, by introducing a short sequence referred to as a "booster." We identify specific cell penetrating peptide nucleotide sequences and their derivatives which allow higher expression of the fluorescent protein, mVenus.

Acknowledgements

I would like to first and foremost thank my supervisor Dr Michael Booth. He has been an incredible and supportive supervisor over the years. I greatly appreciate all that he has done for my development as a scientist and an individual. I would like to thank Prof. Hagan Bayley for accepting me to integrate with his group and providing scientific guidance.

There have been many people during this DPhil that I have forged wonderful friendships with. I would like to recognise Dr Yujia Qing, my friend and desk buddy who has always given me sudden insight during a scientific discussion or given me food, hugs, advice, and conversations. I'd like to give special thanks to Assala Al Samad (for her care and chocolates), Matthew Cornall (so much banter in the lab), Jefferson Smith (scientific guidance on synthetic cells and long chats), Giacomo Mazzoti (being an amazing friend), Brian Ng (for walks and discussions). Special thanks to my very good friends, Diala Al Masri and Barbara Souza, for the love, laughter, deep discussions, overcoming pain, working and surviving well together during COVID-19 lockdown and many other challenges as junior deans.

A few other people that have been special to me throughout the DPhil include Pablo, Denis, Khoa, Zhong, Tika, Tati, Henry, Gabrielle, Ruby-Anne, Maruthi, Shihang, Nasria, Asma, Rubeena for their continuous friendship through the years. I'd also like to recognise and thank St John's College, Oxford for giving me the opportunity to take on the role as Junior Dean since 2019 which opened up an entire world of experiences. Exeter College has also played an important part in accepting me as their student and giving me opportunities. The Doctoral Training Centre, especially the DTP, should be thanked for accepting me into their programme and giving me various guidance throughout.

Few other important people that have supported me in kind and loving ways include Sharmeen Sarkar and my lovely sister, Fahima Chowdhry. I'd also like to give immense thanks to Dr Tuncel and Dr Robert Tack, my in-laws who have given me care, guidance, love, and encouragement in times of need. Finally, I'd like to thank Osman Tack, my partner and the love of my life who has helped me grow in so many ways with patience, care, and wisdom.

Abbreviations

ATP = adenosine triphosphate

CF = Carboxyfluorescein

CMC = Critical Micelle Concentration

CPP = Cell Penetrating Peptide

CU = 7-hydroxycoumaric-3- carboxylic acid

DHFR = Dihydrofolate Reductase

DPPC = dipalmitoyl phosphocholine

DSPC = Distearoylphosphatidylcholine

DSPE-mPEG$_{2000}$ = Carboxy NHS, 1,2-distearoyl-sn-glycero-3-phosphoethanolamine-N-[carboxy(polyethylene glycol)-2000, NHS ester]

Eco-mC = E.coli codon optimised mCherry

Eco-mV = E.coli codon optimised mVenus

EPR = enhanced permeability and retention

FDEL = Freeze Dried Empty Liposome

GOI = Gene of Interest

GTP = guanosine triphosphate

GUV = Giant Unilamellar Vesicles

IVTT = In vitro transcription and translation

LUV = Large Unilamellar Vesicles

Mam-mC = Mammalian codon optimised mCherry

Mam-mV = Mammalian codon optimised mVenus

mC = mCherry

MLV = Multilamellar Vesicles

mNG = mNeonGreen

MPPC = monopalmitoylphosphatidylcholine

MR = Magnetic Resonance

MSPC = monostearoylphosphatidylcholine

mV = mVenus

ORF = Open Reading Frame

PTD = Protein Transduction Domain

PURE = Protein synthesis using recombinant elements

RBS = Ribosome Binding Site

RBS = Ribosome binding site

RNAP = RNA polymerase

SC= Synthetic Cells

SD = Shine Dalgarno

TRD = Texas-Red Dextran

TSL = Temperature Sensitive Liposomes

TSV = Temperature Sensitive Vesicles

TSV = Temperature Sensitive Vesicles

TX = Triton X-100

ULV = Unilamellar Vesicles

UTR = Untranslated Region

w/o = Water-in-oil

β-Gal = β Galactosidase

β-Gal = β-galactosidase

β-Lac = β Lactamase

β-Lac = β-lactamase

Contents

Chapter 1 - Introduction

The production of synthetic cells (SCs) is a rapidly growing field with diverse applications in research, medicine and industry. SCs are designed to mimic biological functions of natural cells, including metabolism[1], division[2] and communication[3]. Two approaches can be taken when creating SCs: a top-down approach, which involves simplifying natural cells into "minimal cells" by removing certain biological functions and potentially adding new ones to observe their impact on cellular activity[4], and a bottom-up approach, which entails producing SCs from simple biomolecules, such as DNA or RNA, a metabolism system and a membrane that creates a capsule separating and protecting the enclosed system from the external environment[2,5]. Bottom-up generated SCs have been referred to by various names, such as artificial cells, protocells, liposomes[6], emulsion droplets[7], polymersomes[8] and proteinosomes[9], all of which have an internal lumen surrounded by a physical barrier which can be made of either a lipid bilayer, lipid monolayer, amphipathic polymers or proteins. For this thesis the term "vesicles" will be used in conjunction with "synthetic cells" which will refer to bottom-up generated SCs.

The internal compartment of SCs can be filled with a variety of molecules, including small molecules[10], nucleic acids[11], vaccine components[12] and enzymes[13]. A mixture of proteins, enzymes, energy molecules and nucleic acid can be loaded into SCs to perform *in-vitro* transcription and translation (IVTT) to produce any proteins, enabling the potential use of SCs as delivery capsules for targeted therapies. Liposomes, which are spherical assemblies of a phospholipid bilayer[14], have been used in the development of SCs for therapeutic drug delivery and has been shown to carry small molecular drugs[15].

1.1 Cell Free Protein Synthesis

Protein synthesis is the process by which cells create proteins, which are essential molecules for various biological functions. It occurs in two main steps; transcription (where the DNA sequence is converted to mRNA sequence) and translation (where mRNA sequence is converted into a polypeptide chain of amino acids). The RNA polymerase (RNAP) binds to the promoter site, then the DNA molecule unwinds, and the DNA is transcribed into mRNA until it reaches a transcription terminator site or until it falls off from the 5' end of the DNA template. Transcription takes place in the nucleus of eukaryotic cells[16] from which the mRNA needs to travel to the ribosomes in the cytoplasm for translation. Eukaryotes require transcription factors to allow polymerase to bind to the promoter site[17]. For prokaryotic cells, transcription only requires RNAP or pre-assembled holoenzyme[18] to recruit free ribonucleotide triphosphates to produce mRNA. Both transcription and translation can take place simultaneously as soon as the mRNA is released from the RNAP and the ribosome binding site (RBS) is exposed[19].

During translation, the mRNA sequence in the untranslated region (UTR) before the gene of interest (GOI) start codon (AUG), contain specific sequences which allows its recognition by the ribosome. The Shine Dalgarno (SD) sequence "AGGAGG" is the main functional element in the 5'UTR, which has been observed in large numbers of prokaryotic mRNAs[20]. It's main function is to bind directly with the complimentary sequence in the 16S ribosomal RNA during the translation initiation step[21]. Elongation of the peptide chain begins when the second codon of the GOI becomes available for the tRNA-aa to bind and ends when it arrives at the stop codon[22]. Specific amino acids are added to the growing polypeptide chain based on the specific codons on the mRNA.

The process of transcription can be conducted in a simple biochemical reaction *in-vitro* in a physiological buffer with RNAP, NTPs, magnesium and spermidine to produce mRNA[23]. Translation, on the other hand, is a more complex process and requires a mixture of various small molecules and proteins for successful protein synthesis. For *in vitro* translation, ribosomes, amino acids, tRNAs, enzymes for loading amino acids to tRNAs, as well as enzymes for regeneration of adenosine triphosphate (ATP) and guanosine triphosphate (GTP) are mixed together. Mixing the machinery of transcription and translation, cell-free protein synthesis can be conducted by adding a specifically engineered DNA to the mix.

Several advantages exist with using cell-free expression systems. Protein expression of high yields[24] can be produced without requiring the use of live cells, which means certain safety parameters do not need to be followed in the laboratory as the opportunities of cross contamination is reduced. This allows broad versatility, scalability and portability[25]. Using cell-free expression systems provides greater control, so the reaction conditions, such as temperature, pH, and substrate concentrations can be fin-tuned. Additionally, modifications and manipulations of the system can be easily implemented to enhance protein yield or incorporate non-natural amino acids into the synthesized proteins[26]. Toxic proteins can also be produced in the cell-free protein synthesis system without damaging the host cell. Most DNA sizes and type (circular, linear, non-native, synthetic DNA sequences) can be used as the template without needing to overcome issues related to cell transformation and cell growth. Cell free expression systems are being studied for use in applications such as biosensing after lyophilising the mixture in paper[27,28], expressing large gene sets, isolating cellular metabolic pathways or using the system for synthetic cell production for the study of origin of life. Cell-free synthesis systems can be performed using cell lysates[29,30] which can be produced in-house or made commercially available such as NEBExpress or by mixing proteins that have

been recombinantly expressed and purified such as the Protein synthesis Using Recombinant Elements (PURE) system[31].

1.2 Liposomes for Targeted Therapy

One of the areas to apply targeted therapy is in cancer treatments. Chemotherapeutics are typically utilized in the treatment of cancer, whereby small drug molecules are intravenously administered and disseminated throughout the tumour site and healthy tissues. Consequently, the administration of chemotherapeutics often leads to harmful side effects and damage to both healthy tissues and cancerous cells, potentially impacting various organs such as the heart, liver, immune system, among others[32].

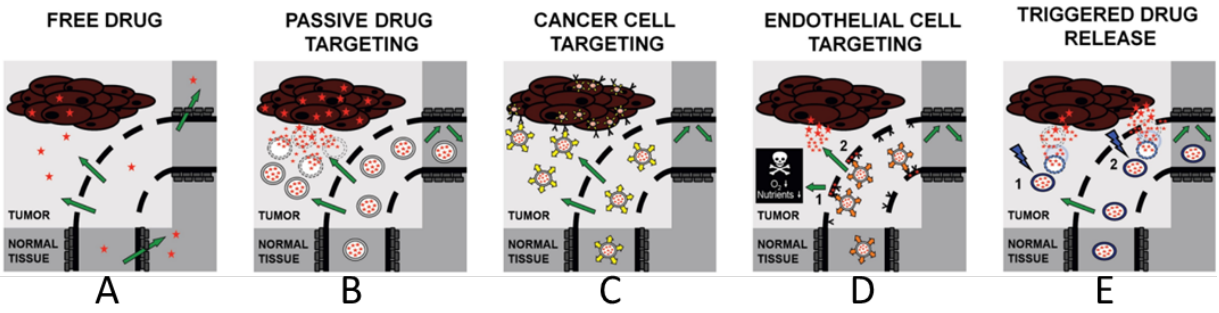

Figure 1.1: The present strategies for drug targeting can be categorized as follows; A) Conventional therapy of free drug movements through the bloodstream and into all tissues. B) Passive targeting through the use of liposomes that take advantage of the EPR effect. C) Active targeting through the use of liposomes that are labelled with tumour-specific antibodies. D) Active targeting through the use of liposomes that are labelled with endothelial cell-specific antibodies. E) Triggered drug release, which can occur either (1) within the interstitial space of the tumour or (2) upon intravascular release. Liposomes that fall into this last category are exemplified by Thermosensitive Liposomes (TSL). Figure from Kunjachan et al. [33]

The unique characteristics of tumour locations facilitate targeted delivery of therapeutics, primarily through the presence of a leaky vasculature resulting from enlarged endothelial pores around the rapidly growing tumours, which enhances drug accumulation (Figure 1.1). This mechanism is known as enhanced permeability and retention effect (EPR)[34], where the blood vessels around the tumour exhibit anatomical deficiencies that lead to poorly aligned endothelial cells, wide lumens, and abnormal smooth-muscle layers[35]. To target the tumour site and reduce impact on healthy tissues, drug delivery systems using lipid bilayer vesicle structures are being investigated[15]. These vesicles can passively accumulate at the tumour site within 24-48 hours and leak out of the vessels through the endothelial pores and onto the tumour sites by passive targeting (Figure 1.1B). Active targeting of cancer cells can be achieved by adding specific antibodies to the vesicle surface, which can be specific to particular ligands either on the tumour cells (Figure 1.1C) or the specific endothelial cells (Figure 1.1D) of the blood vessels surrounding the tumour.

The vesicles can also be internalised into the target cells by receptor-mediated endocytosis. However, the main limitation of a targeted based approach with liposome surface antibodies is that some of the target cells may not have the unique antigen for a specific antibody. To overcome this limitation, an alternative targeted delivery method is to use an external stimulus to trigger release of vesicles at a specific site of interest (Figure 1.1E). Vesicles are preferred as they are biocompatible[36], biodegradable[37], have low immunogenicity[38], low toxicity[38] and the ability to encapsulate a wide range of drug molecules which can have improved stability within the isolated vesicle environment and allow for prolonged blood circulation time[39].

The first PEGylated vesicles carrying doxorubicin that received clinical approval, referred to as Doxil, exhibited reduced side effects compared to traditional formulations[40,41]. However, although DOX vesicles have the ability to accumulate at tumour sites, not all of the drugs are available for optimal therapeutic efficacy[42]. Additional FDA-approved vesicle-based products that contain doxorubicin include Caelyx pegylated liposomal[43], Myocet liposomal[44] and Zolsketil pegylated liposomal[45]. Furthermore, other vesicle based products carrying drug molecules for cancer treatment have been developed and received FDA approval.

Gene therapy is another area of research which can benefit from using targeting drug delivery systems. Nucleic acids have the potential to be used in vaccines to treat human diseases, viral infections[46] and various genetic disorders[47]. However, as nucleic acids are unstable and sometimes require their delivery into specific tissue in order to introduce the genetic materials to specific cells, a firmer strategy of delivery is required. Consequently, researchers are exploring the use of vesicles as carriers for the delivery of plasmid DNA, ribozymes, siRNA and mRNA to address these challenges.[48,49]

Strategic functionalisation of vesicles with specific ligands on the surface can allow for targeted delivery (Figure 1.2). These functional groups can include peptides, antibodies and small molecules which can impact the final surface charge and size of the vesicles[50].

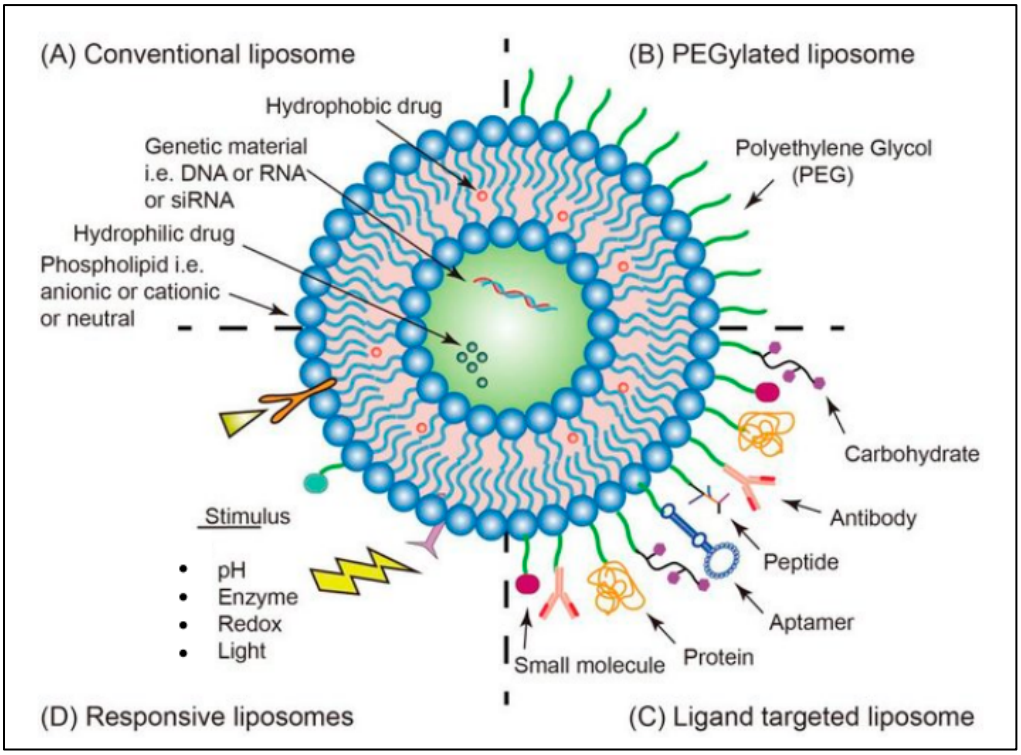

Figure 1.2: Strategies of functionalised liposome delivery for solid tumour therapy. (A) Conventional liposomes can reach tumour tissues through the EPR effect. (B) Surface-PEGylated liposomes can increase circulation time. (C) Functionalised liposomes modified with appropriate ligands can reach the target site and release the drug. (D) Responsive liposomes activate drug release only under specific environmental conditions. Reproduced from Taléns-Visconti et al[51].

1.3 The Need for Stimuli-Responsive Vesicles

Although vesicles can accumulate at a tumour site, the release of the drug can be a slow process[40]. As it is also accepted that the cancer cells take up the released drugs from the vesicles, rather than internalising the liposomes themselves[52]. This phenomenon has prompted a significant amount of research in the development of responsive vesicles that can release its encapsulated contents in response to stimuli after circulating in the bloodstream and localising at a tumour extravasation site[53]. These parameters can eventually modulate targeting of specific tissues and the concentration of the drugs at the target site, as well as its

pharmacokinetic parameters such as its bioavailability and half-life, which are all important factors to consider when designing new drugs[54].

External or internal stimuli can be used to trigger drug release from vesicles. External stimuli includes exposing the vesicles to heat, light or ultrasound and internal stimuli are conditions which may be present at the disease site such as pH changes, enzymes, glutathione or hypoxia[55]. A stimuli responsive drug release from vesicles would be more proactive in providing a higher level of the drug than conventional method of diffusion of the drug across the vesicle bilayers and onto the tumour[56–58].

The use of vesicles to carry drugs means that either hydrophilic, hydrophobic or amphiphilic molecules can be incorporated by either being encapsulated within the inner compartment or incorporated in the hydrophobic lipid bilayer[59]. These vesicles can be used to transport the cargo for the controlled release of the drug at any location[60]. The application of vesicles in the field of nanotechnology has undergone a shift towards the delivery of macromolecular biological cargoes, including peptides, proteins, antisense oligonucleotides and plasmids. Given the heightened sensitivity of these molecules to changes in specific conditions, they are more susceptible to degradation. Therefore, developing techniques to encapsulate them in vesicles has become crucial for protecting them from the external environment and enabling targeted delivery. This approach not only reduces the toxicity of certain encapsulated cargoes but also ensures that sensitive tissues are shielded from exposure to toxic drugs[61].

A major drawback of using lipid-only-based vesicles is their limited ability to remain in the bloodstream for extended duration. When administered intravenously, such vesicles are quickly eliminated by the reticuloendothelial system, which identifies them as foreign bodies using molecules like opsonins, ultimately leading to their removal by the liver[62,63]. However,

vesicles that have been pegylated with either hydrophilic polymers (PEG) or other polymers, can evade immune detection and reach the target site of the disease[51]. This strategy can enhance the efficiency and bioavailability of drugs[64]. PEG is a highly soluble, making it suitable for use in physiological conditions. It is approved by the FDA for human administration due to its non-toxic and non-immunogenic nature, and it can be easily eliminated from the body through the kidneys or liver. PEG polymers can stabilise vesicles by creating a protective hydrophilic layer on their surface, preventing aggregation with other blood components and increasing circulation time. As a result, drug molecules can be more efficiently distributed to leaky vessels at tumour sites[65]. During the development of therapeutic vesicles, it is critical to balance systemic toxicity and therapeutic efficacy. While encapsulating drugs in vesicles reduces toxicity, PEGylation of the membranes can result in increased circulation time as well as a new set of associated toxicity[66].

1.4 Hyperthermia use in Therapeutics

Hyperthermia is the raising of the temperature of a tissue which is a technique used to treat various diseases and has been shown to provide therapeutic benefits[67] especially for tumours. The localised tissue area can have its temperature increased to mild hyperthermia at 39 to 42 ℃ which can allow the target area to become sensitive to other chemotherapeutic and radiotherapeutic treatments. Mild hyperthermia can be used in conjunction with other therapeutic tools such radiation, drugs or even on its own as a form of therapy[68]. The important aspect which can aid with localisation of vesicles, is that the hyperthermia treatment can improve blood flow to the heated area as the vascular permeability increases due to the blood vessel pore sizes becoming larger (extravasation)[69]. This can promote selective drug release at the target tissue as the vesicles can accumulate in the area. This

means that the target cells are more susceptible to the therapeutic drugs being released. This can also increase the direct delivery of vesicles transferred to the target cells by either fusion or endocytosis, all increasing efficacy and decreasing side effects.

The methods of applying heat locally or on the whole-body can vary, depending on the location of the disease site or the type of drugs being administered. Majority of preclinical hyperthermia studies used heated water baths for regional, superficial heating[39]. External electromagnetic applicators emitting microwaves or radio-waves can be used to locally heat superficial tumours. The efficacy of this method can be affected by the tumour location and the type and positioning of the applicator used[70]. To access and heat deeply-seated tumours, minimally-invasive antenna types such as microwave antennas, radiofrequency electrodes, laser fibres and heat sources can be inserted directly into the tumour with ultrasonographic guidance[71]. This approach is effective for tumours less than 5 cm in diameter, but is limited to feasible insertion locations and can require multiple applicators to ensure therapeutic temperatures[39]. High-intensity focused ultrasound (FUS) allows for deep tissue heating in a small focal zone with a high degree of temporal control, making it a leading modality for localized heat-triggered drug release from vesicles[39]. There has been advances in the use of magnetic resonance (MR)-guided focused ultrasound (MRgFUS) which has allowed simultaneous MR-imaging to guide treatment and MR thermometry to monitor temperature changes noninvasively. MRgFUS has shown potential in combination with thermosensitive liposomal therapy for localized chemotherapy, as demonstrated by experiments in rat[72] and rabbit[73] models. However, evidence demonstrating improved clinical efficacy of these systems is currently limited.

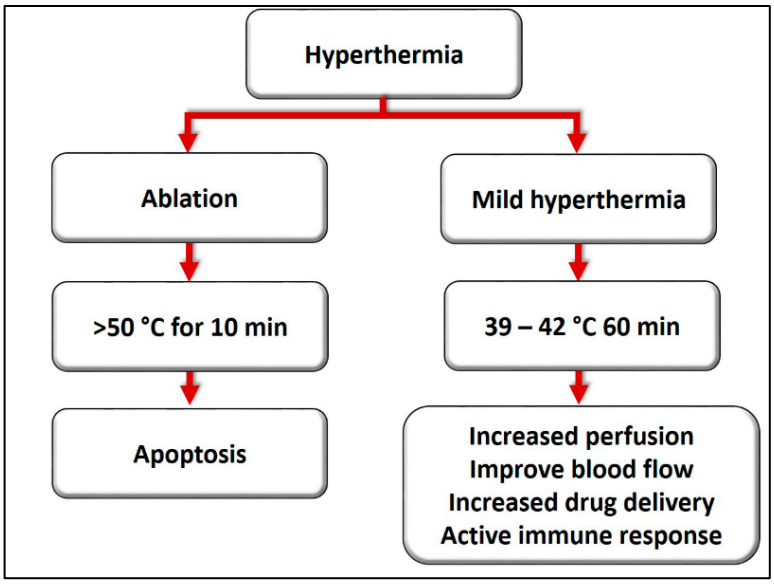

Figure 1.3: Ablation and mild hyperthermia are two different strategies for achieving hyperthermia. Ablation uses high temperatures (above 50 ℃) for a short period and can destroy cells quickly, while mild hyperthermia uses lower temperatures for a longer period and has a distinct physiological response. Ablation is effective for destroying tumour tissue, but heating large tumours can be challenging. Mild heat treatment can induce changes in cellular and molecular physiology without any toxicity, affecting various targets within the cell. It can improve blood flow, intensify drug delivery, and increase sensitivity to ionizing radiation therapy, leading to reduced cell division and inhibited DNA repair mechanisms. Schematic repurposed from Gomes et al.[74]

1.5 Temperature-Sensitive Vesicles

Despite the potential benefits of vesicles as site-specific drug delivery systems, the need for controllable release of encapsulated drugs at specific target sites remains a challenge. To address this issue, researchers have explored the use of external stimuli such as light, magnetic fields, and temperature to achieve controlled release[55,75]. Notably, temperature-sensitive vesicles (TSVs) have shown promise in clinical trials, with ThermoDox© being a successful example that has advanced to phase III[76].

There are various types of TSVs systems that have been described in the literature with various chemical designs with different thermal mechanisms of drug release with various kinetics requiring different heating protocols (Figure 1.4). There are lipid-based TSV, lysolipid-based, polymer-based, metallic nanoparticle-based, and targeted TSVs. The focus of this chapter is on the production of lipid-based and lysolipid-based TSVs. The polymer-based TSVs are designed using amphiphilic temperature-sensitive polymers that are attached to the membrane. These polymers can transition from a coil to globular structure, which can lead to the disruption of the vesicle membrane and the release of its contents[77]. Metallic nanoparticle-based TSVs are hybrids that contain nanoparticles either inside the aqueous core of the vesicle or embedded in the lipid bilayer or absorbed on the surface of the vesicle[78]. These nanoparticles can be heated when exposed to an external alternating electromagnetic field or light and release the encapsulated cargo[79]. Lastly, targeted TSVs possess ligands on their surface, such as peptides or antibodies that can bind to the receptors of target cells[80]. This allows for increased therapeutic potential at the target site as it can result in cellular uptake of the vesicles[81].

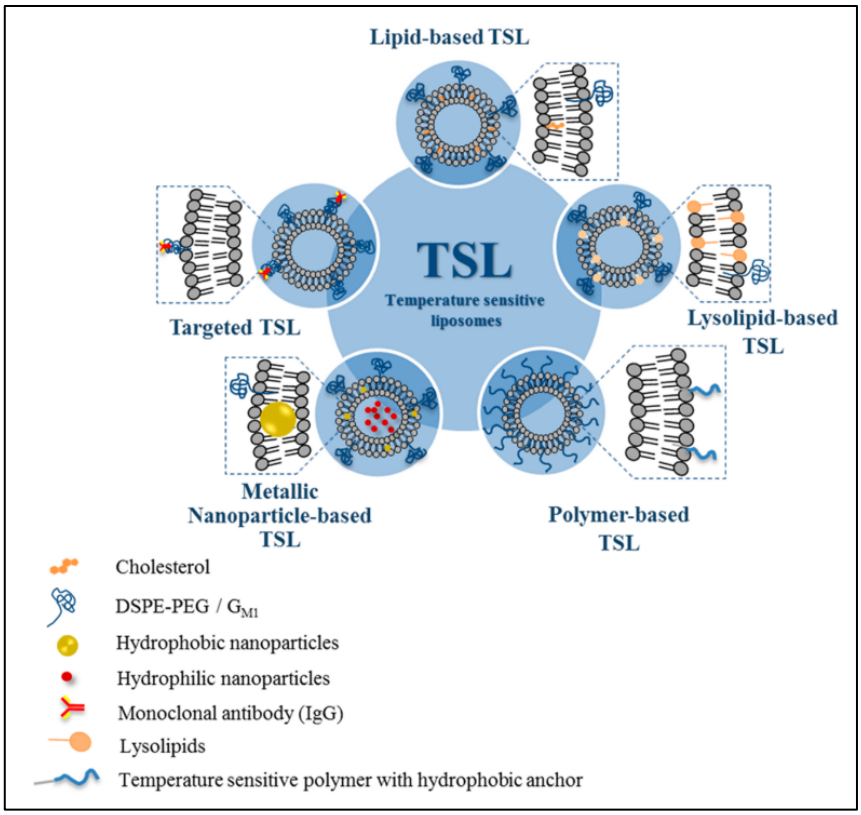

Figure 1.4: Schematic of different types of TSVs with different chemical components that make up their design. Repurposed from Z. Al-Ahmady et al[75].

1.6 Components of Lipid-Based TSV Membranes

The traditional temperature-sensitive lipid that has been used is dipalmitoyl phosphocholine (DPPC), a phospholipid consisting of 16-carbon saturated fatty acid chain. DPPC has a phase transition temperature (T_m) of approximately 42 °C[82]. While DPPC can be combined with other lipids, such as DSPC, to enhance drug release[83], experiments have demonstrated that small unilamellar vesicles containing only DPPC lipids exhibit release at 38 °C, which is less stable, has a broader transition range, and releases at a slower rate and smaller amount[82]. A mix formulation of DPPC and DSPC in different proportions yield a desired T_m between 41 °C and 54 °C such that a 3:1 molar ratio of DPPC:DSPC gives a T_m in the range of 41 °C and 43 °C. This

ratio was first used by Yatvin et al. in 1978 to increase the release of encapsulated neomycin, a pioneering example of thermosensitive drug release from vesicles[82]. The use of lipids with carbon chains longer than DPPC to produce TSVs, can have undesirable effects on the lipid bilayer transition behaviour[82,83]. One of the goals of producing TSV is to ensure that the T_m is above the physiological temperature and can be achieved by hyperthermia for clinical applications[84]. The temperature sensitivity of TSVs is dependent on the lipid components ability to undergo phase transition when heated. Additionally, the maximum release from the vesicles can vary and be sensitive to the protocol used in TSV production.

Incorporation of PEG polymers into DPPC TSVs in the form of DSPE-PEG_{2000} has been found to enhance their blood profile[85]. To achieve a balance between TSV stability at body temperature (37 ℃) and the release of cargo from within at the T_m of the TSV, an optimal concentration of 4-5 mol% of DSPE-PEG_{2000} was determined. Additionally, the presence of DSPE-PEG_{2000} stabilises the pores formed when the temperature reaches the T_m, thereby facilitating the release of the encapsulated contents[85]. These findings suggest that incorporating DSPE-PEG_{2000} into DPPC TSVs may be a promising strategy for enhancing their performance as drug delivery vehicles.

The development of TSVs advanced further with the integration of lysolipids into the conventional PEGylated DPPC TSVs, such as MSPC (monostearoylphosphatidylcholine) or MPPC (monopalmitoylphosphatidylcholine). In 1999, Anyarambhatla and Needham proposed this innovative approach to lower the Tm and facilitate prompt drug release[86]. The incorporation of lysolipids was particularly crucial as the conventional PEG-based DPPC/DSPC TSVs necessitated the heating of tissues to temperatures exceeding 42 ℃ for extended periods of time, ranging from 30 minutes to 1 hour. This posed a significant risk of necrosis to

healthy tissues. Hence, the inclusion of lysolipids offered a promising solution to this challenge[87,88].

Incorporating lysolipids such as monopalmitoyl phosphocholine (MPPC) at approximately 10 mol% with DPPC:DSPE2000 (90:4) has been shown to decrease the Tm from 43 to 39-40 ℃, allowing drug release within seconds. This leads to nearly 50% release within 20 seconds when heated at 42 ℃[76,86]. The formulation of DPPC:MSPC:DSPE-PEG_{2000} in a molar ratio of 86:10:4 was used to produce and clinically approve ThermoDox®. This formulation of TSV would have an improved safety profile and is the most advanced temperature stimulated vesicle that has been introduced in clinical trials[76]. Further investigations have shown that these lysolipid-based TSVs, used in conjunction with hyperthermia heating at 42 ℃ enable rapid drug release and enhanced drug uptake by tumours in animal models compared to controls[89]. Consequently, lysolipid vesicles can maintain low drug toxicity until they reach the tumour site where hyperthermia can control drug release at the specific site. Lysolipids contain one hydrocarbon tail attached to the headgroup with a positive intrinsic curvature resulting in the formation of micelles[90]. This tendency of lysolipids are thought to provide stability of the defected bilayers when the temperature reaches its Tm.

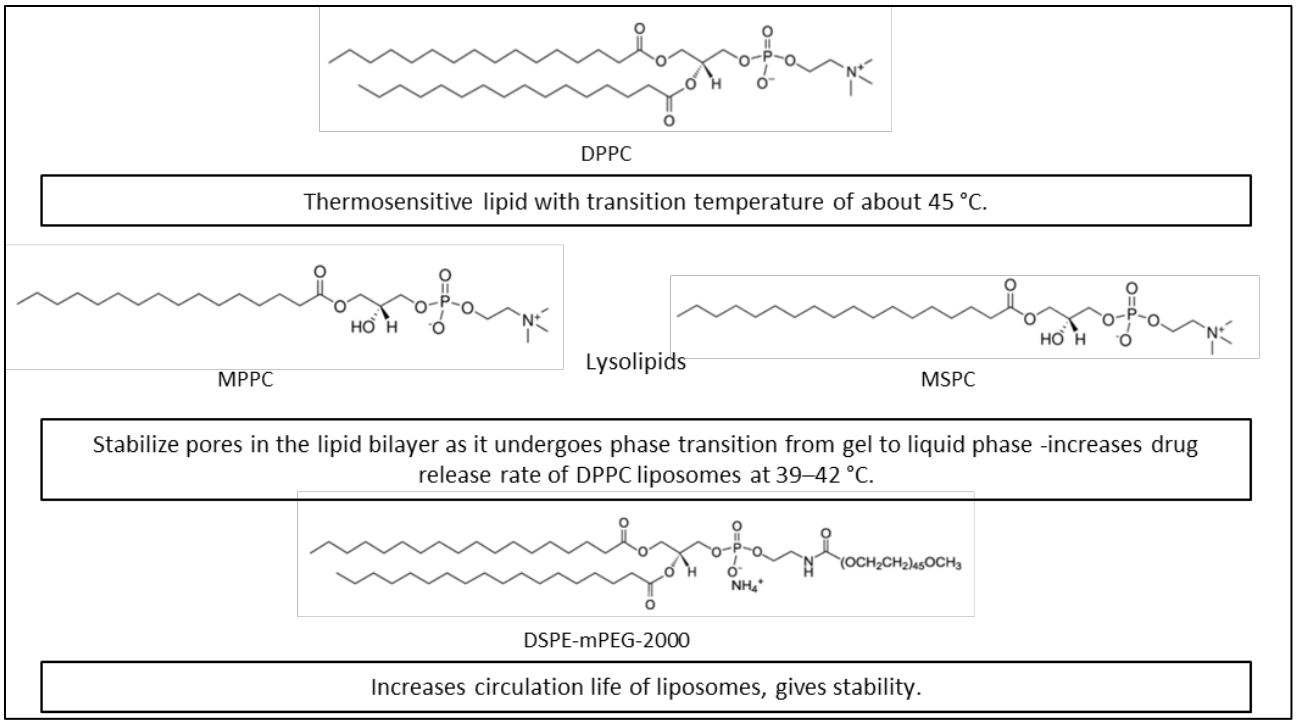

Figure 1.5: Chemical structures of lipid DPPC, lysolipids MPPC and MSPC and PEG polymer, with brief description of their role in TSVs.

1.7 Mechanism of TSV Membrane Transition

The transition temperature (Tm) is a key characteristic of phospholipid bilayers, representing the point at which the acyl chains of the lipids gain configurational entropy[91]. In the case of DPPC lipid molecules, the Tm corresponds to the temperature at which the hydrocarbon chains are fully extended, resulting in an ordered and condensed gel phase[92].

Upon heating to the Tm, the hydrocarbon chains melt and transition to the liquid crystalline phase, as the orientation of C-C single bonds changes from trans to gauche configuration. The resulting increase in the mobility of the head group allows the lipids in the bilayer to freely move in two dimensions, making the bilayer permeable at temperatures above the Tm. (*Figure 1.6*)[39]. The transition temperature of a phospholipid bilayer is influenced by several

factors, including the length and saturation of the acyl chains, as well as the electrostatic properties of the head group of the phospholipids[91].

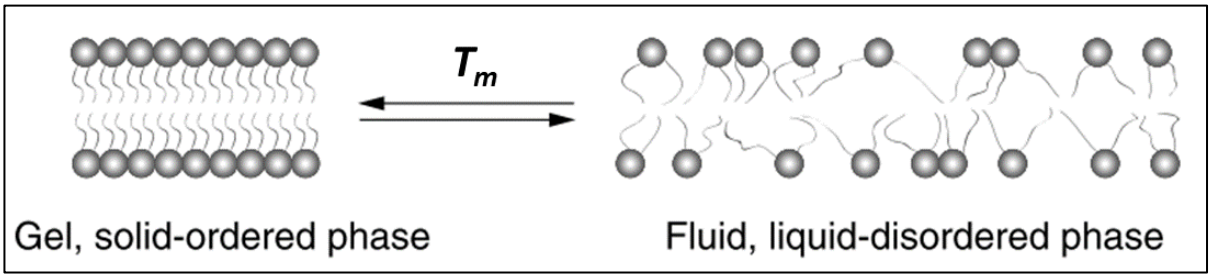

Figure 1.6: Temperature-dependent phase transition of a lipid bilayer. The figure depicts the impact of temperature above the critical temperature (Tm) on the fluidity of the lipid bilayer. An increase in temperature above Tm leads to an increase in lipid bilayer fluidity, which results in an increase in drug release. Schematic repurposed from T. Ta et al[39].

Furthermore, it is important to note that the membrane is not a continuous homogenous sheet, but rather contains domains where the lipids are oriented differently from one another. The points at which these domains meet, are known as the "grain boundaries" which are created during the cooling process when the lipid bilayer goes from a melted liquid structure to a solid ordered phase. These crystalline structures form during vesicle formation and during heating, when melting of the vesicle bilayers is initiated, causing different grains to become energized and defects to form at the boundaries, including the presence of solid/liquid domains as imperfect crystalline arrangements[91] (Figure 1.7).

Drug release can occur through these grain boundaries when heated, particularly in the presence of a certain percentage of lysolipids. Incorporating lysolipid MSPC with DPPC enhances the permeability of the membrane bilayer and slightly decreases the Tm. The characteristics of the grain boundaries at the Tm of the bilayer are dependent on the

concentration of MSPC and polyethylene glycol (PEG), which can impact the permeability of drug molecules. Lysolipids have a tendency to form micelles, allowing them to line and stabilize the pores formed at the grain boundaries during the Tm, but this ability is dependent on the composition of the membrane.

In the presence of pure DPPC during the phase transition temperature, the permeability between the solid phase lipids and the liquid-phase lipids does not align, resulting in a low level of permeability for molecular delivery[93,94]. However, the addition of lysolipid MSPC has been shown to increase the permeability of the encapsulated cargo, as the lysolipids accumulate at the grain boundaries as curved structures, stabilizing the membrane pore. Furthermore, the addition of DSPE-PEG2000 allows for further stability, as it accumulates at the pore due to its tendency to also form micelle curvature structures, resulting in rapid drug release[91].

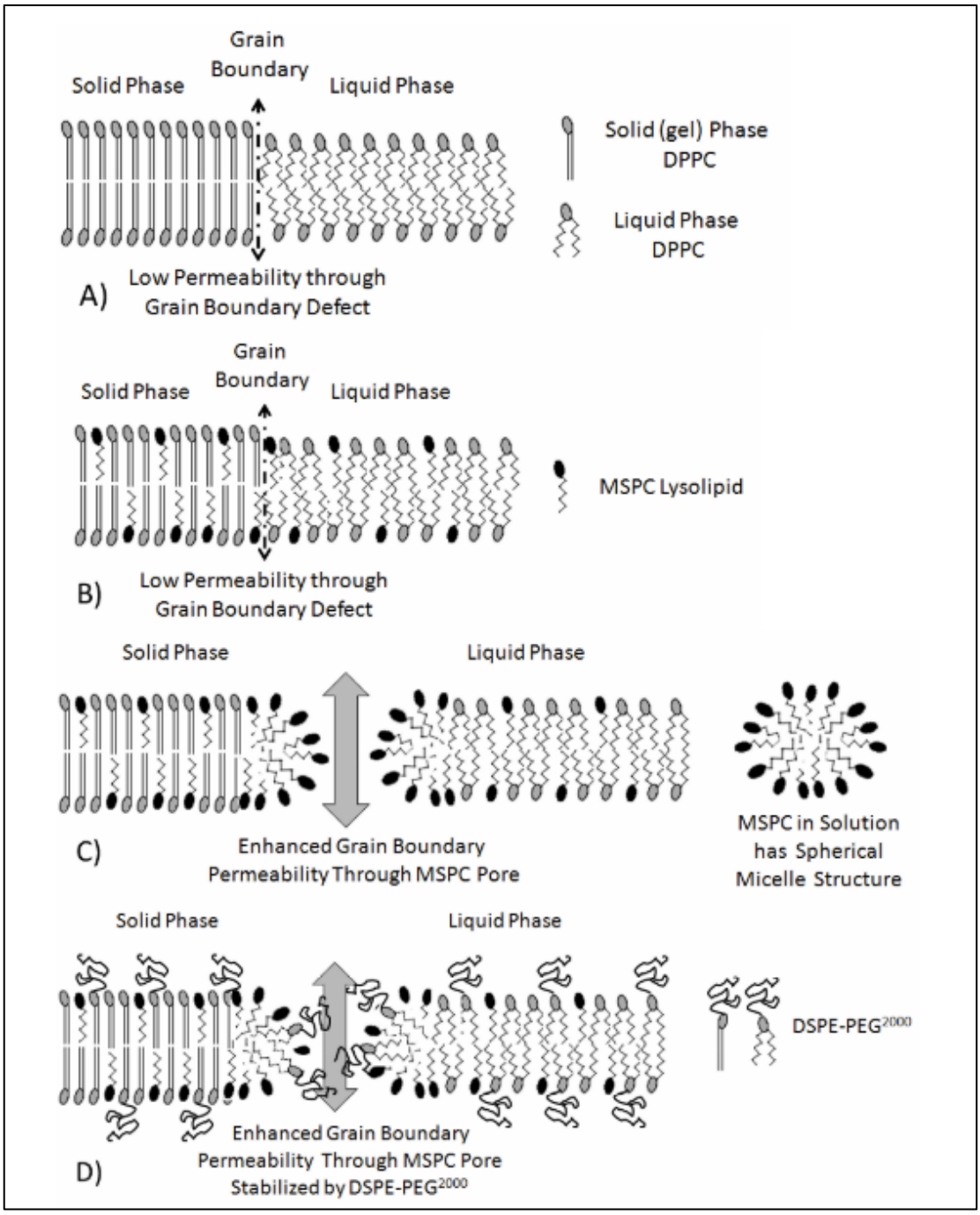

Figure 1.7: Schematics of postulated defect structures that result in membrane permeability for: A) DPPC bilayer in phase transition region with low permeability between grain boundaries for small ions to pass across; B) DPPC:MSPC bilayer in phase transition region, which does not result in a pore as the molar ratio of the lysolipid is too low; C) DPPC:MSPC bilayer in phase transition region with enhanced permeability as MSPC stabilises the pore using its affinity to form a curvature; D) DPPC:MSPC:DSPE-PEG2000 bilayer in phase transition region with enhanced permeability through MSPC pore further stabilised by DSPE-PEG2000. Schematic repurposed from C. Landon et al[91].

1.8 Methods of Making Vesicles

The payload of the TSV are limited by the method by which they need to be made. As the temperature sensitive lipids require a higher T_m during its formation, limited methods are available for the encapsulation of the cargo without damaging their activity. Hence the cargoes that have been loaded into TSV have been drug molecules e.g. doxorubicin[74] or antibiotics[82], fluorescent reporter molecules e.g. carboxyfluorescein[85] or calcein[95] and very short 5-amino acid peptide[96] which are unlikely to be damaged when higher temperatures are applied for a period of time.

For the purpose of producing vesicles which can be considered to be SCs, with the capability to produce any protein within, an IVTT system would need to be encapsulated. However, encapsulation of IVTT system within lipid based TSVs was limited. Therefore, in order to produce thermosensitive SCs, a method needed to be optimised which is able to take in a complicated mixture of proteins and molecules such as an IVTT system without damaging its activity. Below, some methods of producing synthetic cell vesicles are explored and their potential usage for the production of TSVs.

There are many methods of making vesicles that encapsulate an IVTT system to carry out protein expression. Each method has its own advantages and disadvantages which can impact the final properties including the size and electrical charge of the vesicle.

1.8.1 Hydration Methods

The gentle hydration method has been commonly used to produce vesicles[97] since the 1960s. Phospholipids or amphiphilic polymers are usually dissolved in a solvent such as chloroform which is then evaporated under gently flowing gas of argon or nitrogen. This leads to the

formation of thin film of the phospholipid or copolymer on a glass surface (Figure 1.8a). This film is then hydrated with an aqueous buffer solution for proper inflation and hydration of the film. Agitation of the hydrated lipid sheets leads to the formation of large multilamellar vesicles (MLVs) and the resulting particles are typically subjected to sonication or extrusion to reduce their size. For temperature-sensitive lipids usage in the hydration method the lipid and aqueous mixture is heated above the Tm for rehydration[98].

The aqueous lipid mixture can then be processed using different methods[61] to produce a more unilamellar or vesicles of specific sizes including; 1) sonication by ultrasonic waves in a sonication bath or using a probe, 2) membrane extrusion where heterogenous vesicles are pushed through micron sized pores, 3) freeze-thawing where the vesicles are frozen and gradually thawed to produce unilamellar vesicles (ULVs), 4) French-pressurising the MLV by extruding at high pressure through tiny holes.

Other methods of producing vesicles that use solvents include reverse-phase evaporation, ethanol injection, and the formation of double emulsifications as described below[99]. Additionally, a detergent removal technique can also be used to produce Large Unilamellar Vesicles (LUVs), where the concentration of phospholipids in the micelles increases as the detergent is removed by dialysis.

The advantage of using the hydration method is that it is simple and easy to operate but the disadvantage is that it does not allow the control of the membrane structure which results in inhomogeneous vesicle sizes of ULVs and MLVs[100]. Moreover, the introduction of certain cargos is difficult as the type of buffer solutions used can impact the swelling of the membrane structures and hence lead to lower overall yield of encapsulated vesicles. This means that certain cargo encapsulation is not suitable for the hydration method[101].

Gentle hydration method with extrusion has been used to encapsulate purified ribosomes with translation machinery to produce a polypeptide chain of Poly(Phe) inside the vesicles[102]. Fluorescent GFP mutant protein has also been produced with E.coli S30 extract machinery with T7 promoter and T7 RNA polymerase[103] . The gentle swelling method has also been used to produce Giant Unilamellar Vesicles (GUVs) which synthesised rsGFP[104]. The external solutions outside of the vesicles were inhibited from producing the proteins by EDTA, RNase and proteinase K, respectively.

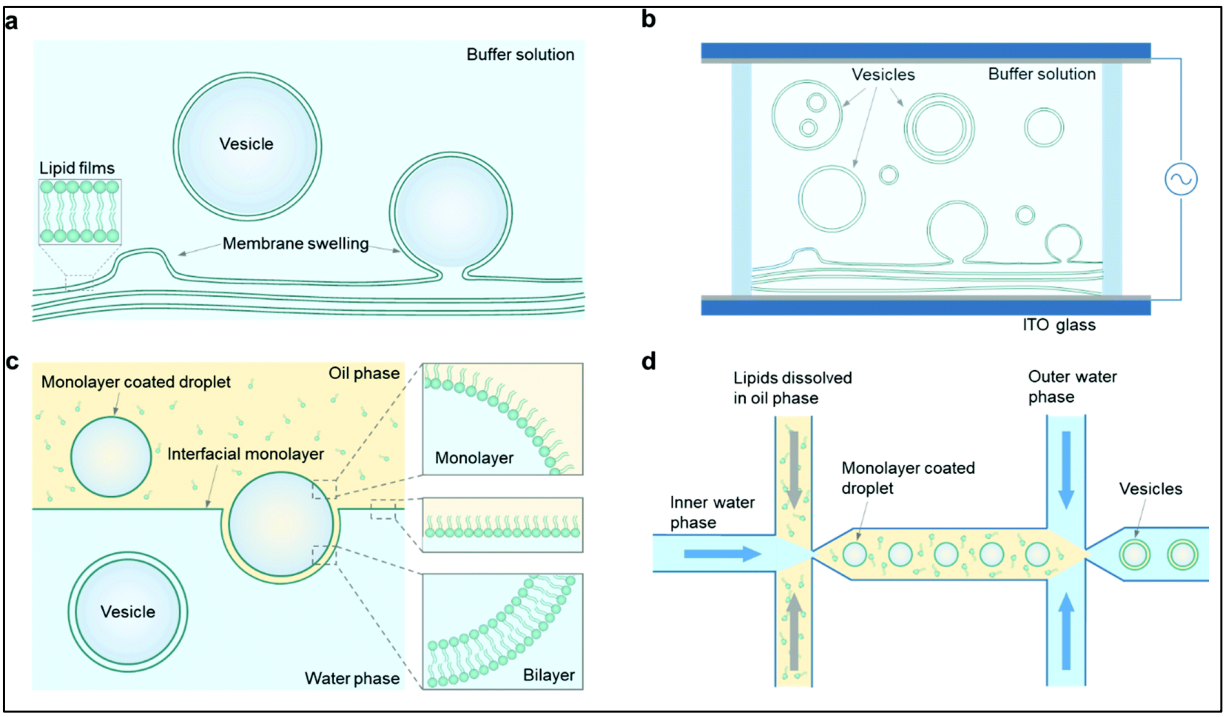

Figure 1.8: Engineering strategies for constructing giant vesicles. (a) Gentle hydration methods. (b) Electroformation of dry lipid films results in the formation of vesicles. (c) Vesicles are generated by droplet phase transfer through a lipid-stabilized oil–water interface. (d) Microfluidic generation of w/o/w double emulsions and subsequent oil extraction results in the formation of giant vesicles. Schematic repurposed from Y. Lu et al[105]

1.8.2 Electroformation Method

The electroformation method is similar to the hydration method, but uses electric fields on the hydrated films to produce giant liposomal vesicles[106]. As the process of hydration requires bilayer separation and bending, an electric field can facilitate this process. This leads to lipid swelling and vesicle formation overcoming intermembrane interaction and bending instability by creating a gentle mechanical agitation[106] (Figure 1.8b). The phospholipid film is dried on glass coated with indium tin oxide, then an alternating current (AC) electric field is applied to the hydrated lipid film for about 2 hours. The frequency and time of the electric field applied is dependent on the type of lipids used and the target size of the vesicles. This results in a more controlled size distribution of the vesicles (5-200 um) being larger and with fewer defects[107]. However, the disadvantage of this method is that it requires low salt solutions so this means charged lipids, proteins and vesicles cannot be used and the electrical current can also denature proteins in an IVTT system[108]. The key aspect for both the gentle hydration and electroformation methods is that a substantial amount of the encapsulating medium is needed as the vesicles are formed in the same medium that it encapsulates. This limits their use of encapsulating precious drugs and molecules which are not available in large quantities.

1.8.3 Microfluidic Method

The technology of microfluidics has been used to produce aqueous droplets which are flowed through microscopic channels. This results in the generation of water-in-oil-in-water (w/o/w) double emulsions. The final vesicles are released into an aqueous solution after extraction of the middle oil phase[109] (Figure 1.8d). Giant vesicles can be

formed by changing the velocity of the solution within the microfluidic devices. Other alternative microfluidic techniques include cDICE[110], jetting[111] and pico-injection[112]. The shape and size of the microdevices can also impact the size and structures of the final vesicles. The efficiency at which the inner solution encapsulates into the droplets is also enhanced. Protein expression systems have been encapsulated into DOPC and POPC based vesicles which can produce a target protein e.g. sfGFP[113]. The main advantage of using microfluidics is that it allows high level of control of the particle sizes that are produced and allows encapsulation of varied types of componenets[112]. However, using microfluidics involves complex instrumental and time-consuming setups and they are not suitable for productions of large amounts of vesicles[114].

1.8.4 Inverted Emulsion Method

The inverted emulsion method allows the rapid production of GUVs which can encapsulate high ionic solutions[99]. The method begins with creating water-in-oil droplet emulsion by mixing an oil and lipid mixture with the solution to be encapsulated (Figure 1.8c). This will eventually become the inner solution of the final vesicle. The lipids form a monolayer around the aqueous droplet which will form the inner layer of the final lipid bilayer. The droplets in oil are placed on top of a mixture of lipid-oil mix containing a second type of lipid which sits on top of an aqueous solution. The use of the second type of lipid allows the control of the outer membrane leaflet which can result in an asymmetric membrane[115].

The water-in-oil droplet sits on the lipid interface, in the oil layer, which is on top of the aqueous buffer solution. Application of centrifugal force allows the droplets from the oil phase to transport across the interface to the aqueous phase, forming a bilayer. This

transfer is possible when the droplet solution has a higher density compared to the oil and aqueous phases. There are several reasons why this method is favoured such as; 1) only small volume of the inner solution is required to produce a high yield of vesicles, 2) during its formation, it is possible to achieve high encapsulation efficiency which are largely uilamellar[99,116] and 3) allows the loading of charged and large macromolecular cargos into the vesicles[117].

One of the main limitations of this method is that the possible presence of oil residues on the vesicle membrane which can pass across the interface with the membrane and into the aqueous buffer. Furthermore, the overall yield of vesicles per experimental sample is very low as well as having varied loading efficiencies which means scaling up is highly resource consumptive.

1.8.5 Freeze Dried Empty Liposome (FDEL) Method

One of the research goals of this thesis was to produce TSVs which encapsulate an IVTT system. In order to fulfil those goals, another method which uses concepts from the hydration method was explored, known as the FDEL method. This method involves the rehydration of freeze-dried empty vesicles with the intended cargo [118]. Considering the hydration method's typical process, which involves multiple steps of emulsification, sizing, or sonication of lipid vesicles above their melting temperature (Tm) and subsequent hydration with a solution containing the desired cargo, it is noteworthy that the high temperatures and shear stress involved in these steps can have adverse effects on the stability of encapsulated proteins or DNA molecules.

In contrast, the FDEL method (Figure 1.9) involves the addition of water to the lipid film, followed by emulsification, resizing, and extrusion steps, all of which can be carried out

above the Tm of the lipid mixture. Next, a certain amount of empty vesicles can be pipetted into individual tubes and lyophilized. When a solution containing the desired cargo is added to the empty vesicles, and the mixture is shaken or vortexed and allowed to swell and re-hydrate and the cargos can then become encapsulated within the vesicles[118]. Various studies have shown that this method was able to successfully encapsulate DNA for transfection of tumour cells[118] and encapsulate a cell-free expression system for fluorescent protein expression[119–122].

This method allows for faster and more efficient preparation steps for vesicle formation, particularly when the empty vesicles are prepared and stored in advance. This is especially significant when encapsulating sensitive cargoes such as IVTT systems containing DNA, enzyme mixtures, and other fragile molecules. As a result, it was determined that the FDEL method would be the most effective approach for producing thermosensitive vesicles, as it would permit the use of various lipid molecules and compositions, enabling the testing of optimal compositions for heat-controlled release.

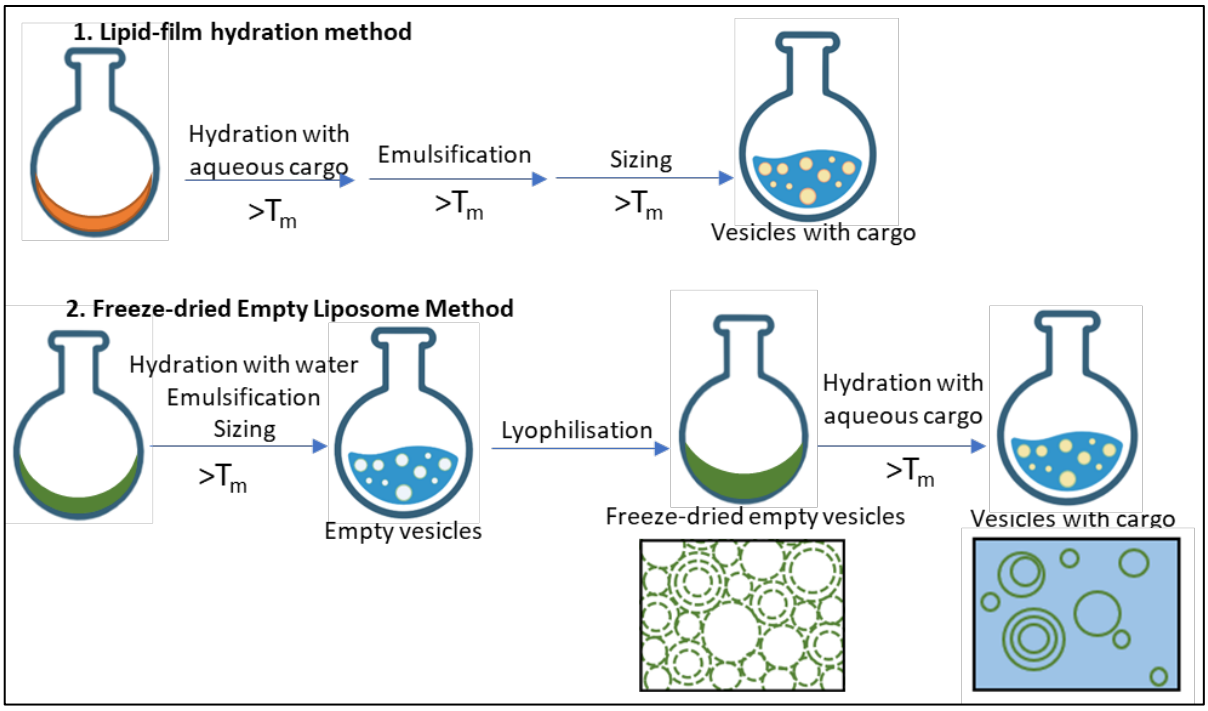

Figure 1.9: Preparation of vesicle formation with 1) lipid-film hydration method and 2) freeze-dried empty liposome (FDEL) method. Both invovle formation of dried thin lipid film but the hydration method invovles adding the encapsulating cargo directly onto the think lipid film. However, for the FDEL method, the encapsulating cargo is added many steps after forming empty liposomes by lyophilisation.

1.9 Summary of Thesis Work

This thesis describes the optimisation steps taken to produce synthetic cells which are capable of encapsulating a cell-free protein synthesis system and provide thermosensitive response leading to the requirement of optimising a release assay. Furthermore, short additional sequences at the 5' end of the encoded gene were explored to boost cell-free protein synthesis yields.

In chapter 2, the inverted-emulsion method was optimised, and various conditions were explored to produce SCs with a protein expression system. Different methods of releasing and measuring expressed enzymes were tested.

In chapter 3, the freeze-dried empty liposome hydration method was explored and adjusted to produce the optimum yield of thermosensitive SCs encapsulating a protein expression system. Different conditions in each step of the method were explored to increase encapsulation of the system. The thermosensitive SCs were heated to explore the impact of heating on the release of the cargo. Various techniques of the FDEL method was altered to identify the reasons for poor encapsulation of the IVTT system.

Chapter 4 explores an alternative method of increasing the yield of a coding region of a gene using short sequences which originated from cell-penetrating peptides. Alternative versions of the sequences were identified which significantly enhanced the yield of mVenus protein synthesis, which were termed as “boosters”. This indicates their potential for further investigation to optimise protein production.

Chapter 2 - Synthetic Cell Production using Inverted Emulsions and Detecting Release of Synthesised Proteins

Various approaches have been attempted for the production of SCs resulting in the formation of these minimal structures, which possess the ability to carry all sorts of cargo. Encapsulating specific proteins inside the SCs or reconstituting the membrane with membrane proteins can endow cellular functions such as metabolism[123], division[124] or communication[125]. The aims of this chapter were threefold: to produce a high yield of SCs using the inverted emulsion method, which encapsulates an IVTT system; to optimize an enzymatic assay compatible with the produced SCs; and to express protein enzymes inside the SCs and release the contents.

During SC production, different oils, lipids, and lipid concentrations were investigated. To optimize an enzymatic assay, various enzymes were tested for their feasibility and usability with the SCs. Once the enzymes were expressed inside the SCs, the method of releasing them from the SCs was explored to conduct the enzymatic assay and measure the level of release.

2.1 Introduction

The motivation behind this project was to produce synthetic cells which could be capable of delivering therapeutic proteins to living cells. To add an element of control

to the release of the cargo, it was decided to use thermosensitive SCs as delivery compartments that would release the cargo upon application of heat. Heat can be used as an external stimulus for targeted drug delivery as it can enable release from SCs in a controlled manner. The SCs in this thesis were constructed using a bottom-up approach, allowing for the selection of individual components as required.

To construct these SCs, the inverted-emulsion method[99] was employed, which allowed the use of phospholipids for membrane construction. This method not only enables encapsulation of large biomolecules inside the vesicles but has also been demonstrated to be a reliable approach for producing GUVs. Additionally, the method enables handling of low volumes of encapsulated samples, which is crucial for managing costly and sensitive products. Hence, the inverted-emulsion method was considered ideal for producing vesicles that could encapsulate large biomolecules and offer control over the yield and size of the vesicles generated[126–128].

The inverted emulsion method has demonstrated successful encapsulation of macromolecules, including enzymes[129], DNA[130], polymers[131], cells[132] and micron-sized particles[133]. Moreover, SCs produced via the inverted emulsion method have been shown to communicate with living cells, leading to neural differentiation[134], initiation of asexual sporulation of fungal cells[135] and induction of endothelial cell proliferation in mice models[136].

The preparation steps of the emulsion is important as this eventually affects the final yield, quality and size of vesicles produced in the aqueous solution. The typical procedure for this method involves initial dissolution of a specific lipid mix in an oil. The efficiency at which cargos are encapsulated and the vesicles are formed depends on the

oil as one of the factors. Various types of oils have been investigated to produce the droplets in the inverted emulsion method including dodecane[99,137], squalene[137,138], mineral oil[139,140] and paraffin oil[141] which have increasing viscosity respectively. These oils have different viscosity and surface tension which affects the property and behaviour of the emulsion droplets[137]. This can impact the final number of vesicles formed even when other features are exactly the same[137]. Therefore, to obtain a specific type of vesicle the optimisation of the type of oil used, the method of emulsion production and the lipid concentrations used were explored in this chapter.

In this chapter, various enzymatic assays including DHFR, β-lactamase, and β-galactosidase assays were examined. These enzymes were selected based on their diverse protein sizes, offering a range of options for experimentation. Additionally, the selection of different enzymatic assays allowed for the generation of varied results, aiding in identifying the most suitable assay for measuring release.

2.2 Results and Discussion

The objective of this chapter was to produce vesicles capable of serving as a cargo carrier for an IVTT system, enabling the expression of any target proteins, such as fluorescent proteins or enzymes. This could facilitate the production of therapeutic proteins and enable control of protein production on demand at any site in the future. Additionally, further aims of this chapter was to investigate a mechanism to release all contents from the vesicles for use as a control sample in an enzymatic assay, which would be compared to samples of cargo released in response to a stimulus, as explored in chapter 3.

In this chapter, it was recognized the advantages of using the inverted emulsion method to efficiently encapsulate an IVTT system at a low cost, compared to other methods. Since the IVTT system requires a low and chilled temperature in all steps to ensure the enzymes remain stable and active, implementing other methods of producing SCs that encapsulate an IVTT system can be challenging. However, the inverted emulsion method was found to be simple enough to allow for all steps to be carried out at low temperatures. Furthermore, the method results in less waste of the encapsulating system, as most of it ends up inside the vesicles[99]. This means that large volumes of expensive IVTT systems are not required for simple experiments.

The subsequent section of this thesis chapter will explore the investigation of diverse enzymatic assays that were examined to quantify the expression levels of synthesised proteins from the vesicles. The selection of suitable assays presented a complex task as it required the assays to be sufficiently sensitive to detect quantities of proteins produced within the vesicles, while also ensuring that they functioned effectively in the presence of the varied components commonly found in an IVTT system.

2.3 Producing Synthetic Cells Using Inverted Emulsion

The preparation of SCs using the inverted emulsion method begins with the creation of a water-in-oil (w/o) emulsion, where the desired inner solution is combined with a lipid and oil mixture to form a monolayer of phospholipid around the aqueous droplets. The choice of solvent oil is critical as it can impact the final properties of the vesicles formed, as each solvent has unique characteristics such as specific gravity, surface tension, and viscosity[137]. There are several criteria that need to be taken into account when producing SCs using the inverted emulsion method, including the type of lipid used, the

incubation time, the gravity of the emulsions, the osmolarity of the inner and outer solutions, the method used to disperse the droplets, and the centrifugation speed.

2.3.1 Lipid and Emulsion Preparations

Dodecane and squallene have been shown in the literature to be suitable for emulsion formation as they can form an oil free bilayer[99] along with mineral oil[139,140] and paraffin oil[129,133,141]. The selection of an appropriate oil is contingent upon the particular properties sought in the resulting vesicles. It is essential to strike a delicate balance between ensuring the lipids can dissolve in the chosen oil, maintaining the stability of the inverted emulsion, and minimising or eliminating the presence of the oil in the final vesicles.

The methodology for dissolving the dried lipid with four different oils was investigated. Initially, the lipid in chloroform was dried in a glass vial under a stream of nitrogen and allowed to desiccate for several hours to remove excess chloroform. To disperse the dried lipid into the oil, several techniques were tested: 1) vortexing for several minutes, 2) heating the lipids to 80 ℃ for 30 minutes followed by vortexing, 3) sonication in a sonication bath for 4 hours at room temperature and 4) combination of all three methods (vortexing for about 1 minute, heated to 80 ℃ for 20 minutes with a 1 minute interval of vortexing in the middle, and then placed in the sonication bath for 1 hour at 50 ℃). It was observed that the last method of combining the first three methods gave rise to higher number of droplets than just using each of the methods. Therefore, this last method was used to prepare the lipid and oil mix.

Next, emulsions consisting of carboxyfluorescein (CF) were produced using the lipid-oil mix prepared above (Figure 2.1). During this step, four emulsion preparation techniques

were tested to produce the droplets in the emulsions including vortexing[99], extrusion[99], sonication[141] using a probe and mechanical agitation by running the tube across a tube rack[126]. Depending on the method used to dissolve the lipids in the oil, and the method of emulsification, determined the different sizes and dispersity of the emulsion droplets formed within the different oils.

All four oils produced different properties of the emulsions. Dodecane and squalene produced very small sized droplets within the emulsions whilst mineral and paraffin oil produced larger sized droplets. The greyscale images in Figure 2.1 show the structures of the droplets when different techniques were applied for emulsion preparations. A few properties of the emulsions were observed when the different techniques were applied. During vortexing of the oils, the different oils needed different amounts of time to break up the droplets. The droplets in the oil for example did not easily break apart so longer vortexing time was needed. This is not ideal as the vortexing of an IVTT system for a long period of time can result in denaturing of the proteins in the system. Extrusion of the droplets in oil was attempted, but this was not very successful for dodecane, squalene or mineral oil as the droplets tended to become stuck on the extruder sides and the extrusion membrane which meant that the droplets were not forming effectively (although in paraffin oil the droplets were able to pass through the membrane pores possibly due to high viscosity of the oil and better stability of the droplets). Using a sonication probe was effective in forming homogenously sized droplets but they ended up being too small in all the oils. We were also conscious that using a sonication probe could introduce contaminants and has increased chances of damaging proteins due to the heat. But this is a method to consider for potential use in the future for handling large volumes of emulsion. The final technique of mechanical

agitation where the tube of emulsion was run across a tube rack allowed the formation of small droplets very quickly and efficiently without needing difficult equipment.

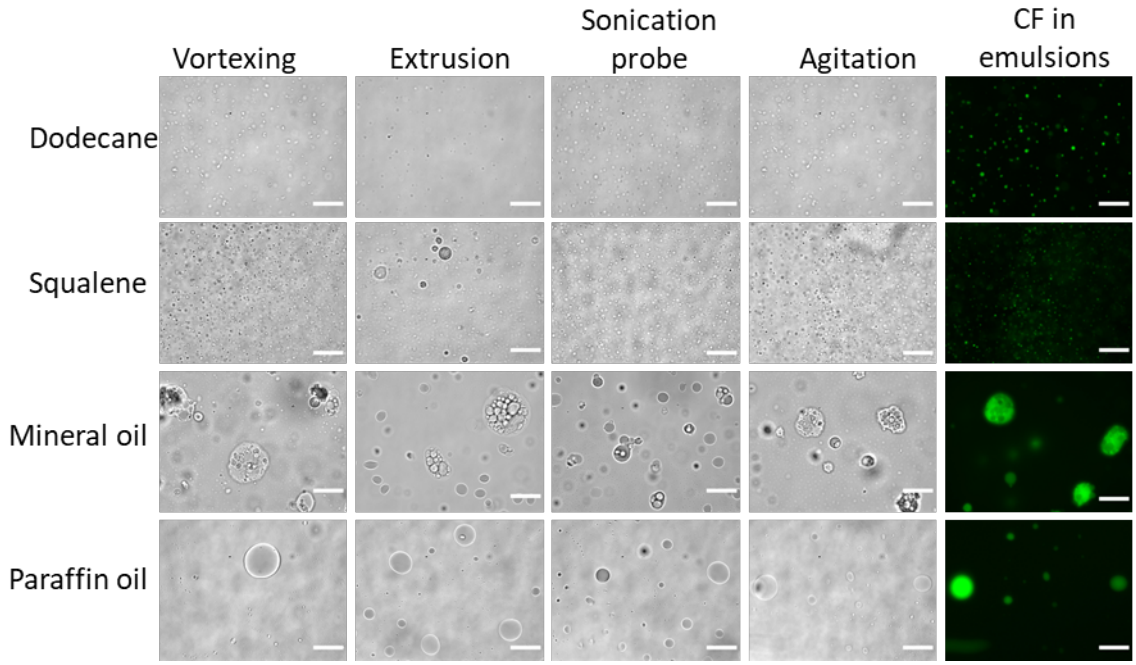

Figure 2.1: Water-in-oil emulsion droplets were produced using different oils and different techniques to use for the inverted emulsion method. Egg PC lipids were used to encapsulate CF and sucrose. Brightfield images and fluorescent images (far right) of the CF are shown. Sizes of the emulsions in dodecane and squalene were far smaller than the emulsion droplets made in mineral and paraffin oil. Scale bar = 20 µm

The droplets formed in dodecane and squallene were far smaller than the droplets observed in mineral oil and paraffin oil. They were also observed to coalesce very quickly within few minutes. This is not ideal as the incubation of the emulsion phase on top of the aqueous phase is essential for stabilisation of the monolayers around the droplets and at the interface before centrifugation for transfer and formation of vesicles in the aqueous layer. Therefore, the next steps towards producing SCs in the aqueous phase used mineral and paraffin oil.

2.3.2 Testing Centrifugation Speeds

To investigate the production of the vesicles, the PURExpress IVTT system with CF was used as the inner solution. An emulsion of this mixture was placed on the oil-lipid phase on top of the aqueous phase. Equilibration of the lipid monolayer interface was required for the interface to become saturated and stable with the lipids[99]. In order to transfer the water-in-oil droplets across the oil layer into the aqueous layer, gravity or centrifugation[99] can be used. The density of the droplets also needs to be higher than that of the aqueous solution. Therefore, sucrose was added to the inner solution with the IVTT system which made the droplets heavier than the outer solution. To ensure the balance of the osmotic pressure difference between the inner solution of the vesicle and the outer solution, the same concentration of glucose was added to the outer solution to balance the osmotic pressure and avoid shrinking or rupturing of the vesicles[141].

The inverted emulsion system was centrifuged at 120 g[99], 5000 g, 12,000 g[116] or 16,000 g for 30 minutes. Although dodecane and squalene were both used to attempt production of bilayer vesicles in the aqueous phase, no vesicles were observed. However, vesicles were observed in samples that used mineral and paraffin oils only (Figure 2.2). It was clear that the higher the centrifugal force, the higher the numbers of vesicles observed. It is possible that the lower speeds could also eventually produce higher number of vesicles if centrifuged longer but this was not tested. It was shown that mineral oil produced far higher number of vesicles consistently than paraffin oil in all the speeds. This could be due to the viscosity of the paraffin oil being higher than mineral oil. It was also observed that the lipids became trapped on the oil-water interface on the inverted column, rather than transporting across into the aqueous

phase. For the next optimisation steps, it was decided that mineral oil will be used for further studies as this gave the most amount of vesicles.

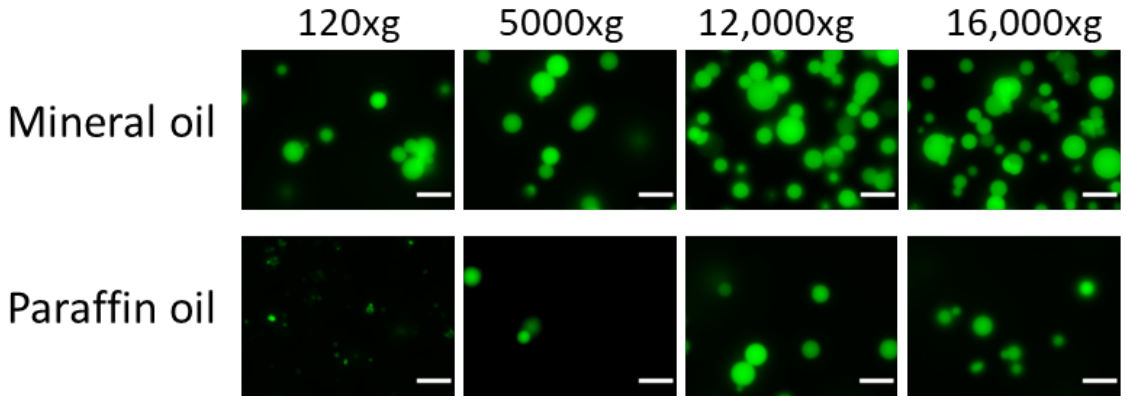

Figure 2.2: Bilayer vesicles produced using different centrifugation speeds using emulsions made in mineral oil and paraffin oil. Scale bar = 20µm

The above experiments were tested with lipids at concentration of 2 mg/mL. The concentration of lipids in the oil phase have been shown to have a direct impact on the time it takes to form monolayers at the oil-water interface[126]. It has been demonstrated that an adequate amount of lipid is required to allow enough lipids to be available to cover the interface and then enough to replenish the areas that cross with droplets when forming vesicles. Otherwise, an incomplete monolayer would affect the final yield of the vesicles produced. This wuld be because when an aqueous droplet makes contact with the aqueous outer solution if gaps form on the interface monolayer, it would release its content to the aqueous solution instead of forming a vesicle and hence decreasing the yield of the GUVs.

The lipid Egg PC concentrations that were tested was 2 mg/mL, 5 mg/mL and 10 mg/mL

in mineral oil. It has also been shown that enough incubation time to form the interface monolayers is important for the yield of vesicles[126]. We found that incubating the top lipid-oil phase for 5 minutes and then further 5 minutes after adding the emulsion was enough to observe levelling of the interface monolayer and to yield vesicle.

Although all lipid concentrations did result in the formation of stable vesicles, the different concentrations seemed to show different properties. The yield of the vesicles made from 2mg/ml lipid in mineral oil appeared to be lower than 5 mg/mL whilst the 10 mg/mL samples had more oil contamination as the brightfield images shows oil highly present with the vesicles. Further, the vesicles and lipids show to be more aggregated together in the higher 10 mg/mL concentration. This could be because the high concentration of lipids meant that the emulsions could not easily transport across the highly saturated lipid interface. And the droplets that did go across pulled the high lipid content along with some oil. For future vesicle preparations, the 5 mg/mL concentrations of the lipids was used.

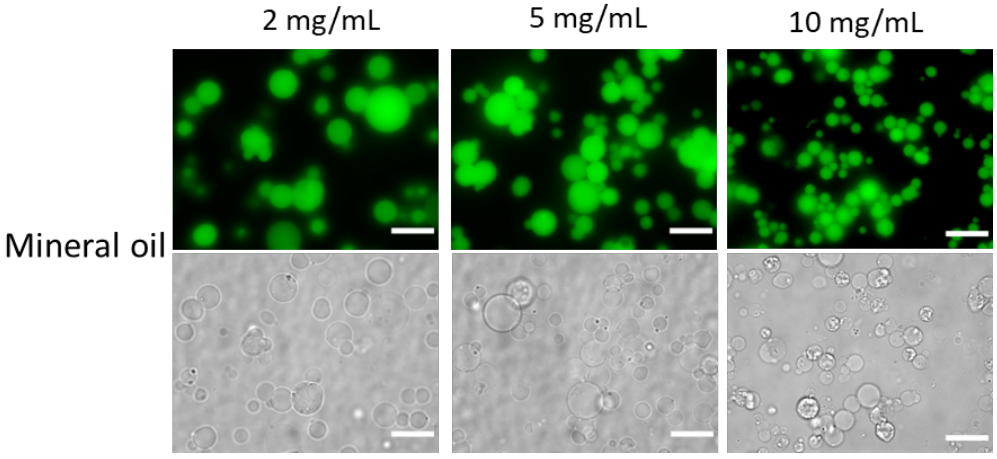

Figure 2.3: Different concentrations of Egg PC lipids were used to test for the production of vesicles using mineral oil. The 5 mg/mL and 10 mg/mL concentration of lipid in oil resulted in higher number of vesicles compared to 2 mg/mL. However, the vesicles made from 10 mg/mL had a larger amount of oil present in the brightfield images. Scale bar = 20µm

With the above optimised conditions in mind, vesicles were produced with PURExpress and mNG DNA template using Egg PC lipid concentration at 5 mg/mL in the oil phase (Figure 2.4). The vesicles also had Texas Red Dextran (TRD) molecules present at a concentration of 25 µM as well as sucrose at 200 mM to balance the osmolarity with the outer solution buffer which had 200 µM glucose. Fluorescent images of SC were captured using a green chana lactamase nel for monomeric mNG and a red channel for Texas TRD. The combined image of mNG and TRD fluorescence indicates that both the red and green fluorescence levels varied, but the green showed a higher degree of variation. This could potentially be due to the better encapsulation of TRD, a small molecule. Nonetheless, noticeable variability was observed in the mNG fluorescence among different synthetic cells, suggesting that the production of mNG protein in each SC was inconsistent. These observations underscored that the encapsulation efficiency of the in IVTT system varied across individual vesicles, with some demonstrating sufficient IVTT components to support higher levels of protein expression than others. On the other hand, some vesicles retained their red fluorescence, implying these vesicles faced difficulties in encapsulating the IVTT system components.

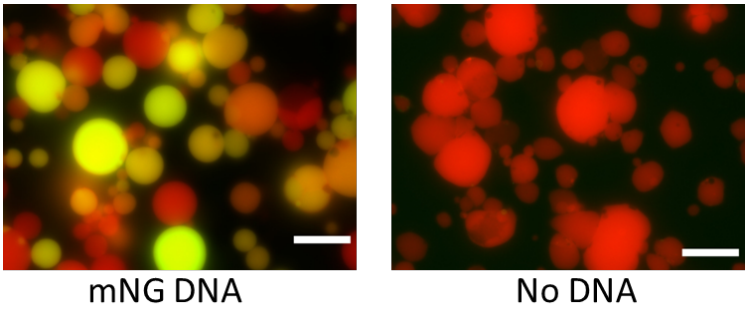

Figure 2.4: Merged images of vesicles from green and red channel representing mNG DNA and TexasRed Dextran respectively. The more mNG was present, the more green the vesicles. The vesicles without DNA were all red as no mNG was present. Scale bar = 20 µm

The above protocol was used in conjunction with blue-light activated DNA prepared by another DPhil student in the group, Denis Hartmann. Light-activated DNA templates have been developed in the Booth group which can be encapsulated within SCs with the PURExpress IVTT system that can produce a gene on demand when illuminating the system with UV[142] or Blue light[143]. This system allowed exploration of quorum-sensing based communication between SCs and bacteria which was controlled by light[144].

The light-activated DNA used was a linear DNA which included a T7 promoter site upstream of the gene. The T7 promoter region of the DNA was modified where photocleavable blockades were installed with biotinylated nitrobenzyl (UV activatable) or coumarin derivative (blue-light activatable) on amine modified nucleotides. Monovalent streptavidin was bound, which provided steric bulk which repressed transcription and allowed regulation of transcription. The use of this light-activatable DNA can allow temporal control of gene expression in SCs.

The coumarin-derived, blue-light-activatable DNA was encapsulated within SCs, aling with PURExpress, 25 μM of TRD and 200 μM of sucrose (Figure 2.5). Upon illumination using a 455 nm light-emitting diode (LED), the steric group was successfully cleaved, thereby enabling the transcription process. Interestingly, fluorescence was detected exclusively in the SCs subjected to blue-light exposure, while the unexposed SCs demonstrated no such fluorescence. These findings underscore the potential of vesicles for future applications in the medical field, particularly in the realm of targeted drug delivery. However, in this thesis we were focused on using temperature as an external stimuli to study the possibility of its usage in targeted delivery as this would allow controlled release of the synthesised proteins from the SCs.

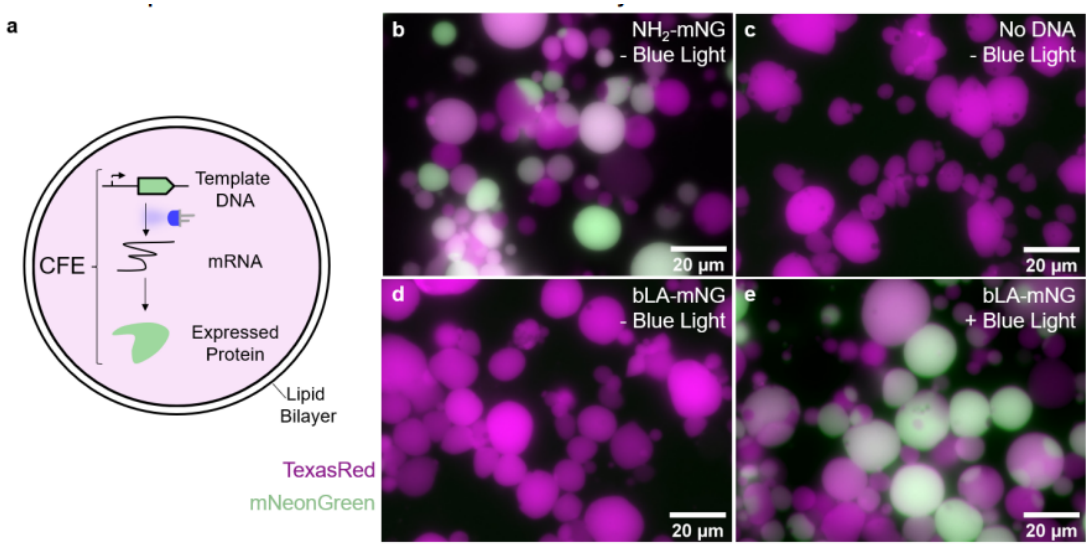

Figure 2.5: Blue light-activated expression within giant unilamellar vesicle (GUV) synthetic cells. a, Schematic of a GUV synthetic cell. A lipid bilayer encapsulates a cell-free expression system and a template DNA, from which RNA and protein are expressed in situ. b, When NH2-mNG DNA in the absence of blue light was included in the synthetic cells high fluorescence was observed. c, When no DNA was added within the synthetic cells in the absence of blue light no fluorescence was observed. d-e, When encapsulating bLA-mNG DNA inside synthetic cells, fluorescence was not observed in the absence of light (d), however, following 1 minute of 455 nm illumination, fluorescence was observed to a similar level as b (e). Scale bar = 20 µm. Figure repurposed from D.Hartmann et al[143].

2.3.3 Optimising Vesicle Release Assays

The production of bilayer vesicles with the ability to encapsulate an IVTT system to produce a target protein was successful. The next part of the project was to investigate the release of these proteins from the vesicles. Measuring release would be important because in chapter 3, we investigate thermo-controlled release of IVTT synthesised proteins from the vesicles. This meant that we had to generate an assay to measure release, which required a positive control release mechanism. We decided to release the protein content from the SCs using a detergent (Triton X-100), which allowed all vesicle membranes to be broken down and contents to be released for measurement (Figure 2.6). This would provide a control to compare with the samples of vesicles releasing its contents by heat in the next chapter.

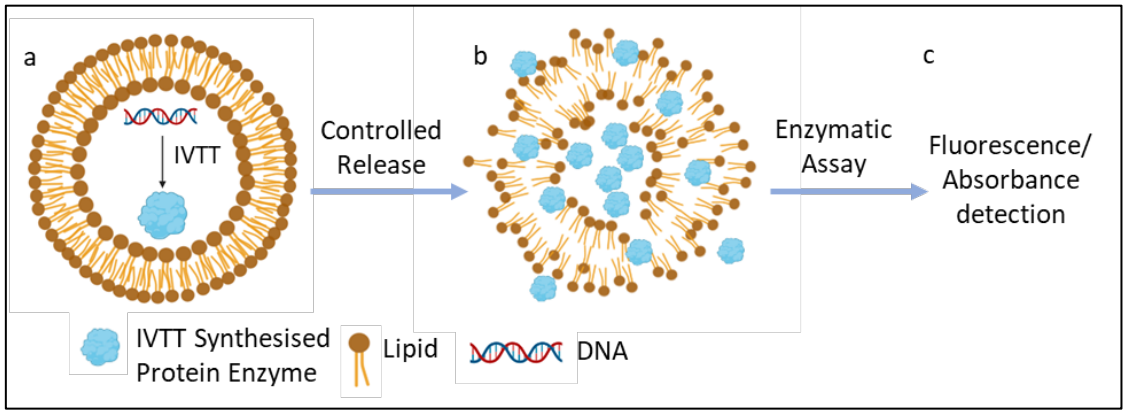

Figure 2.6*:* Schematic of vesicles and intended use for controlled release. a) Vesicles are produced encapsulating an IVTT system and DNA containing a T7 promoter with the gene sequence of a protein enzyme. b) Vesicle phospholipid membrane is disrupted to release the synthesised enzyme and c) an enzymatic assay is carried out to determine the fluorescence or absorbance level to give an indication of the amount of the enzymes that is released.

However, before encapsulating the IVTT system with the appropriate protein enzyme DNA, several enzymatic assays were investigated and optimisations were carried out in bulk

reactions. The enzymes tested were dihydrofolate reductase (DHFR), β-lactamase (β-La) and β-Galactosidase (β-Gal). Respective assays were tested to judge the simplicity of the assays and see if small amounts of the enzyme could be detected. This is important as the assay would need to be sensitive enough as the amount of enzyme that would be eventually released will be small, correlating with the small amount of the vesicles which would be produced in each experimental samples, especially vesicles from the inverted emulsion method.

2.3.4 DHFR Assay

Firstly, the aim was to synthesize dihydrofolate reductase (DHFR) enzyme in vesicles and employ it in an enzymatic assay. DHFR is an enzyme that is ubiquitous in most living cells and plays a crucial role in the catalysis of dihydrofolate reduction to tetrahydrofolate, utilizing NADPH as a cofactor[145] (Figure 2.7a). DHFR is also responsible for RNA and DNA synthesis, and its inhibition can lead to cell death[146]. The oxidation of NADPH by DHFR results in a measurable decrease in absorbance at 340 nm, corresponding to the decline in NADPH availability[147] (Figure 2.7b). The DHFR enzymatic assay was performed in bulk by varying the volume of the DHFR enzyme. As expected, the absorbance level decreased in both samples, with the sample containing a higher volume of the DHFR enzyme exhibiting a faster decrease in absorbance (Figure 8c). This outcome indicated the functional competence of the DHFR enzyme in the enzymatic assay, where a higher concentration of enzyme led to a more rapid reaction rate.

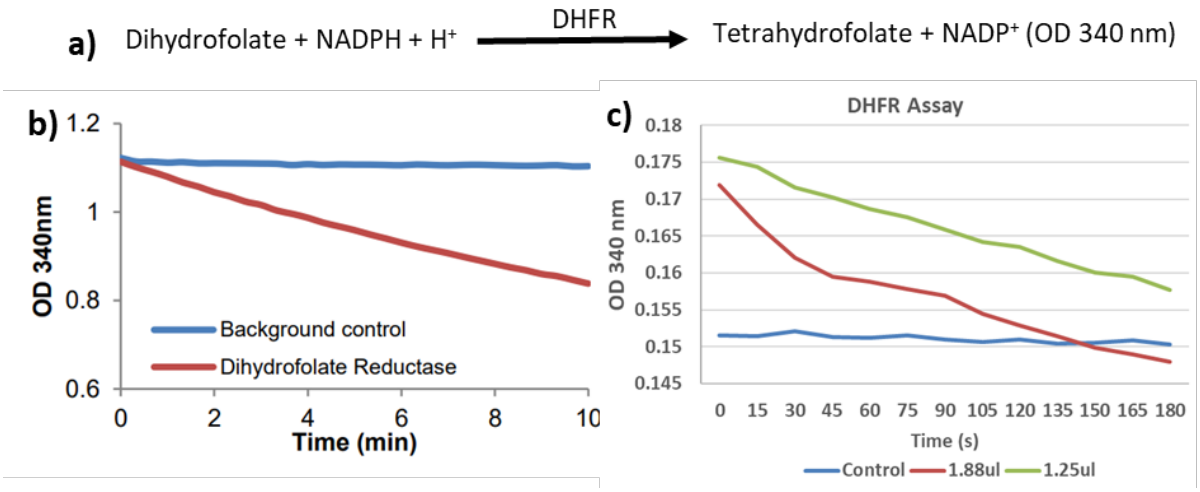

Figure 2.7: a) Dihydrofolate Reductase assay reaction uses NADPH as cofactor which absorbs at wavelength of 340 nm. b) Expected graph of reaction from abcam DHFR assay kit[148];as the reaction proceeds, the amount of NADPH in the reaction decreases in the presence of DHFR (red) whilst the control sample without the enzyme remains stable (blue). c) Bulk assay carried out with DHFR enzyme in Assay Buffer from Sigma Aldrich DHFR assay kit which showed that the assay gave similar decreasing assay reading as expected. Higher amount of DHFR enzyme in the assay (red) led to the absorbance decreasing faster.

This similar enzymatic assay was tested with DHFR synthesised in the PURExpress system (

Figure 2.8). The PURExpress system was incubated with or without DHFR-encoding DNA for three hours before the assay was conducted. Results revealed that the presence of DHFR synthesised in the PURExpress system led to a decrease in absorbance compared to the absence of DNA, indicating the successful production of functional DHFR enzyme that can catalyse the hydrolysis of NADPH.

The activity of purified DHFR in the presence of the PURExpress system was also evaluated. The results indicated that the DHFR enzyme functioned in the PURExpress solution, but the absorbance was slightly higher than in the buffer solution (

Figure 2.8). It is possible that the PURExpress system may inhibit NADPH absorbance or decrease the rate of the DHFR reaction. The latter hypothesis is supported by the observation that the absorbance levels of the DHFR reaction in the presence of the PURExpress system fluctuated, unlike the buffer control solution which absorbed NADPH at a lower level.

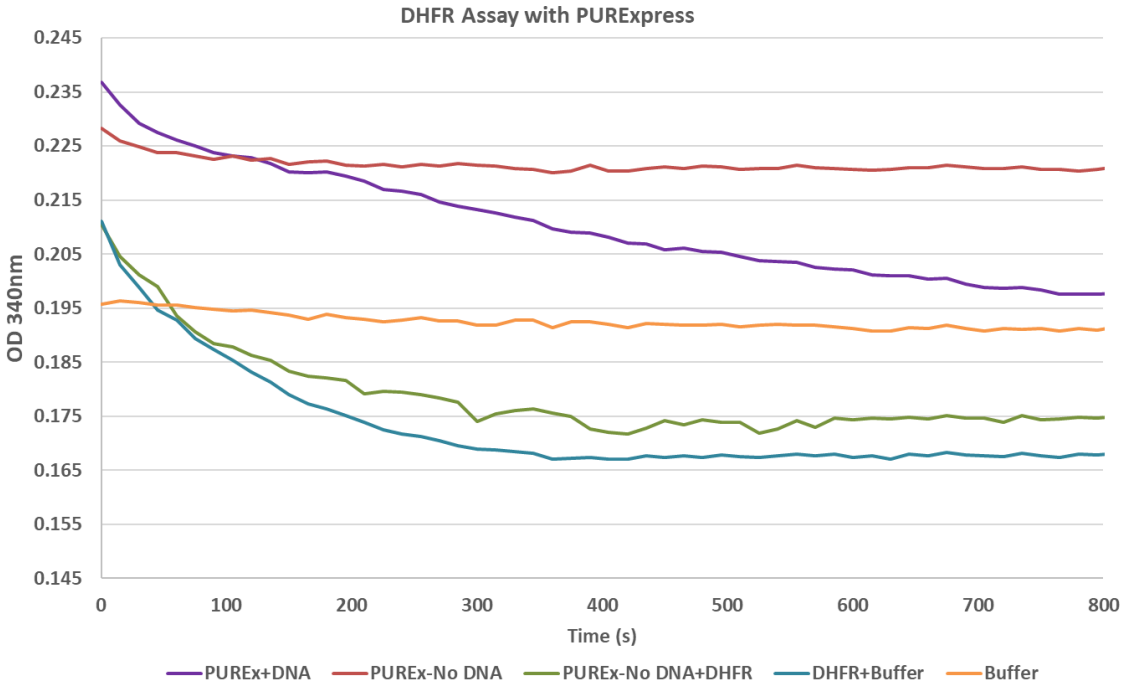

Figure 2.8: DHFR enzyme was synthesised using PURExpress system and bulk assays carried out to test for its activity and compare the absorbance of DHFR assay in the assay buffer compared to the absorbance when the assay is carried out in the outer solution buffer. DHFR enzyme was successfully synthesised in the PURExpress system as the OD decreased over time in the sample with DNA (purple) and purified DHFR enzyme (green) whilst the sample without DNA remained constant (red). The DHFR assay carried out in the assay buffer with purified DHFR enzyme showed a more consistent decrease in absorbance (blue) indicating the presence of the PURExpress system affecting the absorbance consistency of the assay (green).

To explore the impact of detergent on vesicle release, the DHFR enzymatic assay was conducted in the presence of Triton X-100. After the expression of DHFR in PURExpress, Triton X-100 was added, which showed that the DHFR activity was completely inhibited in the presence of the detergent (

Figure ***2.9***). This was not the result we wanted to observe as it was important that the enzyme activity was not inhibited components of the reaction. Even in the presence of DHFR alone, the reaction appeared to be inhibited by Triton X-100.

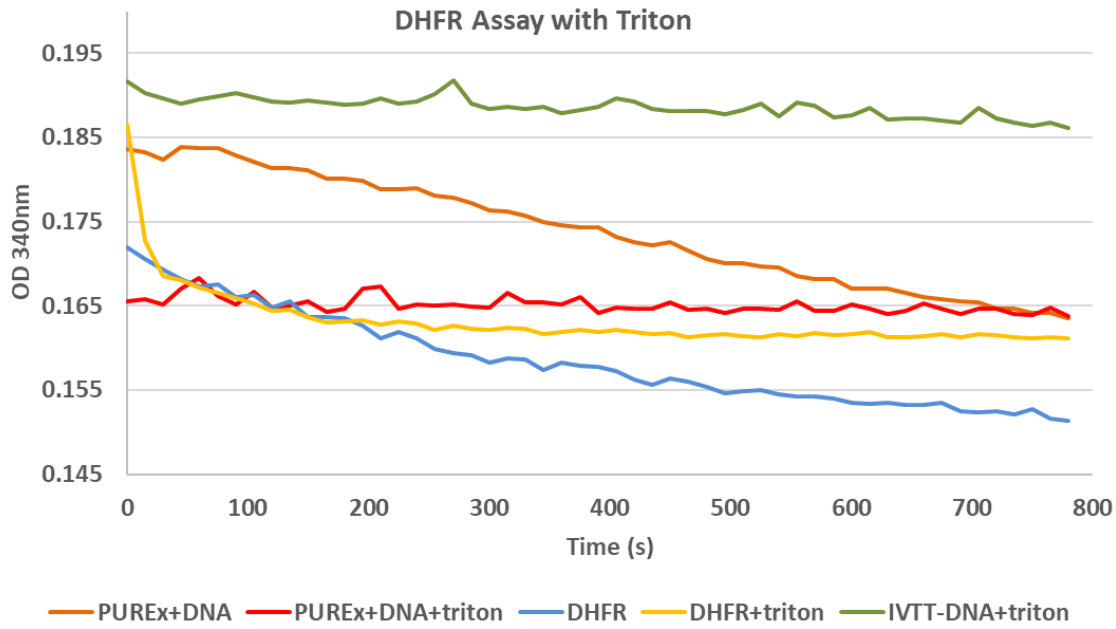

Figure 2.9: DHFR was tested for its activity in the presence of Triton X-100 (red and yellow) which showed that the DHFR activity was inhibited when using purified DHFR a well and PURExpress synthesised DHFR. As before, the absorbance decreased in the presence of DHFR enzyme over time (orange and blue). This showed that the DHFR assay could not be used when using Triton X-100 as detergent to release protein content from vesicles.

As a result of the these, it was determined that the DHFR assay was not suitable for detecting the presence of enzyme release from vesicles. The assay lacked the required sensitivity for detecting the small levels of enzyme release we aimed to measure, and was also inhibited by detergent Triton X-100. Since our goal was to quantify the amount of protein released from vesicles, the DHFR assay was not useful. Consequently, we proceeded to investigate a different enzyme and its corresponding assay.

2.3.5 β-Lactamase Assay

β-Lactamase (β-La) is an enzyme commonly expressed in both Gram-positive and Gram-negative bacteria, capable of hydrolysing β-lactam rings found in many antibiotics, rendering them inactive against harmful bacteria[149]. As such, β-Lactamases pose a significant clinical threat in antibiotic-resistant bacteria[150]. The enzymatic activity of β-La can be detected using a chromogenic cephalosporin, nitrocefin, which produces a red-coloured product with absorbance at 490 nm upon hydrolysis[151] (Figure 2.10). In bulk assays, the catalysis of nitrocefin by β-La was observed to increase over time, both in the presence of purified enzyme and β-La synthesized in the PURExpress system (Figure 2.10d). The addition of triton to the reaction resulted in higher absorbance, indicating either an increase in the rate of the reaction or an effect of triton on the absorbance at 490 nm.

The assay was then carried out using Egg PC vesicles encapsulating the PURExpress system, with or without DNA (Figure 2.10). Vesicles containing DNA showed an overall increase in absorbance over time, though with significant fluctuations. The addition of Triton X-100 caused a decrease in absorbance, suggesting that β-La was non-functional in the presence of

the Triton X-100 and lipids, resulting in an inhibition of the enzymatic reaction. Furthermore, the results of the assay were sometimes inconsistent, yielding similar or different results upon repeated testing. It was assumed that the presence of lipids and components of the PURExpress system impacted the enzymatic activity of the protein or hindered the absorbance of the nitrocefin. As a result, it was decided that the β-La assay with nitrocefin was not suitable for achieving the objectives of this chapter.

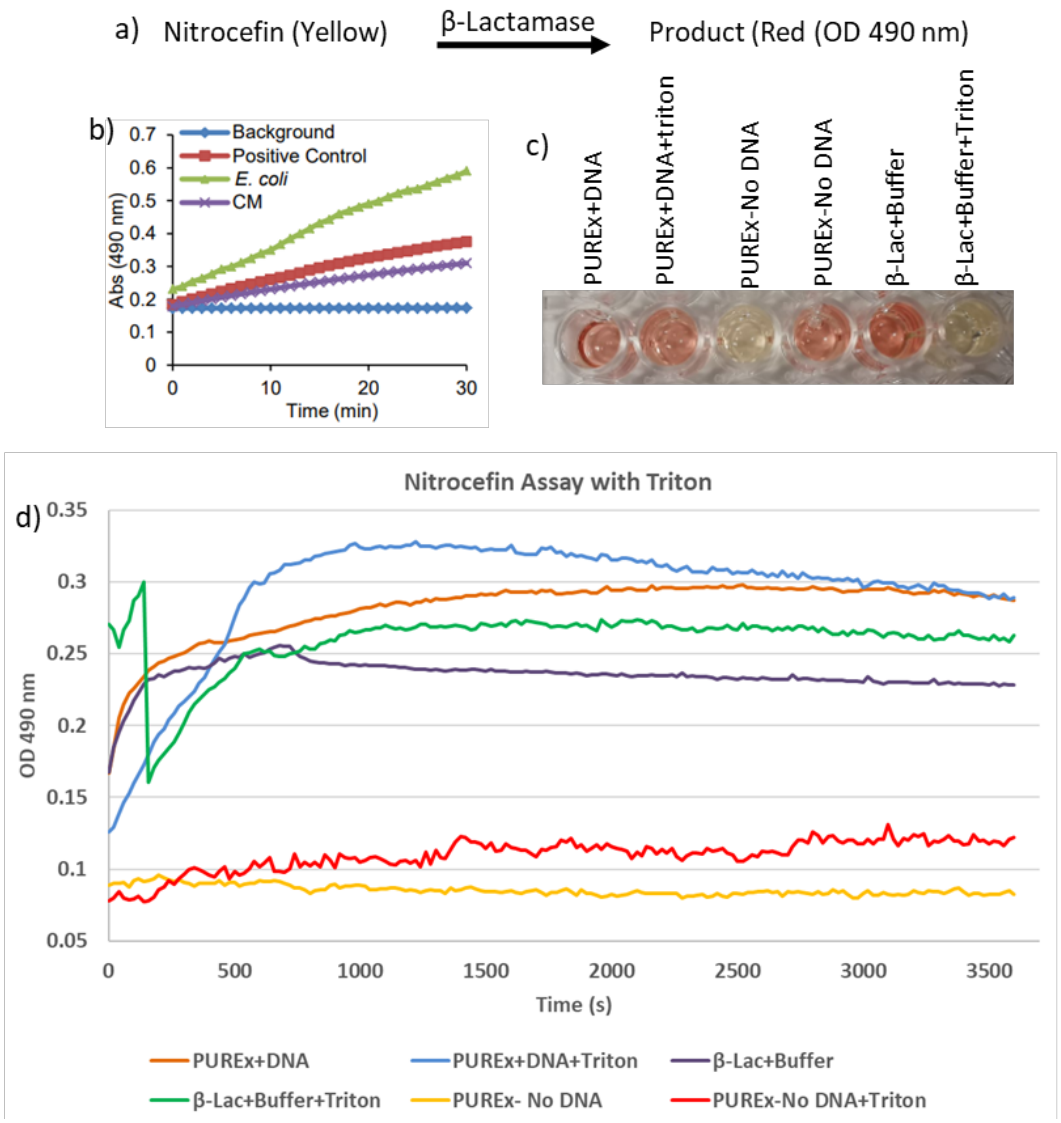

Figure 2.10: a) β-Lactamase assay reaction using the chromogenic substrate nitrocefin which is hydrolysed by β-La into a red product with absorbance at 490 nm. **b)** Expected graph of a β-La assay reaction from abcam β-La Assay Kit[152]. Absorbance of samples with β-La had increasing absorbance at 490 nm over time (green, red and purple) whilst the control sample maintained the same absorbance level over time (blue). **c)** Image of samples with nitrocefin where the samples turned red in the presence of the β-La enzyme. **d)** β-La assays were carried out using purified β-La enzyme in sodium phosphate buffer (purple) or PURExpress synthesised β-La in the outer solution buffer (orange). The bulk reaction was also carried out with Triton X-100 using purified β-La (green) or PURExpress synthesised β-La (blue). The overall absorbance seem to increase in the presence of Triton X-100 for both samples as it can also be seen for the control reactions of PURExpress without Triton X-100 (yellow) and with Triton X-100 (red).

2.3.6 β-Galactosidase Assay

The next enzymatic assay tested was using β-Galactosidase (β-Gal). The β-Gal discussed in this thesis is encoded by the *Lac Z* gene, found in E.coli, which is responsible for the hydrolysis of lactose into glucose and galactose by hydrolysing β-glycosidic bond[153]. It exhibits a complex structure, typically consisting of multiple subunits arranged in a tetrameric form. β-Gal has been used as a reporter protein for detecting the gene expression inside the vesicles in this thesis. The fluorogenic substrate 3-carboxy-umbelliferyl β-D-galactopyranoside (CUG) can be used for the sensitive detection of β-Gal activity as it is a substrate which is cleaved by the enzyme and forms a highly fluorescent product (CU) which can be detected in a plate reader.

A series of optimisations was conducted in order to identify the best method and condition at which the assay should be caried out. The final working concentration of CUG was at 1 mM and the reaction was incubated for 20 minutes before being read on a black-bottom microplate using a fluorescent plate reader with excitation filter at 390 nm and emission filter reading at 460 nm.

It was decided that we needed to identify what the smallest volume of PURExpress IVTT that could be detected by the assay. This was important as the PURExpress kit is highly expensive and high number of experiments would need to be carried out during the optimisation stage, so a minimal volume of the IVTT system was intended to be used. Furthermore, the amount of β-Gal enzymes produced in each vesicle samples were thought to be of low amount, which also needed to be measurable. Therefore, bulk assays were carried out using decreasing volumes of the diluted IVTT system (Figure 2.11). IVTT volumes from 0.5 µL to 0.001 µL were used to carry out the fluorescent assays. The fluorescence level were significantly higher for volumes that were 0.1 µL or. This showed that the PURExpress system did synthesise the enzyme which was active and was able to break down the CUG substrate. Furthermore, we were able to see the impact of different amounts of IVTT expressed β-Gal on the level of fluorescence of the CUG products.

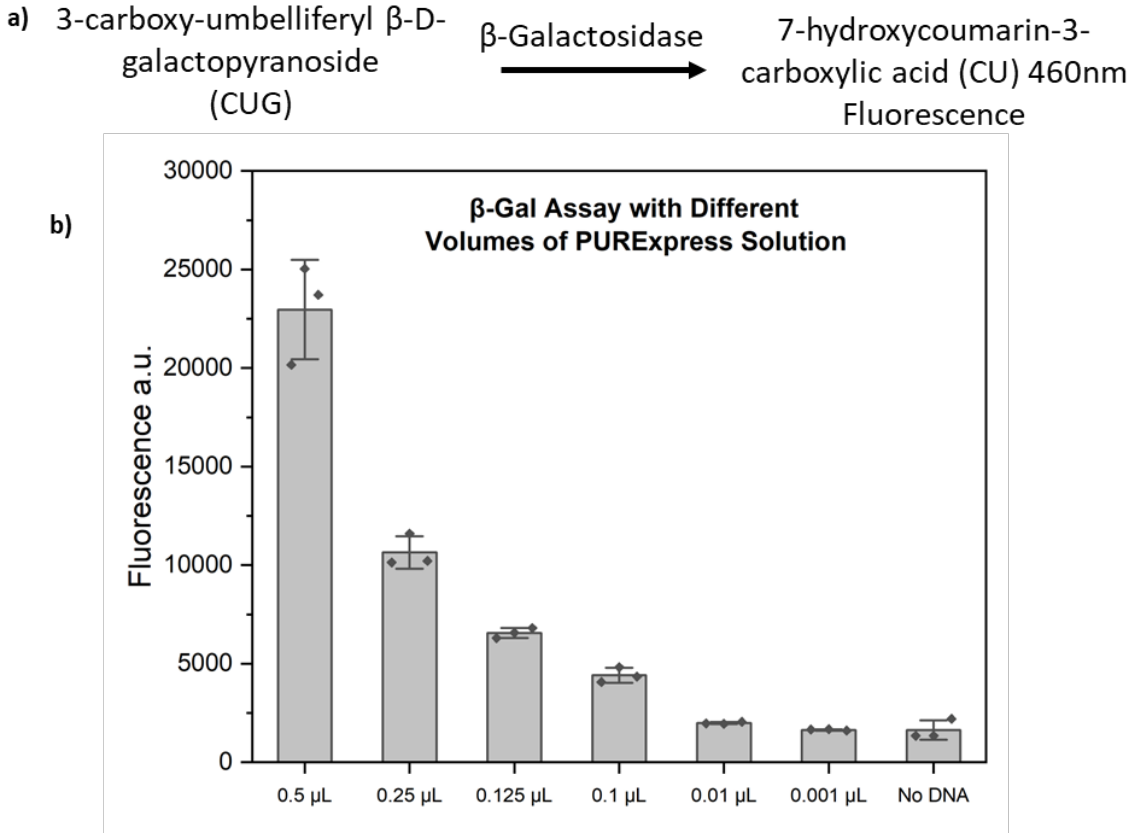

Figure 2.11: a) β-Gal assay reaction using the fluorescent substrate CUG which is hydrolysed into the fluorescent molecule CU with an excitation filter at 390 nm and fluoresce at 460 nm. b) β-Gal assay conducted with decreasing volumes of β-Gal enzyme expressed in PURExpress system.

2.4 Testing Release Using β-Gal Assay

To break down the vesicles completely, different methods were explored. This was needed to measure the total level of fluorescence observed when all the enzymes have been released from the vesicles. This would then allow a comparison with vesicles that are disrupted using heat as the control.

2.4.1 Lipase Controlled Release

A lipase enzyme was an option which was explored to enzymatically breakdown the membranes by catalysing the hydrolysis of the lipids. But first β-Gal assay was tested with IVTT expressed LacZ in the presence of the lipase which showed that β-Gal was still functional as an enzyme, albeit the fluorescence level was slightly lower in the sample with lipase (Figure 2.12). This could be due to slight inhibition of the β-Gal activity. Next, vesicles were produced with PURExpress and DNA to express mNG for 3 hours. Lipase were then added to the outside of the vesicles and incubated for 1 hour to determine if all the vesicle membranes broke down to allow the encapsulated proteins to release which should lead to diminishment of the fluorescent vesicles as the contents are released. However, fluorescent images of the vesicles shows that vesicles did not break down after incubation with lipase and the vesicles were in fact still intact. Therefore, it was decided lipase would not be the appropriate method to use for complete release of proteins from the vesicles.

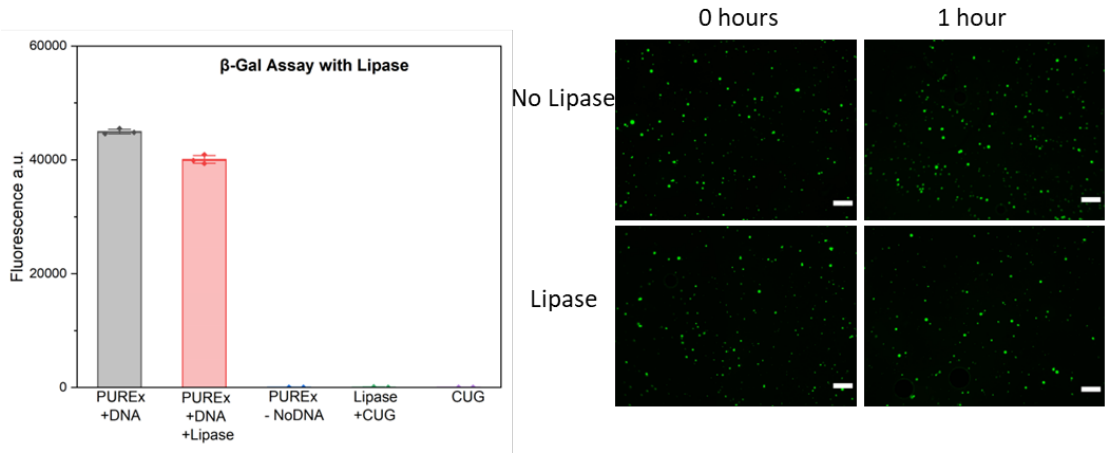

Figure 2.12: Lipase enzyme was added and to PURExpress system after β-Gal synthesis for 3 hours, and incubated for 1 hour. Then β-Gal assay was conducted (left). Egg PC vesicles were produced with PURExpress and mNG DNA (right). Lipase was added to observe if vesicle numbers decreased after 1 hour. No significant change in vesicle numbers were observed. Scale bar= 200 µm.

2.4.2 Solvent Controlled Release from Vesicles

Next, different organic solvents to break down the lipid bilayers were tested. Organic solvents can interact with the hydrophobic tails of the lipids, affecting the interaction of the membrane bilayers. This can lead to release of contents from the vesicles into the surrounding solution. The effectiveness of the organic solvents bursting vesicles depends on several factors including the type of solvents being used, the concentration of the solvent and the composition of the lipid bilayer. It is worth noting that organic solvents can cause damage to the encapsulated substance, especially proteins so careful testing was required. Three organic solvents were chosen to be investigated; hexadecane, silicone oil and chloroform.

Firstly, the activity of β-Gal was tested by mixing the solvents for either 1 minute or 5 minutes with the PURExpress system which was then allowed to separate naturally and pipetted out to a different tube. Then CUG assay was conducted with the PURExpress system (Figure 2.13a). Fluorescence was still observed in the samples that were pre-mixed with the solvents. This showed that the proteins were still functional even after coming in contact with the harsh

solvents. This method was then tested to see if vesicles could release the PURExpress synthesised β-Gal. The vesicles were produced as described above and mixed with the solvents by inverting the Eppendorf tube several times and then allowed to separate. The solvents were removed and the remaining vesicle samples were used to conduct the assay. Figure 2.13b shows that fluorescence was higher than the "No DNA" sample as well as the sample not mixed with a solvent. Hexadecane showed the largest amount of fluorescence compared to silicone and chloroform. The silicone and chloroform sample had similar fluorescence level as the non-solvent sample. This shows that hexadecane potentially allowed membrane disruption the most and consequently releases the β-Gal enzymes, and/or the silicone and chloroform samples had inhibitory impact on the β-Gal enzyme before it was used in the assay. This method required careful pipetting technique to separate the two mixtures to ensure that remaining solvents were not present in the sample, which was especially difficult to do as the volumes were very small and it was challenging to not remove the vesicle samples whilst trying to remove the solvent. It was decided that using this technique to detect the release from vesicles would not be the best option.

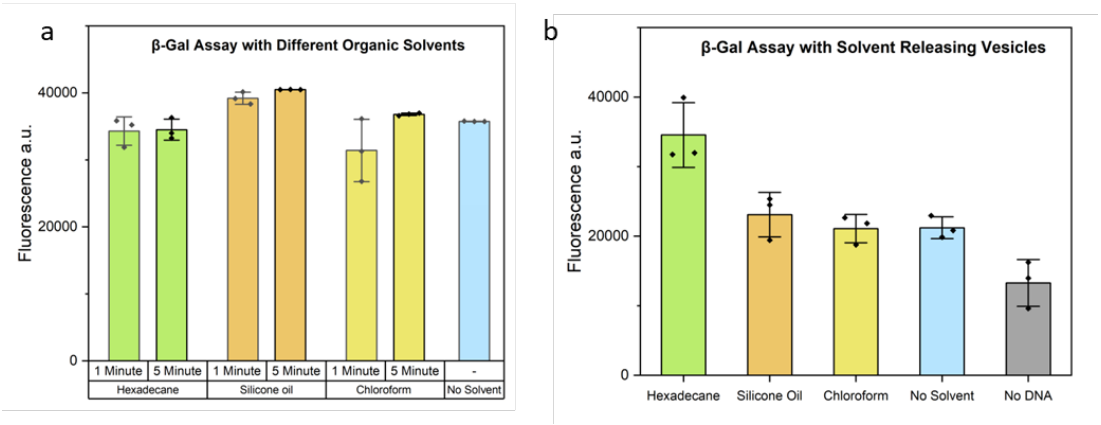

Figure 2.13: Fluorescence measured after β-Gal assay conducted using a) bulk IVTT synthesised β-Gal mixed with different solvents, B) β-Gal synthesised inside Egg PC vesicles produced by inverted emulsion method which was mixed with different solvents.

2.4.3 Detergent Controlled Release

The next method tested to release contents from vesicles was by using different detergents. Detergents are amphipathic molecules with hydrophobic and hydrophilic regions in their structure[154]. When detergents are added to vesicles, the hydrophobic region can interact with the hydrophobic regions of membrane lipid leaflets causing disruption in the bilayer structure[155] (Figure 2.14a). This can cause the lipids to become solubilized in the detergent and form micelles and as a result the content of the vesicles gets released into the solution. The choice of detergent and concentrations are important as some detergents are more effective in solubilizing lipid bilayers than others and some may have greater effect on the proteins leading to denaturing. Therefore, testing was carried out to optimise the use of detergents to release proteins from vesicles.

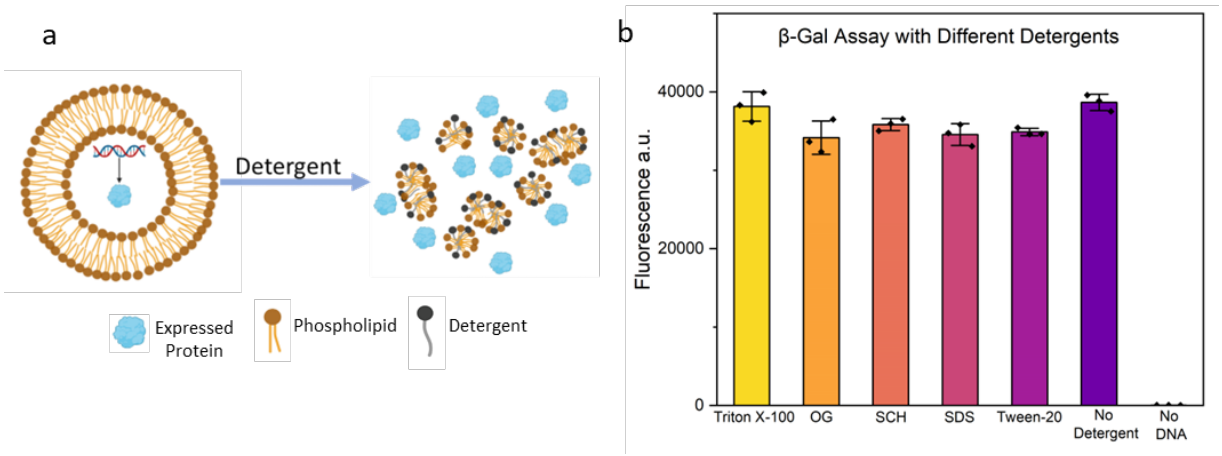

Figure 2.14: a) Schematic of vesicles encapsulating PURExpress IVTT system and DNA of enzyme and their release when detergent is added. Micelles of phospholipids and detergent are formed, b) B-Gal assay carried out with CUG in the presence of different detergents.

Different detergents were tested including Triton X-100, octyl-beta-Glucoside (OG), sodium cholate hydrate (SCH), sodium dodecyl sulfate (SDS) and Tween-20. β-Gal was expressed in bulk and then the different detergents were added in individual samples at a concentration that was higher than the known Critical Micelle Concentration (CMC) for each detergent. CMC of a detergent is related to the ability of a detergent to disrupt the membranes of the vesicles[156]. The concentrations of detergents below the CMC means that the detergent-lipid complexes are small which do not cause significant disruption to the vesicle membrane. However, as the concentration of the detergent goes above the CMC, the complex of detergent and lipid become larger and this leads to eventual solubilisation of the vesicle membrane. Therefore, the concentrations used for the different detergents were 0.08%, 40 mM, 4 mM, 4 mM and 0.07% for Triton X-100, OG, SCH, SDS and Tween-20, respectively, in the final volume of the assays. Measuring the fluorescence of each of the β-Gal assays in the presence of the different detergents show a similar level of activity from. Triton X-100 was chosen as the detergent to release the contents from the vesicles as it is also widely used for cell lysis and protein extraction as it solubilises lipid membranes whilst being mild and non-denaturing to proteins. The final concentration Triton X-100 that was used was usually between 0.1 – 1% for releasing vesicles which is the range the next of experiments were focused on using. The β-Gal assay was next tested to determine if the protein release from vesicles could be detected. Different lipid vesicles made of DOPC, POPC and Egg PC were produced, encapsulating PURExpress kit and DNA of mNG or β-Gal. Epi-fluorescent images of the vesicles show that all the vesicles samples released their contents in the presence of the detergent (Figure 2.15).

β-Gal assay was conducted with vesicles producing β-Gal and Triton X-100 was added, mixed well with the pipette tip, ensuring not to pipette up and down to avoid formation of bubbles (which was a major issue during this optimisation stage). CUG assay was carried out and the fluorescence was measured. Each assay that was caried out in various experiments produced different results for the different lipids. However, the Egg PC seemed to show that when Triton X-100 was added, fluorescence was higher, indicating more β-Gal release in the outer solution. However, it can be seen that the samples without the detergent also had a significant level of fluorescence which could indicate quite a high level of enzyme available in the solution or the vesicles were bursting over time in the absence of detergent. Also, the gain for this sample was very high when taking measurements in the plate reader, indicating the very low level of fluorescence being detected and hence the very low level of enzyme in the solution.

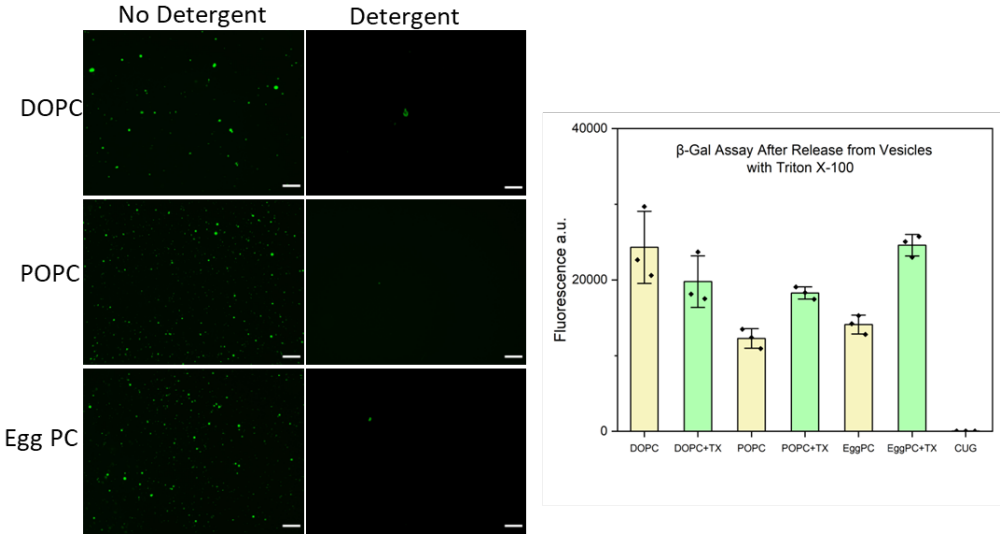

Figure 2.15: Epi-fluorescent images of vesicles of different lipids. Triton X-100 was added as the detergent which disrupted all the vesicles, eliminating the fluorescence in the images (left), scale bar= 200 µm. B-Gal assay conducted with the different lipid vesicles in the presence or absence of Triton X-100 (right).

2.4.4 Drawback of the Inverted Emulsion Method

As the CUG assay experiments were carried out using the vesicles made by the inverted emulsion method, it was apparent that the background fluorescence of the non-detergent treated vesicles remained high as the experiments shown above. It was presumed either the vesicles were bursting during the preparation of the assay or the background was observed to be high as there were not enough vesicles to provide a larger comparison. Furthermore, the total volume of β-Gal present was presumed to be reflective of the amount of β-Gal produced from IVTT volumes of 0.25 µL to 0.5 µL based on the fluorescence level observed for different volumes of IVTT in Figure 2.11. This is significantly low compared to the total 4 µL of the of the PURExpress IVTT system used for the preparation of each sample. It was recognised at this stage that the use of the inverted emulsion method to produce vesicles of high numbers were not feasible. The next chapter will also further explore how using this method was also not possible with certain type of bilayer components. This meant producing thermosensitive vesicles with this method would be a challenge.

2.5 Conclusion

This chapter has described optimisations that were undertaken to produce vesicles in an attempt to encapsulate an in-vitro transcription and translation system for the production of a target protein. The aim was to also measure the release of the encapsulated proteins and optimise an assay that can detect the proteins being released.

This project began with the idea of using the vesicles as carriers of therapeutic proteins which would be produced inside. These vesicles would then be applied to live cells where they could controllably release their inner contents and stimulate a physiological response within the

live cells. This led to exploring various ways of producing the vesicles and it was decided that the inverted emulsion method was the most advantageous. Therefore, this method was optimised and several iterations of the methods to produce the vesicles were explored. This included the investigation of various oils, method of producing emulsions, testing different lipids and lipid concentrations, and encapsulating the PURExpress system ensuring successful production of protein within. Eventually, the iterations led to using mineral oil in the inverted emulsion method, Egg PC as the lipid in concentrations of 5 mg/mL which encapsulated PURExpress IVTT kit to allow expression of various proteins.

This chapter also investigated methods that can be used to release the encapsulated synthesised protein from the vesicles. Different enzymatic assays were tested to identify the best approach that could be taken to detect the proteins that were being released from the vesicles.

The assays that were tested were DHFR, β-lactamase, and β-galactosidase assays. The β-Gal assay was eventually chosen to test for protein release from vesicles as it provided clear significant difference in fluorescence level between samples that contained the enzyme compared to samples that did not. However, when vesicles were produced using the inverted emulsion method, and the β-Gal assay was carried out, it was realised that the yield of the overall released proteins from the vesicles were very low. This suggested that the yield of vesicles were also too low. This would mean if the inverted emulsion method was used to create a vesicle with materials that can control protein release, then a real understanding of the amount of controlled protein release would not be detectable. Although the β-Gal assay was fluorescent enough to detect low levels of the enzyme, it was decided that a higher amount of vesicle yield would be required to have higher amount of proteins. This would also

be important because if the vesicles are used for application in live cells, a high amount of the proteins would be required to observe any physiological impact.

Therefore, the next chapter investigates a different method of producing vesicles with the aim of producing high yield of the vesicles and subsequently, high yield of a target protein. It also explores the production of vesicles that can be controlled to release when it is heated.

Chapter 3 - Synthesising Thermosensitive Vesicles

3.1 Introduction

The preceding chapter described the production of vesicles utilizing the inverted emulsion method to encapsulate an IVTT system[99]. These vesicles were capable of producing detectable fluorescent or enzymatic proteins which were detected by fluorescence imaging and a reporter assay. Assessing the degree of protein release from the vesicles was crucial to determine the extent of encapsulation and compare it with the amount of proteins released when utilising controllable stimuli-responsive lipids. Therefore, various methods for releasing the synthesized proteins were tested, resulting in the use of the detergent Triton X-100 to achieve complete release of IVTT-expressed β-Gal reporter protein. This protein was detectable through the optimized fluorescent CUG assay. However, the inverted emulsion method had several issues when using thermosensitive lipids, which will be discussed in this chapter. Moreover, the low yield of vesicles resulting from this method limited the number of β-Gal enzymes available for detection through the chosen assay. As a result, this chapter focuses on utilizing the freeze-dried empty liposome (FDEL) method to enable the use of thermosensitive lipids to encapsulate an IVTT system at higher temperatures and in greater quantities, showing that they can be thermosensitive. The chapter also delves into the challenges encountered while attempting to encapsulate an IVTT system using the FDEL method. Ultimately, it was determined that this method had potential to encapsulate an IVTT system within vesicles that are challenging to produce, although the yield was low. Further work would need to be explored to improve the conditions of the method and perhaps the

materials used to encapsulate an IVTT system within thermosensitive lipid structures that give high yield of the vesicles.

3.2 Results

The objective of this chapter was twofold; to develop thermosensitive vesicles capable of encapsulating an IVTT system and to produce sufficient quantities of these vesicles to enable detection of IVTT products through an enzymatic assays after the release of the cargo from within. The FDEL protocol has been shown to be used to encapsulate IVTT systems for GFP expression and other protein productions within the vesicles[120,122]. This method was chosen because it was thought that a higher encapsulation of IVTT could take place as a larger proportion of lipids can be used in each batch which can result in a higher yield of vesicles compared to the method using inverted emulsions. Moreover, the FDEL method enables the use of various compositions of lipid mixes, which cannot be achieved using the inverted emulsion method due to the need to manipulate lipids at a temperature above the Tm, which is not feasible for when using this method.

3.2.1 Attempt at Producing TSV with Inverted-Emulsion Method

Before testing the FDEL method, the efficiency of the inverted-emulsion method was assessed for producing vesicles using heat responsive DPPC lipids. Vesicles produced with DPPC and Egg PC of various molar ratios were tested which encapsulated IVTT and DNA of mNG (Figure *3.1*). It can be seen that as the proportion of DPPC increases in the mix with Egg PC, there is a significant decrease in the number of vesicles being produced. The conditions that were used to produce the vesicles were the same as the previous chapter, which means that the temperatures of each step was kept at 4 ℃. This is important because the IVTT systems need

to be kept at this low temperature to ensure premature transcription and translation is not taking place. Given the lengthy nature of each step of the inverted-emulsion method, maintaining a low temperature of 4℃ was imperative.

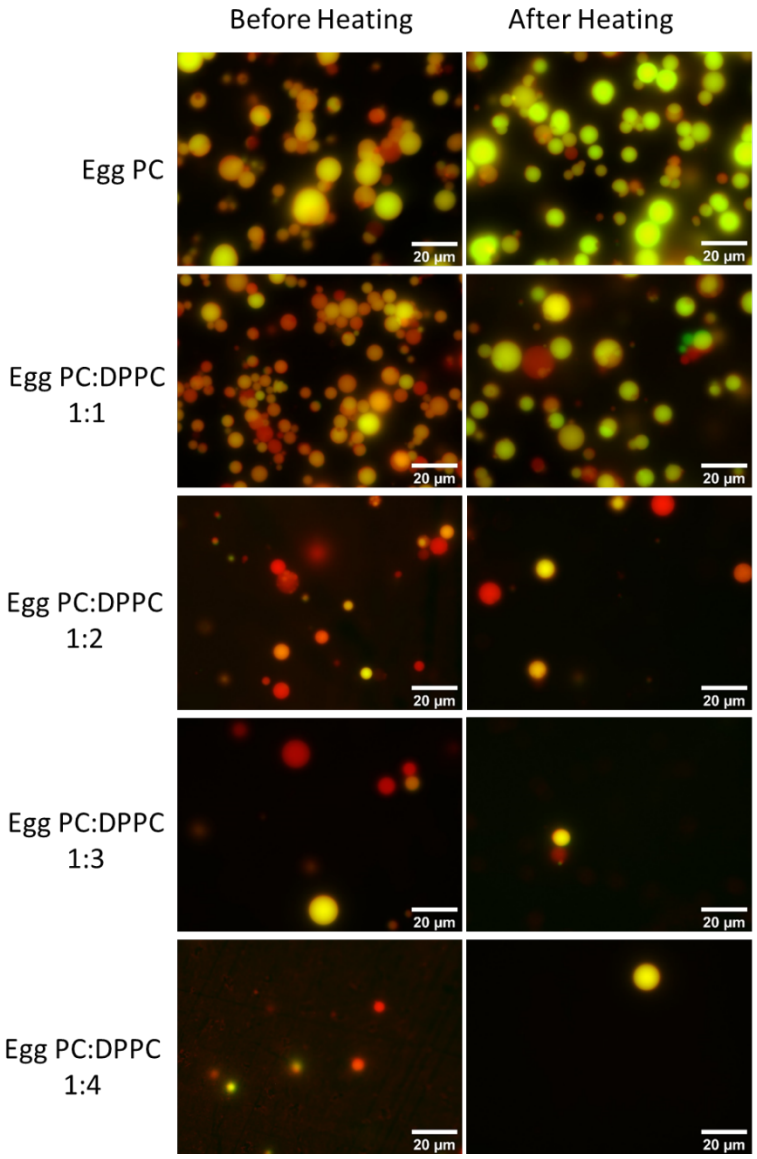

Figure 3.1: Epi-fluorescent images of vesicles generated via the inverted-emulsion method using varying molar ratios of Egg PC to DPPC are presented. Upon heating, Egg PC vesicles exhibited no significant difference in the overall number of vesicles; however, in the case of DPPC vesicles, a reduction in the number of vesicles was observed after heating for 10 minutes at 45 ℃, potentially indicating controlled release. Each image is an overlap of vesicles containing the background encapsulated vesicle with Texas-Red indicating a colour towards red or more green, indicating vesicles carrying out IVTT expressing mNeonGreen. Scale bar=20 µm

Subsequently, the vesicles were subjected to heat to assess whether the cargo was released. Upon heating of the vesicle samples consisting of DPPC, a lower number of the fluorescent vesicles were observed in comparison to unheated samples, suggesting that some vesicles released their contents during heating. Nevertheless, there were intact vesicles that did not release their contents.

Efforts to generate vesicles using the inverted emulsion method comprising lysolipids and DSPE-mPEG$_{2000}$ were made. This was however not possible as PEG was not miscible in the mineral oil, rendering it unsuitable in its use for this method. Consequently, it became necessary to explore an alternative vesicle production method, leading to the adoption of the FDEL method.

3.2.2 Preliminary Tests for Producing Vesicles with the FDEL Method

To evaluate the feasibility of using the FDEL method for producing vesicles capable of encapsulating and releasing contents, a simple testing methodology was devised using circular plasmid DNA. The plasmid of 3kb size, containing restriction sites for XbaI and BamHI, was encapsulated in vesicles using the hydration FDEL method. To determine the degree of encapsulation, some samples of the vesicles were treated with XbaI and BamHI enzymes, which digested the plasmid outside the vesicles, leaving the encapsulated DNA intact. EDTA was added to inhibit the enzymes, and Triton X-100 was used to release the contents without digesting the encapsulated DNA. The level of available DNA was then measured using gel electrophoresis (Figure 3.2). The experiment was carried out using two sets of samples: one with POPC lipid vesicles encapsulating the plasmid and treated in different ways (as indicated below the gel image), and another set in carried out in bulk reactions.

The first lane consisted of encapsulated vesicle samples which were not treated with the restriction enzymes and not released with Triton X-100. Therefore, DNA bands indicating the presence of uncut plasmids were seen as expected at around 3kb mark as well as concatemers of 10 kb size. These band patterns are the same as the control samples in lane 5, 7 and 8 which were carried out in bulk where the plasmids remain intact. When the two restriction enzymes were added, the plasmid was cut at specific locations, presumably outside the vesicles as the enzymes cannot enter across the membrane, resulting in the expected production of linear DNA of sizes 2.2 kb and 0.9 kb. There were other bands that were also detected in the same lane which were the same DNA profile as the undigested plasmid lane 1 indicating the presence of undigested plasmid DNA inside the vesicles which remained undigested and protected by the vesicles. In lane 3, EDTA was added after incubating the vesicles with the restriction enzymes to inhibit them which showed the same bands as the pervious lane as expected. The EDTA ensured that the restriction enzymes were inhibited when Triton X-100 was added so the released plasmid from the vesicles would not be digested, which could be seen on lane 4. This lane also shows DNA bands for the linear DNA as well as the plasmid DNA. However, in lane 6, all the DNA incubated with the enzymes were digested, indicating the only two bands as the final products. In this lane, the plasmid DNA bands are not present. This simple experiment shows that it was possible to produce lipid vesicles which encapsulate and protect molecules inside. And it also shows that the contents can be released when Triton X-100 was added. Images of the vesicles by the FDEL method, using Egg PC, was taken (Figure 3.2b), which encapsulated the NEBExpress IVTT system with mNG DNA template. The fluorescence observed in these vesicles were not as obvious as the vesicles produced by the inverted emulsion method. The vesicles sizes appeared to be smaller and not as spherical. As fluorescence of mNG could be observed, it was assumed that the IVTT system was being

encapsulated to be able to synthesise proteins. It was decided that the hydration FDEL method can be used to produce thermosensitive vesicles. This would allow the production of a higher yield of the vesicles and allow the incorporation of various other lipid bilayer components such as PEG and lysolipids.

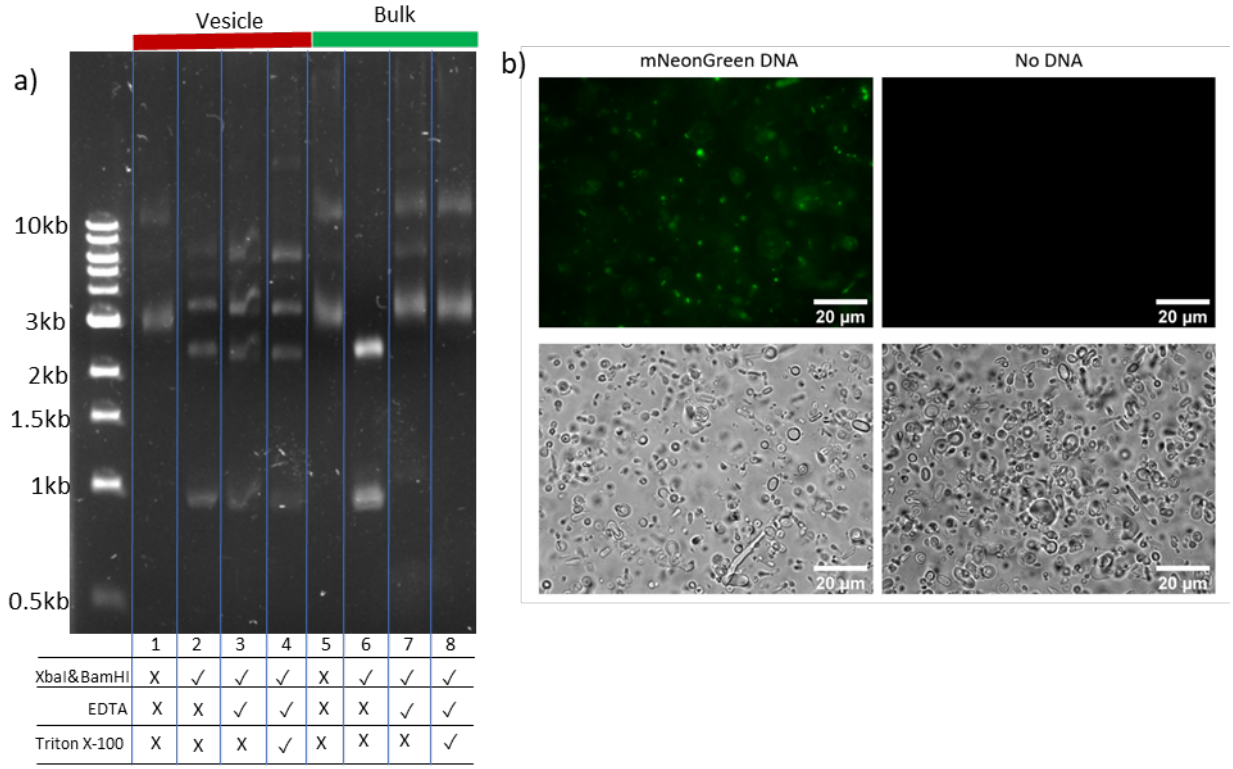

Figure 3.2: Initial testing to produce Egg PC vesicles using the FDEL method. A) Electrophoresis DNA gel of vesicles made by the FDEL method and samples of reactions made in bulk. Samples were treated with restriction enzymes XbaI and BamHI. EDTA were added to inhibit the enzymes. Triton X-100 was added to release the DNA from inside the vesicles. DNA profiles show that the vesicles protected encapsulated DNA whilst digesting any DNA outside of the vesicles. B) Fluorescent images of Egg PC vesicles made by the FDEL method consisting of an IVTT system with mNG DNA or without DNA.

3.2.3 Optimising Release Assay for Vesicles Made by Lipid Hydration

It was decided that the vesicles would be produced to incorporate NEBxpress as the IVTT system. Using the FDEL hydration method to produce vesicles would require a larger volume of the encapsulating substance compared to the inverted emulsion method explored in

chapter 2 which only requires 2-4 µL. For the FDEL method, about 10 µL of NEBxpress system would be used for each sample so it was chosen for the subsequent experiments in this chapter as it was a lot cheaper than PURExpress. There are several differences between the FDEL method and the inverted-emulsion method and the type of vesicles that can come out of the two techniques. The inverted emulsion method uses an oil to prepare the lipids, whilst the FDEL method does not require oils. The inverted emulsion method requires a small volume to produce vesicles, whilst the FDEL method requires a larger amount of the encapsulating system, which then requires further diluting so that the IVTT system outside of the lipid vesicles do not synthesise the target protein. As the cheaper IVTT option, NEBExpress was to be used, it meant that there would be background β-Gal enzymes present in the system which would need to be considered when calculating the final fluorescence level.

The aim was to produce the β-Gal enzymes inside the vesicles and get an indication about the amount of protein expression being made inside the vesicles. This required the optimisation of the β-Gal release assay using vesicles made by the FDEL method.

After the vesicles were produced with the lyophilised lipids, and the IVTT system was encapsulated within the vesicles, the outer solution was diluted enough so that protein expression would not take place outside of the vesicles. DNAseI was also added to digest DNA that was outside of the vesicles. After incubation of the vesicles at 37 ℃ for 5 hours, the contents of the vesicles were released using the detergent Triton X-100 which disturbed the membrane allowing the expressed β-Gal proteins to be released. This could then be used to conduct a CUG assay where the fluorescence level of intact vesicles should be significantly lower than the vesicles that were disrupted.

As it was decided that Triton X-100 was to be used to break open all the vesicles, the percentage of the detergent that was required to release all the contents from an individual sample of the vesicles was optimised. The impact of the different concentrations of the detergent on the CUG assay was tested in order to identify how much Triton X-100 should be used for optimum release without inhibiting the fluorescence.

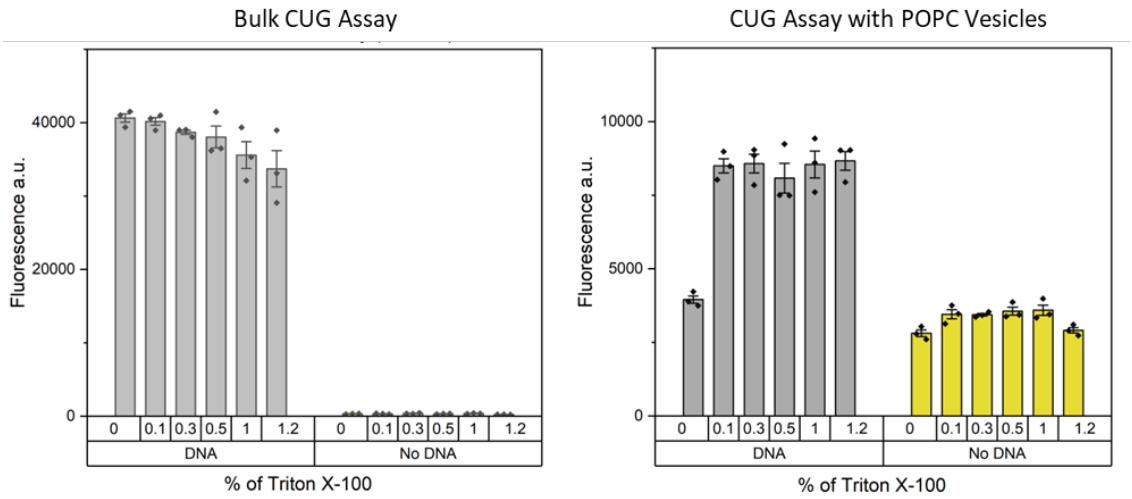

Figure 3.3: Fluorescence level of IVTT bulk reactions (left) and vesicle reactions (right). Different amounts of the detergent was added leading to decrease in fluorescence in the bulk reaction. Increasing the Triton amount with the vesicles did not show an increase in fluorescence, which means that 0.1% was enough to release all the encapsulated content from the vesicles.

When β-Gal CUG assay was carried out in the presence of 0.1 – 1.2% of Triton X-100, the fluorescent levels overall decreased with the increasing detergent level in the samples. This was repeated in the presence of POPC vesicles and it was observed that fluorescence was higher for the vesicle samples after Triton X-100 was added (Figure 3.3). This indicated that a higher amount of the β-Gal enzyme was available from the released vesicles compared to the intact vesicles of the sample without Triton X-100 which had similar level of fluorescence as

the samples without β-Gal DNA. Although all vesicle samples with Triton X-100 showed similar level of fluorescence, it was decided that 0.1% of Triton X-100 would be enough to release vesicle content as this percentage was high above the CMC of the detergent[157] and it did not inhibit the fluorescence level of the samples compared to the higher Triton X-100 level.

3.2.4 Inhibiting IVTT by Dilution

The FDEL method used by the Mansy group[120] added 10 uL of the IVTT system to the lyophilised lipids and vortexed for less than 30 seconds. The mixture was left for 30 minutes on ice for the vesicles to swell and allow encapsulation of the IVTT system. They diluted the mixture 20-fold with a buffer containing Proteinase K to break down the protein components of the IVTT system on the outside of the vesicles. This similar method was also used and tailored to encapsulate the NEBexpress system within the vesicles.

Using this approach however, meant that both the inner and outer solutions was made up of the IVTT system. To prevent the expression of the β-Gal protein on the outside of the vesicles and allow its expression exclusively within the vesicles, the outer solution was diluted to varying degrees with a buffer. DNAse I was also used, but it was not enough to inhibit the target protein expression as shown in Figure 3.4. To determine the optimal dilution factor required to inhibit protein expression on the outer surface of the vesicles, different dilutions of the IVTT samples were incubated at 37 ℃ for protein expression. In addition, an undiluted sample was also tested in the presence of DNAseI to assess any residual expression of β-Gal protein. CUG assays were then performed on the different dilutions of the samples to identify the appropriate dilution factor. Notably, the control sample without DNA exhibited some background fluorescence, which may have been due to the presence of background β-Gal protein in the NEBExpress bacterial lysate. The expression of β-Gal protein from the IVTT

system was effectively inhibited with a 1:2 dilution of the outer solution. However, in the presence of DNAseI, the fluorescence was higher, indicating that some β-Gal protein was still being produced, possibly due to incomplete digestion of the DNA. Therefore, for future vesicle production using the FDEL method, it was decided that the outer solution of NEBExpress would be diluted to a 1:2 ratio of IVTT with buffer to effectively inhibit protein expression on the outer solution of the vesicles.

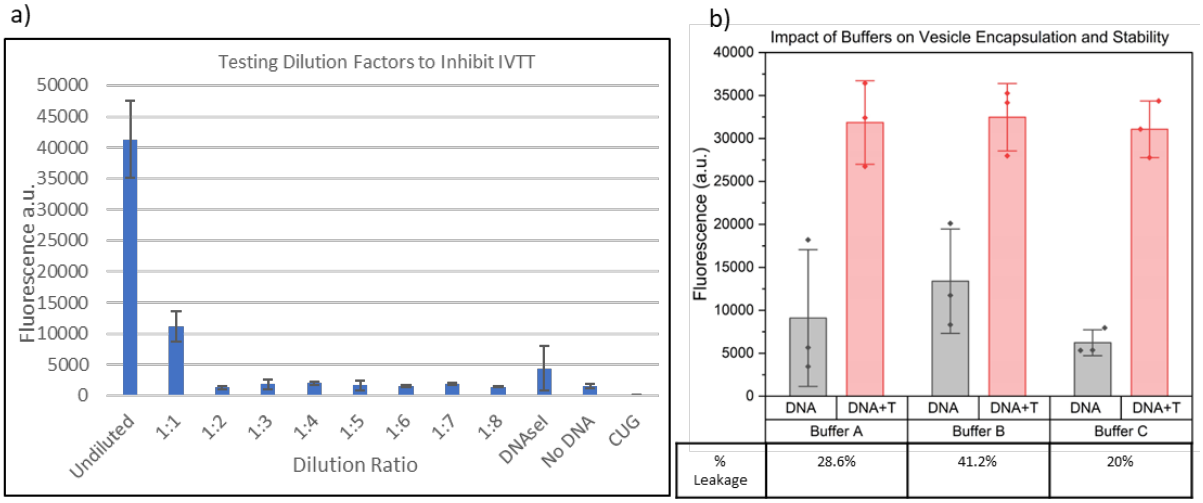

***Figure* 3.4**: Testing NEBExpress IVTT system. a) NEBExpress IVTT system diluted by different proportions of the outer solution buffer and then incubated at 37 ℃ to test for protein expression and CUG assay was carried out and fluorescence was measured. 1:2 ratio of IVTT with buffer was enough to inhibit IVTT in the absence of DNAseI. (Right) Different Buffers were used to check for vesicle stability as a balanced osmolarity was required. Buffer C provided the lowest background indicating better stability of vesicles. Adding Triton X-100 released all the encapsulated β-Gal enzyme hence the fluorescence should be at its highest for these samples. T = Triton X-100, error bars represent 1 Standard Deviation.

3.2.5 Impact of Outer Solution Buffer on Vesicle Stability

In order to achieve osmolarity balance between the buffer outside of the vesicles and the NEBExpress system inside the vesicles, the osmolarity of the NEBExpress system was measured. Table *1* provides a summary of the osmolarity of different buffers, as well as the

measured osmolarity of the NEBExpress system. Initially, Buffer A was used, which had been utilized in the encapsulation of PURExpress vesicles in the previous chapter. However, it was observed that the fluorescence of the intact vesicles remained high (**Figure *3.4***b). Upon adjusting the buffer concentrations to match the osmolarity of the NEBExpress mix and producing vesicles using the IVTT system, the fluorescence level remained the same as Buffer A, indicating the presence of unstable vesicles in the buffer. Subsequently, it was discovered that the NEBExpress mix had a high glycerol concentration of approximately 2%. Therefore, the buffer was modified to include glycerol in the mix, and the produced vesicles were evaluated for CUG fluorescence. The results demonstrated a reduction in fluorescence for the intact vesicles in Buffer C which had 2% glycerol. The fluorescence levels were corrected with the background fluorescence level and the leakage percentage was calculated. Buffer C had the lowest percentage of leakage at around 20% compared to Buffers A and B which had higher level of leakage at 28.6% and 41.2% from the intact vesicles. This indicates the increased stability of the vesicles in Buffer C due to possibly the osmolarity being almost the same between the outside and inside of the vesicles. It is worth noting that the standard deviation of each experiments was shown to be wide which illustrates how the repeats of each samples can had varied fluorescence levels.

Table 1: Compositions of the buffers used and their osmolarity values.

Buffer	**Osmolarity**
Buffer A: 50 mM HEPES, 400 mM Potassium Glutamate, 200 mM Glucose, pH 7.6	1050 mOsm
Buffer B: 50 mM HEPES, 321.5 mM Potassium Glutamate, 200 mM Glucose, pH 7	893 mOsm
Buffer C: 50 mM HEPES, 188.5 mM Potassium Glutamate, 200 mM Glucose, 2% Glycerol, pH 7	893 mOsm
NEBExpress	893 mOsm

3.2.6 Optimising the FDEL Method

Although various papers have used the FDEL method following a specific protocol already mentioned in the introduction section, there were steps that needed adjusting for the purpose of this study. This was because this was the first time that a thermo-sensitive lipid formulation of a clinical composition had been attempted to be used to encapsulate an IVTT system to observe controlled heat responsive release. As this method has been used to encapsulate IVTT systems in the past but with only neutral lipids that did not have such high T_m as DPPC (42 ℃), we were unsure how to go about encapsulating the cargo without damaging the IVTT system with high temperatures, vortexing and premature expression. Furthermore, the TSV formulation of the membrane components have been used for encapsulating small drug molecules in the past rather than large molecules of proteins which are sensitive to heat and agitation as IVTT systems. Hence, this project involved a lot of exploratory research with many optimisation steps to improve the vesicle production steps, releasing the cargoes in a controlled way and ensuring the assay measurement was representative.

3.2.7 Testing Different Concentrations of Lipids

Following the Mansy paper[120] which made vesicles using POPC with the FDEL method to encapsulate a cell lysate extract IVTT system, they used concentration of the lipid at 47 mM. The lipid preparation involved forming a thin lipid film, adding water and vortexing. This mixture was emulsified using a homogeniser tip which was then extruded and lyophilised. A very similar set of steps were taken in this study as well to prepare the lipids but a sonication bath was used for the homogenisation step. Also, all the steps were carried out at 45 ℃, including the extrusion and the hydration.

IVTT was added to lyophilized lipids, which were presumed to be dried liposomes in each tube. When IVTT was added, the lipid became hydrated, allowing for varying amounts of macromolecular components to be encapsulated within the vesicles. To prevent protein expression on the outside of the vesicles, the un-encapsulated molecules were diluted by Buffer C with two portions of buffer to 1 portion of the IVTT added to the lipid, as demonstrated in Figure 3.4. The vesicles which were produced by the FDEL method used final vesicle lipid concentrations at around 47 mM in the literature but different concentrations of lipids were also explored in this study.

As well as optimising vesicle formation for TSV, POPC vesicles were also produced as they would be needed for control experiments for comparison with the TSVs. The optimal concentrations of lipids to form the POPC vesicles were also determined by testing different concentration from 105 mM to 5.2 mM. After the vesicles were produced, they were diluted as determined above and the vesicles were then incubated for 5 hours at 37 ℃, and CUG assay was carried out either in the presence or absence of the detergent Triton X-100 (**Figure *3.5***). The concentration at 46mM showed the best amount of encapsulation and release when detergent was added for these POPC vesicles. 105 mM of the lipid concentration gave inconclusive fluorescent readings and it was noticed that 105 mM was complicated to work with as 10 µL of IVTT was not enough to dissolve all the lipids, so the DPPC vesicles that were produced ranged in concentrations from 46 mM to 6 mM (Figure 3.5). It can be seen that encapsulation occurred in all concentrations but to varying degrees. The highest amount of fluorescence was observed at the concentration of 46 mM, indicating that this is the optimal concentration for encapsulation and subsequent release upon detergent addition. Lower concentrations resulted in less protein release when detergent was present. Encapsulation was observed to occur at concentrations ranging from 46 mM to 12 mM, with a decreasing

amount of encapsulation observed at lower concentrations. At a concentration of 6 mM, the encapsulation fell, and the higher fluorescence of CUG was not observed when Triton was added. This could possibly be due to a lower amount of lipid being available to provide enough vesicles to encapsulate the IVTT system for protein expression.

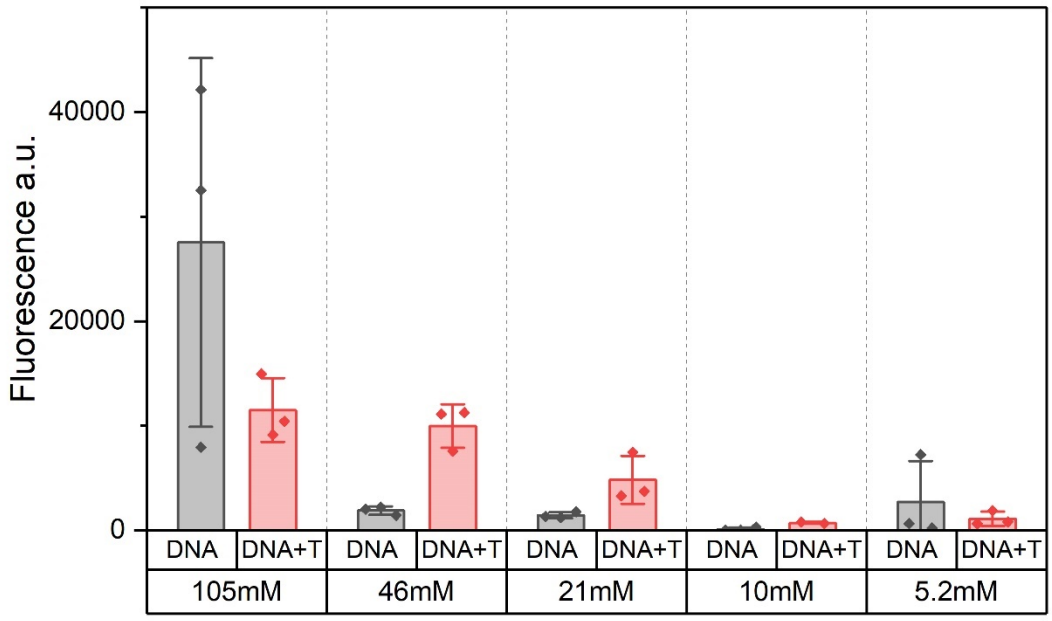

Figure 3.5: POPC vesicles consisting of different concentrations of lipids. These vesicles were made by FDEL method and diluted with Buffer C. 46mM and 21mM concentration gave reasonable encapsulation and release level. Each samples were compensated for the background and the leakage percentage calculated for the intact DNA vesicles. T=Triton X-100.

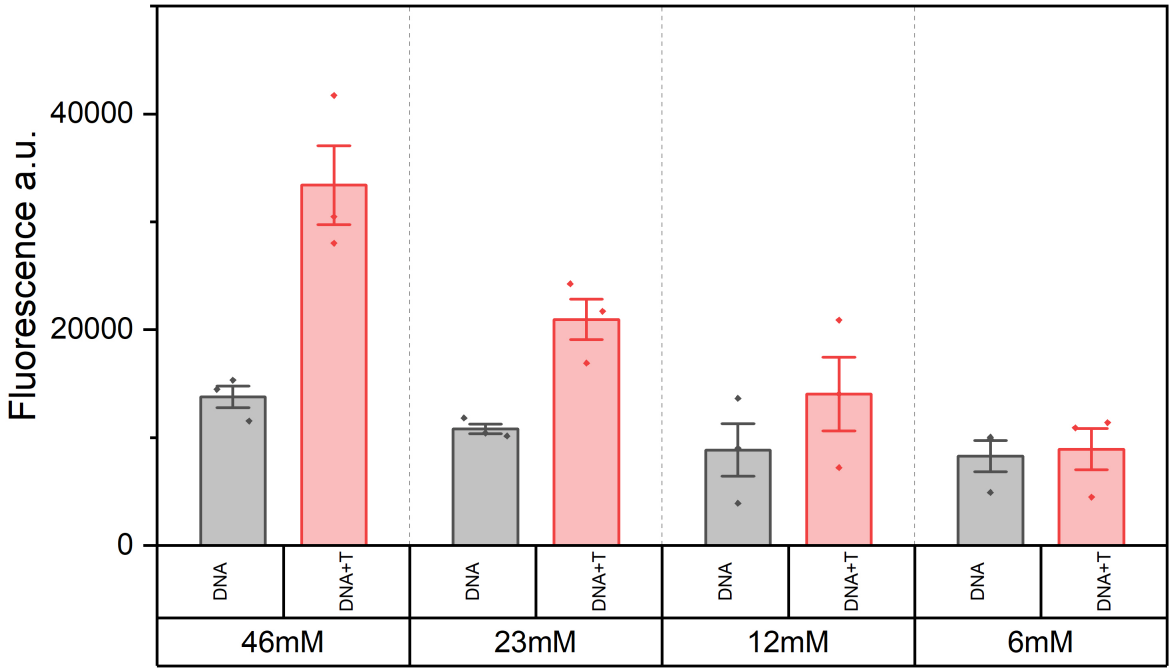

Figure* 3.6:* DPPC vesicles made of different concentrations of the lipid. These vesicles were made by FDEL method and diluted with Buffer C. Concentrations from 46 mM to 12 mM showed varying levels of encapsulation and release when Triton was added. 46 mMmshowed reasonable amount of encapsulation as there was a significant difference between the intact DNA vesicles and the release vesicles when Triton was added with leakage being the lowest in this group at 42%. T=Triton X-100.

3.2.8 Lysolipid and PEG in Thermosensitive Vesicles

Thermosensitive DPPC vesicles have been incorporated with lysolipid and PEG which have been used in clinical studies as it results in enhancement of release rate. The most clinically advanced thermosensitive vesicle formulation was composed of DPPC/MSPC/DSPE-PEG_{2000} which was tested in this chapter. As this work focussed on the encapsulation of cell extract system consisting of large macromolecular proteins, various parameters were tested; including the usage of another lysolipid MPPC, and testing different pore sizes for extrusion of the empty lipid vesicles before encapsulation. It is worth noting that throughout the study, it seemed the amount of encapsulation and hence release of the proteins varied from batch to batch or experiment to experiment. This indicated to us that the usage of the FDEL method

was not as consistent, as originally thought, in encapsulating an IVTT system. This was a challenge for the purpose of this thesis as it was important that the amount of IVTT components being encapsulated was high to ensure an overall high yield of the protein to achieve the aim of the goal-which was the production of enough proteins to be detectable to test the stimuli responsive lipids.

Vesicle formulation of DPPC:MPPC:DSPE-mPEG$_{2000}$ or DPPC:MSPC:DSPE-mPEG$_{2000}$ in the molar ratio of 86:10:4 was produced. The lipids were prepared as mentioned above by bath sonication, extrusion and lyophilisation as expected in the FDEL method. The NEBExpress system was encapsulated and released using Triton and CUG assay was conducted. First, MPPC was tested as it is also a well used lysolipid in encapsulating drug molecules within TSVs. Figure 3.7 shows this formulation provided some encapsulation at 46 mM. However, the fluorescence level of the released vesicles with Triton X-100 in the decreasing concentrations seemed to not be significantly different to the unreleased vesicles. On the other hand, the vesicle samples of the lipid mixture with MSPC showed indication of better encapsulation and hence better release (Figure 3.7b). When Triton was added to release the contents, the fluorescence for these samples were higher than the intact vesicles for concentrations 46 mM, 23 mM and 12 mM. Furthermore, the leakage was very low at only 10.5% for the 46 mM lipid concentration. This showed that MSPC with DPPC and PEG allowed a good amount of encapsulation as well as good stable vesicles compared to the MPPC formulation. So going forward, MSPC was used as the lysolipid in the mix to produce the thermosensitive vesicles.

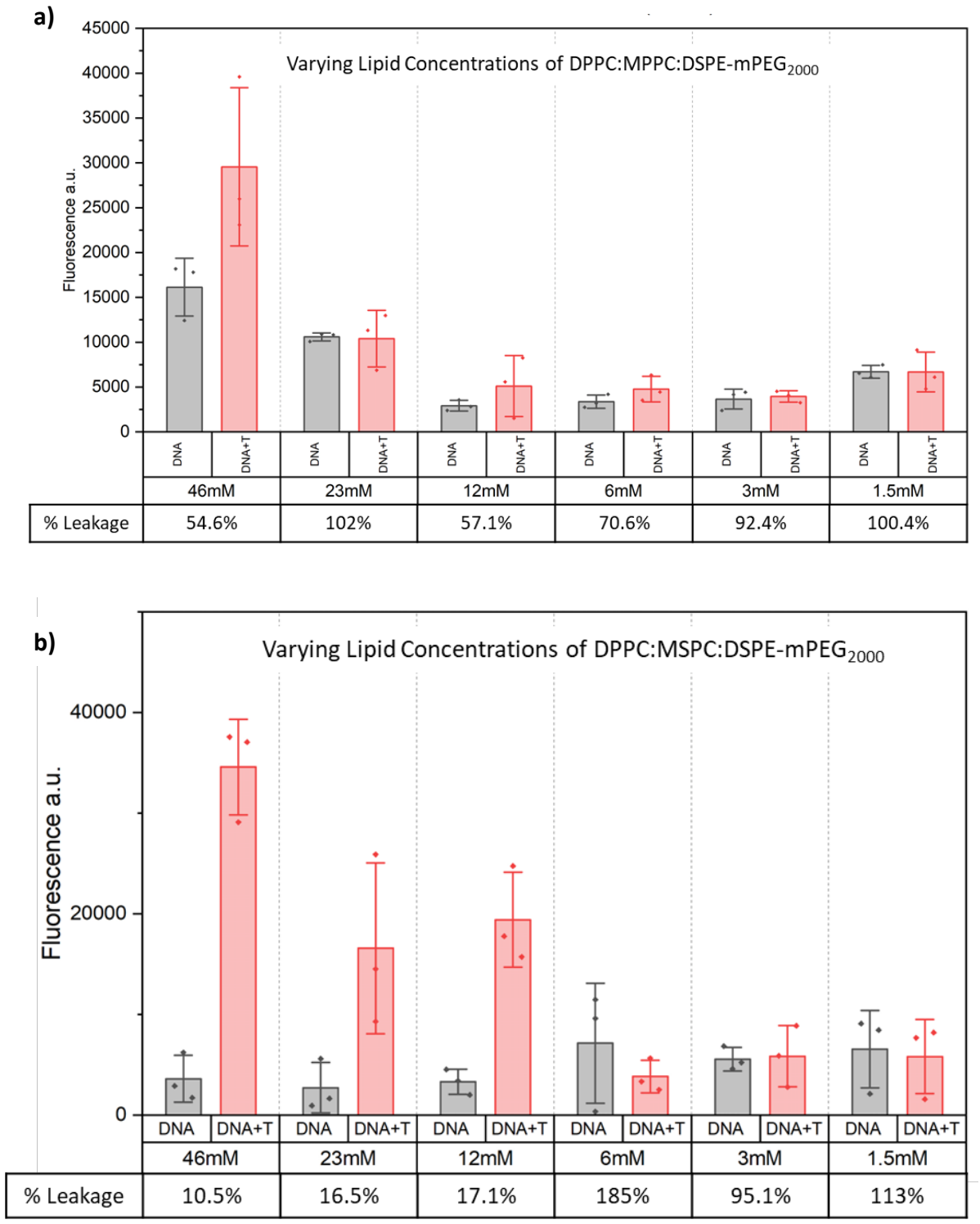

Figure 3.7: CUG assays of vesicles produced using the FDEL method encapsulating IVTT system with DNA of β-Gal which are either released with Triton X-100 or kept intact. (Above) Vesicles produced with lipid composition of DPPC:MPPC:PEG_{2000} in a molar ratio of 86:10:4. Very low encapsulation overall in all concentrations with high leakage. (Below) Vesicles produced with same molar ratio but the MPPC lysolipid was relaced with MSPC. Better encapsulation was observed as a high level of

release could be seen compared to the unreleased vesicles. The leakage was also observed to be low from the unreleased vesicles. T=Triton X-100.

3.2.9 Testing Extrusion Sizes

When preparing the TSV, the vesicles above were extruded with 0.4 µm sizes of extrusion filter membranes. In the next steps, different sizes were studied to understand if the sizes of the empty lipid vesicles produced with water and lyophilised before adding the IVTT system had an impact on the encapsulation and release of the proteins. Sizes of 0.2 µm, 1 µm and 12 µm were used to test the impact of different sizes of the empty dried liposomes on the final encapsulation of the vesicles. The different sizes of extrusion filter membranes with different lysolipid TSV compositions were produced which showed different amounts of encapsulation and hence different amount of release of proteins from the final vesicles that were produced (Figure 3.8). The MSPC vesicles with the varying membrane sizes gave better level of encapsulation and release than the MPPC vesicles. During freezing and drying, the lipid molecules become compact but with possible packing defects as the water molecules are not present to provide regular stability. During rehydration of the lyophilised vesicles, when heat is also applied, the added aqueous solution is able to enter through the defects especially as the lipids are in a liquid-crystalline phase where they are more fluid and can allow movements of large macromolecular molecules. It is possible, this is when the lysolipids and the PEG can stabilise these temporary lipid gaps when the empty liposomes get filled with the contents, which can then become closed as the lipid bilayer becomes a gel-crystalline phase when the samples are chilled on ice.

It was observed that the smaller the extrusion membrane pores that were used, it appeared the better the stability and encapsulation by the vesicles as a low fluorescence level was seen on the intact vesicles, encapsulating IVTT system with DNA, whilst high fluorescence is seen on the released vesicles, indicating a good level of encapsulation. This indicated that the specific size of the extrusion membrane used to prepare lipids before lyophilisation did impact the overall encapsulation of molecules. Extrusion membrane pore sizes greater than 0.2 µm will lead to the formation of multilamellar vesicles. This could mean that the use of 1 µm and 12 µm sized membrane results in multilamellar vesicles which could be difficult to fill with the IVTT components as there are more layers to get through in the vesicles. But using the 0.2 µm sized membrane possibly results in more unilamellar vesicles which might be easier to fill as the IVTT components have only one layer to pass through.

Hence, the subsequent vesicles which were produced used a lipid mix consisting of MSPC as the lysolipid and the lipids were prepared with a 0.2 µm sized filter membrane for extrusion.

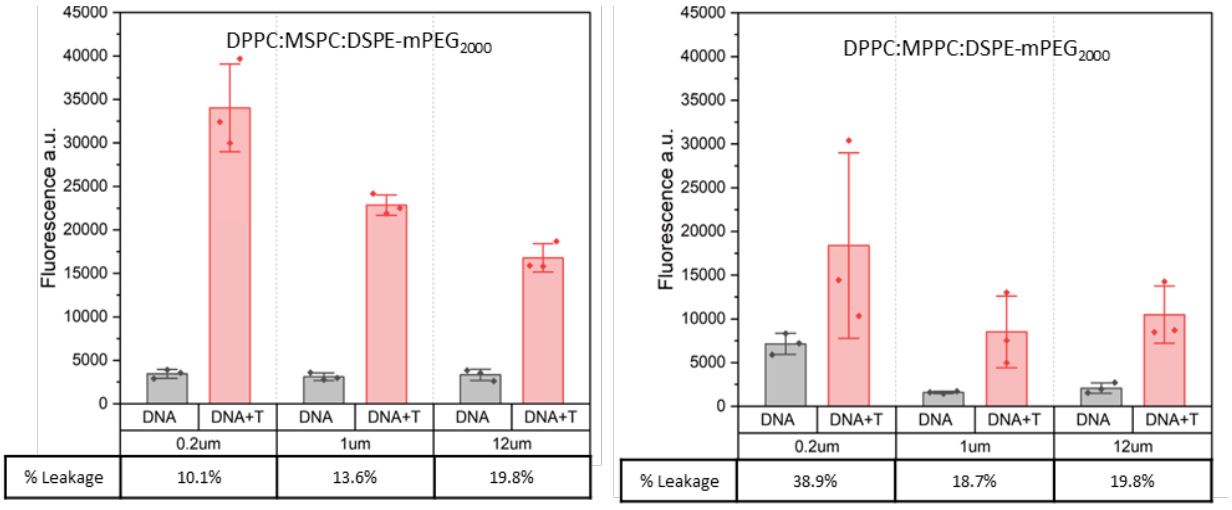

Figure 3.8: TSVs produced using FDEL method with lysolipids MSPC (left) and MPPC (right). Vesicles were extruded with different sizes of filter membranes. MSPC TSVs gave overall better encapsulation and release of the IVTT expressed β-Gal from within the TSVs. The smaller size of the filter membrane for MSPC based TSV also showed the lowest leakage level. T=Triton X-100.

3.2.10 Heating the TSVs

The next steps was to test controlled heat induced release from the vesicles produced with the FDEL method. Vesicles were produced with the optimised MSPC lysolipid with DPPC and PEG with the mentioned composition of 86:10:4 molar ratio (Figure 3.9). The vesicles were then heated for either 10 minutes or 20 minutes to 43 ℃ to test the release of the encapsulated cargo and compare this value with vesicles released using Triton. The heating experiments showed that the TSVs with MSPC as the lysolipid had potential for controlled release upon heating to hyperthermia temperatures. Although the level of release is shown to be low, if the incubation temperature was to be increased, this could increase the release level. This is the first time showing controlled release of in-situ synthesised proteins from thermosensitive vesicles. When the POPC vesicles were heated in a similar manner, no increased release was seen compared the control samples, further highlighting the potential of the TSV for usage in heat controlled protein release. The amount of leakage from the unaffected vesicles were only at around 14% whilst the vesicles heated for 10 minutes leaked to 34.9% and when the heating time increased to 20 minutes, the leakage was seen to be higher at 42.7%. This showed that the vesicles were being affected by the heat and the membrane was undergoing changes in its structure when heated above its T_m causing pore formation and substances to move across the membrane bilayer. It is possible that the β-Gal is moving across the pores and into the outer solution leading to the slight increase in fluorescence.

One thing to notice in these experiments was that the encapsulation and hence the level of release of the β-Gal proteins and fluorescence level was a lot lower than previous samples. As further experiments were repeated, the level of encapsulation remained low, which is why

a significant portion of time was given to identifying issues that were causing low encapsulation.

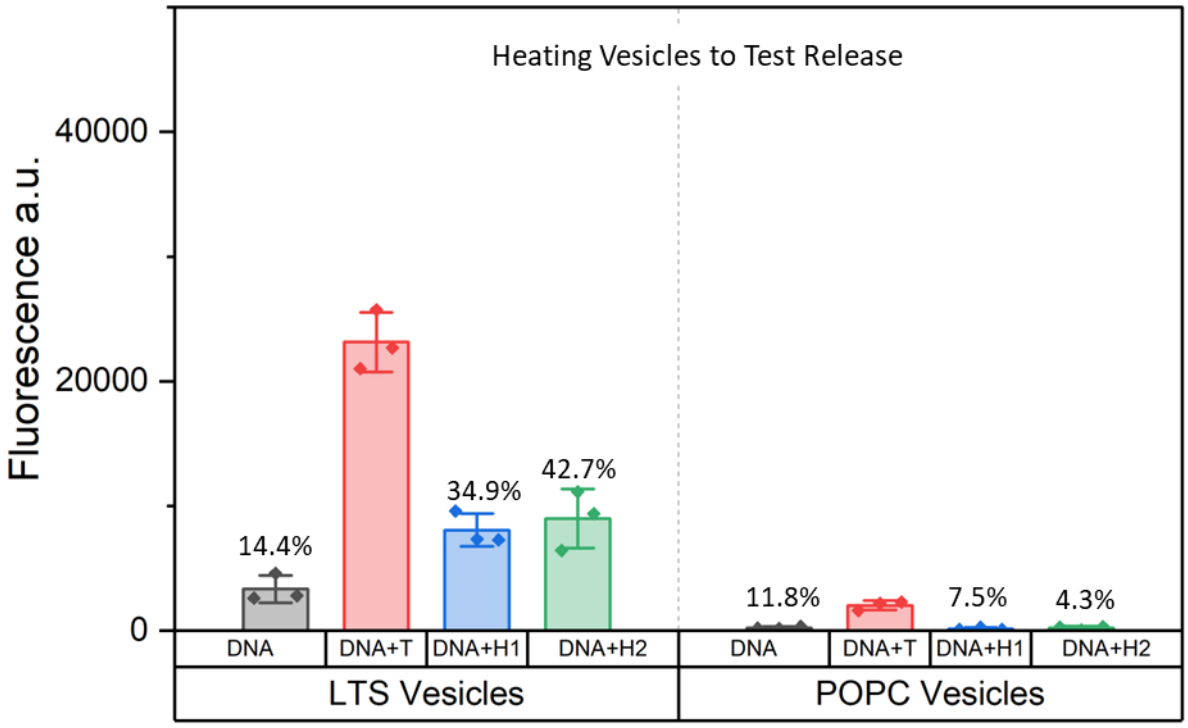

Figure 3.9: TSVs produced with FDEL method and heated for 10 minutes (H1) or 20 minutes (H2). Higher percentage of leakage observed when the TSVs were heated longer at 43 ℃. POPV vesicles also heated (right) but no increase in leakage observed.

3.2.11 Challenges with the FDEL Method

During the usage of the FDEL method to produce vesicles with the IVTT system, there was noticeable challenges that were faced. Throughout this research project, the level of encapsulation and leakage was not always favourable. It was observed that the experiment above was repeatable several times, but it was not always successful. The issues that was observed was that the encapsulation was significantly lower at times and the leakage from

the vesicles was so high that the fluorescence levels that had been observed were not always reachable and the unreleased vesicle levels was the same as the Triton treated vesicles. This necessitated the allocation of a significant amount of time to address these challenges.

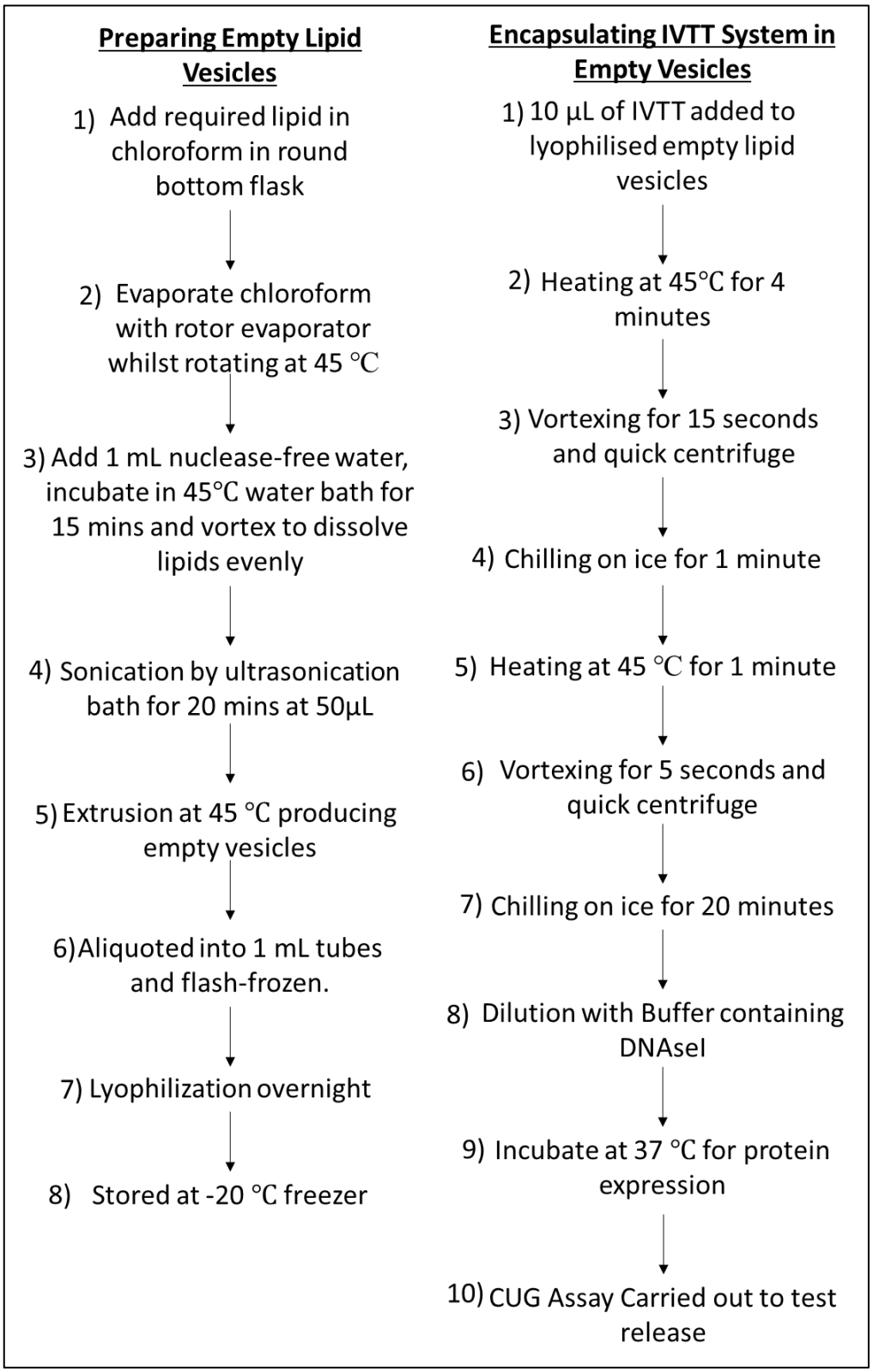

Figure 3.10: Steps in the FDEL method. Left; steps to prepare empty vesicles with thermosensitive lipid composition. Right; steps to encapsulate IVTT system within the empty vesicles. Conditions of the various steps were altered to overcome encapsulation challenges.

The identification of the underlying issues and experimentation with various techniques to restore the vesicles' ability to encapsulate the IVTT system and maintain stability proved to be a formidable task. This was primarily due to the inability to ascertain the cause of the decreased encapsulation and such low level of fluorescence. Troubleshooting efforts involved modifying various conditions during the lipid preparation and vesicle production stages. Figure 3.10 depicts the various steps in the vesicle preparation method. The literature has established that the method employed for the formation of the thin lipid layer significantly affects the characteristics of the resulting encapsulating vesicles[158]. As such, several modifications were made in the various steps towards making the empty vesicles in order to investigate the impact of these alterations.

In step 1, new stocks of lipids and chloroform were used (Figure 3.11a) which showed that the use of new lipids and new chloroform stocks slightly improved the encapsulation compared to the use of old lipid and old chloroform stocks. But the leakage from the vesicles were still very high with the standard deviations of the intact DNA vesicles and released DNA vesicles overlapping with the IVTT vesicles without the DNA, although the samples using new chloroform and new lipid stocks did show slightly better encapsulation and release.

In Step 2, the amount of time that the lipids were left to rotor evaporate was usually 2 hours, but a longer and shorter time was also tried to observe any impact on the encapsulation. In Step 3 where the lipid is allowed to dissolve in water by incubating in a heated water bath at 45 ℃ and vortexed, different factors were changed in this step which included trying different

sources of water, increasing the incubation time at 45 ℃ and increasing vortexing-all of which did not show any difference in the encapsulation capability from Figure 3.11b.

The next parameters that were tested were the use of two sonication techniques to homogenise the lipids in the water into smaller sizes and testing two different drying techniques. An ultrasonic bath had been used to homogenise the lipids in the methods. To test a different sonication technique, a probe-type ultrasonication tip was used. In step 7 the lipids were dried using the usual lyophiliser as well as a Speed-Vac concentrator overnight. Figure 3.11b shows that the first three conditions did not show any encapsulation. However, the fourth condition of using the ultrasonic bath and lyophiliser showed some encapsulation confirming the same results as the previous Figure 3.11a, indicating that the ultrasonication bath to homogenise the lipids and using a lyophiliser to dry the lipids is better for empty vesicle preparations than the ultrasonic probe and speed-vac. In step 8, the amount of time the empty vesicles were stored in the -20 ℃ freezer was also altered but this did not impact the encapsulation and so the results for these experiments are not included here.

The technical changes that were made, did not impact the final encapsulation and stability of the vesicles. Instead, the original method showed formation of vesicles but the leakage was still very high (around 77-78%) and the encapsulation very low (as the overall fluorescence was far below previous experiments.

As the steps in the preparation of the empty vesicles did not result in improved encapsulation, it was decided that the encapsulating steps after adding IVTT would be changed. The timings of the steps 2 to 4 of heating, vortexing and chilling were altered to times that were below and above the timings mentioned in Figure 3.10. These are the steps when the lipid bilayers undergo transition from the solid ordered phase to the liquid disordered phase, allowing for

a)

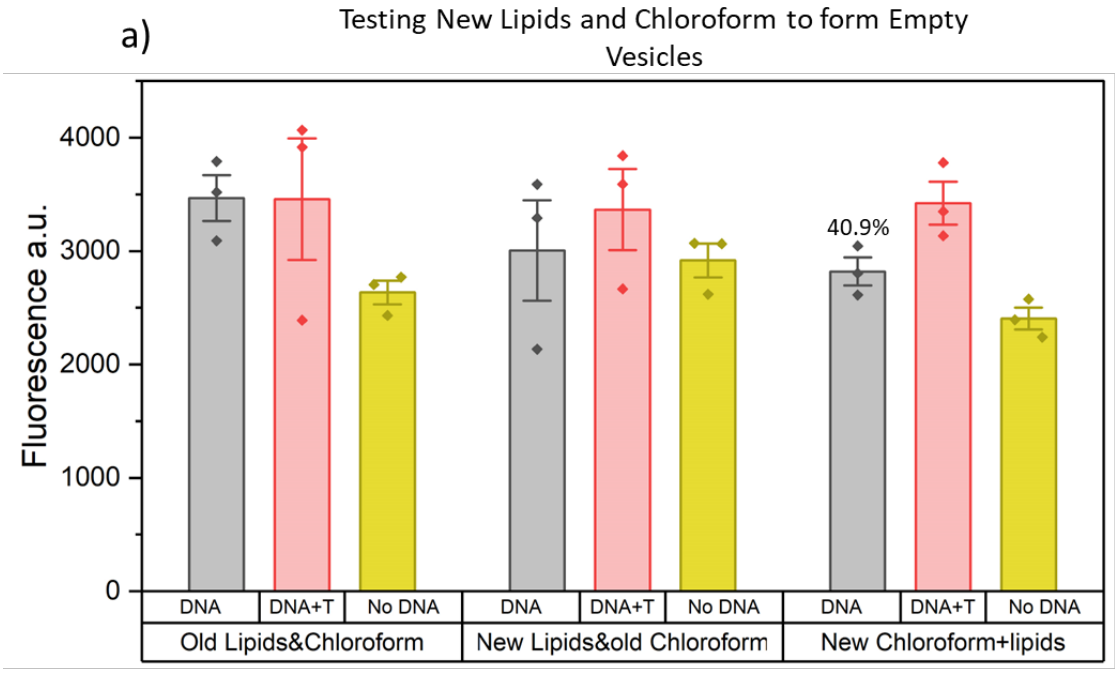
Testing New Lipids and Chloroform to form Empty Vesicles
Fluorescence a.u.
4000
3000
2000
1000
0
40.9%
DNA
DNA+T
No DNA
Old Lipids&Chloroform
New Lipids&old Chloroform
New Chloroform+lipids

b)

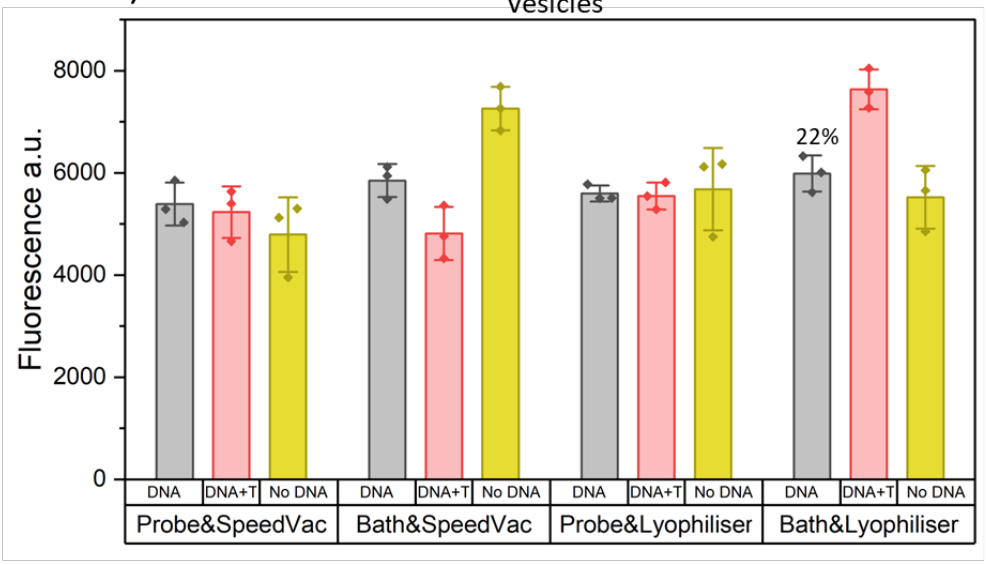
Testing Sonication and Drying Techniques to form Empty Vesicles
Fluorescence a.u.
8000
6000
4000
2000
0
22%
DNA
DNA+T
No DNA
Probe&SpeedVac
Bath&SpeedVac
Probe&Lyophiliser
Bath&Lyophiliser

c)

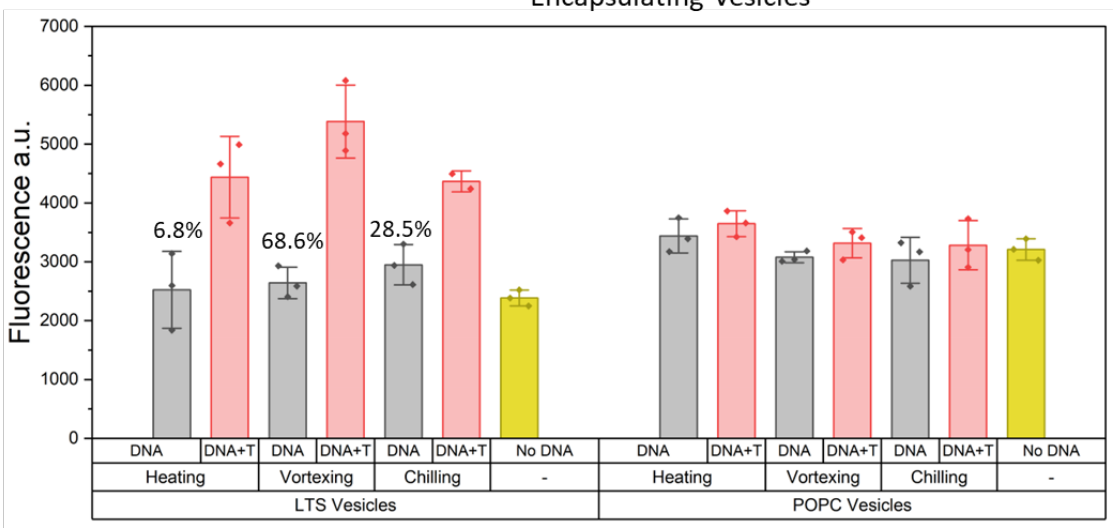
Testing Timings of Heating, Vortexing and cooling on Encapsulating Vesicles
Fluorescence a.u.
7000
6000
5000
4000
3000
2000
1000
0
6.8%
68.6%
28.5%
DNA
DNA+T
No DNA
Heating
Vortexing
Chilling
-
LTS Vesicles
POPC Vesicles

Figure 3.11: Changing various conditions of the FDEL method to improve encapsulation. A) New lipid and chloroform stocks were tested, B) different method of sonication and drying the empty vesicles were tested, C) The time taken to heat the lipid with IVTT mix, vortexing and cooling periods were increased to 5 minutes, 10 seconds and 30 minutes respectively for these samples.

the temporary pores to form and allow the IVTT system to transport across the membrane into the vesicular structures. In step 2, the heating of the vesicles were changed from 4 minutes to 1, 2, 3 and 5 minutes. The vortexing time in step 3 was also changed from 15 seconds to 10, 20 and 30 seconds. The chilling time on step 4 was changed from 1 minute to 30 seconds, 2 minutes and 3 minutes. In step 7, the timing for the incubation on ice was increased to 30 minutes from 20 minutes. All of these changes, however, showed similar pattern of low encapsulation and therefore low level of release (Figure 3.11c). When they FDEL method was used to produce vesicles with POPC at this stage, encapsulation was not observed for any samples even when various conditions were changed (Figure 3.11c-right). It was difficult come to a conclusive reason as to why the encapsulation had completely stopped for POPC lipids and the LTS vesicles were overall low.

As the encapsulation was not improving, one avenue that was tested was to produce and use a bacterial lysate extract without background β-Gal proteins. This was thought to perhaps bring down the background fluorescence and provide a better idea of encapsulation efficiency. Figure 20a shows that the production of the bacterial lysate extracts were successful. There were two bacterial extract that were produced; BL21 DE3 E.coli lysate extract and ΔBL21 DE3 lysate extract which did not have β-Gal gene in the bacterial genome. Fluorescence was observed in the presence of β-Gal in the samples of BL21 DE3 extracts with both DNA and no DNA samples. But for ΔBL21 DE3 lysate extract, fluorescence was absent in the sample without DNA indicating the absence of background β-Gal protein.

Encapsulation of the thermosensitive vesicles were attempted (Figure 20b) using the new lysate which showed better level of encapsulation compared to the last sets of difficulties with the NEBExpress system. However, leakage was still observed from the encapsulated vesicles at 37%. This further demonstrated that this FDEL method was quite feeble and sensitive to changes in the conditions and equipment used which meant vesicle production and encapsulation of the IVTT system was not consistent especially when using such small volumes (10 µL).

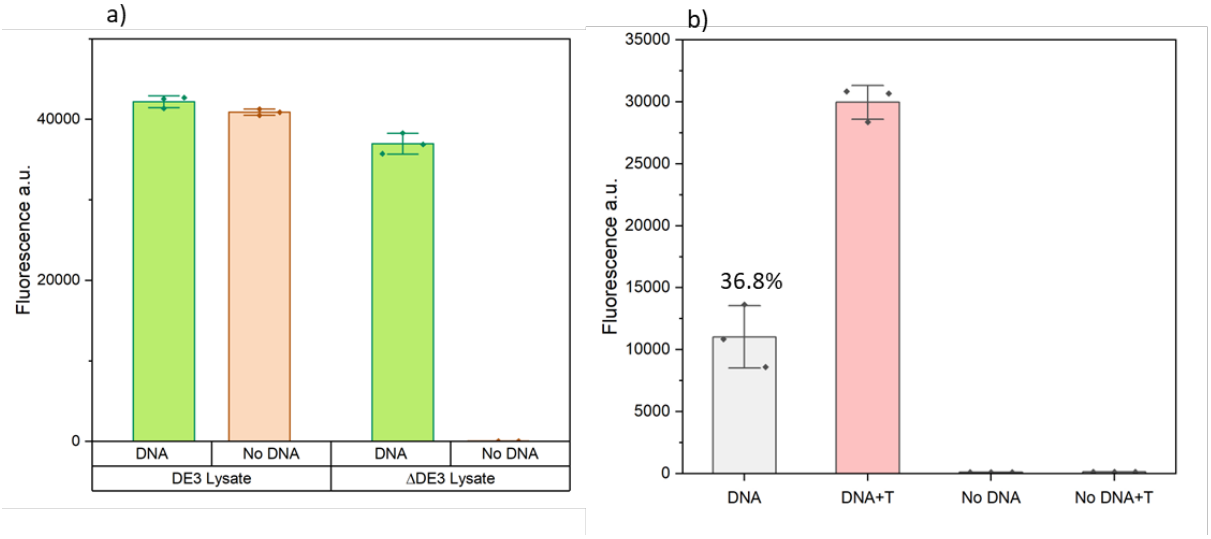

Figure 3.12: a) BL21DE3 lysate extracts were produced and CUG assay carried out on the presence or absence of β-Gal DNA. DE3 lysate both of samples with and without β-Gal DNA gave large fluorescence when CUG was added. But for ΔBL21 DE3 lysate extract, no background fluorescence was present in the none DNA sample when CUG was added, indicating the absence of background β-Gal from the extract. B) Vesicles produced using the ΔBL21 DE3 lysate extract which eliminated the background fluorescence from the sample as shown. Encapsulation was successful but the leakage was still high as DNA samples of vesicles without Triton X-100 had 36.8% leakage. T=Triton X-100.

3.3 Conclusion

This chapter explored various methods aimed at generating thermosensitive vesicles (TSVs) capable of encapsulating an IVTT system. The Freeze-Dried Empty Liposomes (FDEL) technique, a hydration-based method, was our primary tool for producing the vesicles. We found that other techniques weren't suitable for using thermo-sensitive lipids in encapsulating an IVTT system. Initially, we employed the inverted emulsion method to create vesicles composed of DPPC in varying ratios with Egg PC. The primary goal was to test this lipid blend's capability to form vesicles and trigger the release of its contents upon heating. Fluorescent imaging revealed a decrease in the number of vesicles post-heat treatment. However, a concurrent increase in the DPPC molar ratio resulted in diminished vesicle production using this method. As a result, we shifted our focus to explore the potential of the FDEL technique.

Next, we demonstrated that thermosensitive vesicles could be produced and showed a release of β-Gal upon heating. Despite this accomplishment, the optimization of this method presented several challenges. Our main focus was on ensuring consistent encapsulation and controlled release, which wasn't always achieved. As a result, we undertook multiple rounds of testing and optimisation under various conditions to enhance encapsulation efficiency, an endeavour that remained challenging.

Finally, it's important to note that hydration methods typically yield vesicles capable of encapsulating small molecules and are suitable for working with larger volumes. Therefore, optimising the use of the ΔLacZ DE3 lysate extract or OnePot PURE system[159] for the large-scale production of TSVs, may be the key to achieving more consistent and high-yield TSV production.

Chapter 4 - Increasing Yield of Cell-free Protein Synthesis Using Short Additional 5' Sequences

4.1 Introduction

We explored the potential to increase the yield of protein production in SCs. It was identified that adding specific nucleotide sequences at the beginning of the open reading frame (ORF), increased the yield of protein production. The sequences that were used were known as cell-penetrating peptides (CPPs) which are short peptides of less than 40 amino acids that can cross cell membranes and transport cargoes of genes, proteins, as well as nanoparticles[160]. Although the CPPs were intended to be used for other purposes, it was identified that the presence of the CPP nucleotide sequence at the beginning of a fluorescent protein gene, impacted the yield of a yellow fluorescent protein, mVenus. Therefore, we decided to study this phenomena further to look into the potential of using these short sequences to increase the yield of a mammalian codon optimised and E.coli codon optimised mVenus and mCherry gene in a PURExpress system. The success of using short sequences at the beginning of a gene sequence would mean that the yield of protein could be observed easily.

Although the main principles of gene expression have been uncovered, there are still additional factors that require understanding. This is important as the designing of synthetic proteins require an understanding of various contributing elements during transcription, mRNA stability and translation. An identical protein can have a different codon sequences (CDS) where the final amino acid sequence might be the same but can influence translation efficiency and result in different protein production levels, different folding abilities as well as

affecting the final function[161,162]. It has been observed that a certain organism uses specific codons more frequently than another codon for its species, possibly due to an abundance of a the corresponding tRNA[163], which has led to the use of Codon Adaptation Index (CAI) [164] where the bias of using a specific codon leads to a more efficient translation and therefore a high CAI. Recent studies have also shown that CAI is not the main determining factor for high protein production[165–167]. The weight of various components on protein production can vary depending on the type of organism, the environment, the tissue or even the position of the codon on the ORF[168,169]. It appears that many questions pertaining to the role of codons still remain unanswered and only using CAI of codons would be an oversimplification to estimate efficiency in protein translation. It is important to understand the usage of specific codons as this could be significant to understand the translation of mRNA into proteins. Furthermore, having precise control of transcription and translation efficiency is important for the field of synthetic biology to allow greater predictability during the process of protein production.

The amount of protein produced are dependent on the efficiency of transcription, the stability of the mRNA, the efficiency of mRNA translation and the final stability of the protein product. The UTR consists of a series of DNA sequences which are important for assembling the transcription machinery. The RNA polymerase (RNAP) binds to the promoter site of the DNA, which contain conserved elements, to convert the UTRs and ORF into mRNA. The initiation of translation of mRNA to polypeptide chains is considered to be one of the most important steps that contributes to the efficiency of the overall translation. In prokaryotes, which are the system of focus in this thesis, the 30S ribosomal subunit recognises a RBS on the 5' UTR (Figure 4.1). The RBS has a Shine Dalgarno (SD) sequence consisting of GGAGGU on the mRNA which interacts with the anti-SD sequence on the 16s rRNA of the 30S ribosomal subunit[20]. Studies have shown that high secondary mRNA structure around the RBS and SD site can

severely slow down the initiation of translation[165,166,170]. However, there are also mRNA sequences in large numbers of bacteria and archaea that are lacking the SD sequence[171] and very little is known about the translation initiation mechanism for these.

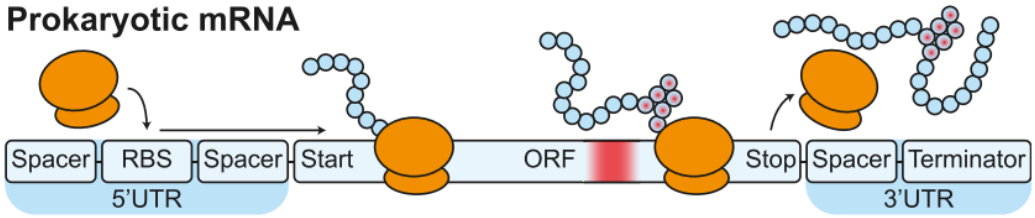

Figure 4.1: Schematic overview of prokaryotic mRNA being translated by ribosomes (orange). RBS, ribosome binding site; ORF, open reading frame; 50/30 UTR, 50/30 untranslated region. The co-translational folding phenomenon is indicated with a red gradient in the mRNA and the associated amino acids. Figure repurposed from T. Nieuwkoop et al, 2020[172].

During gene expression, it has been demonstrated that the mRNA sequences which are at the vicinity of the start codon to the gene, contains information for ribosome recognition and hence has impact on the rate and yield of protein production. This is evident as computer analysis has shown significant non-randomness around the start codon of genes[173,174]. The binding affinity of the RNAPs and other transcription factors with the promoter sequence also plays a role in the mRNA synthesis rate[175]. The non-coding regions such as the promoters and untranslated regions (UTRs) also have regulatory functions on the overall gene expression which can be impacted by the strength of the promoter sequence binding to the RNAP[176].

There have been studies revealing the importance of the first few codons of a gene having major effects on recombinant protein production in E. coli[177,178]. The main suggestion for this

is the role of mRNA secondary structures around the ribosome binding site (RBS) and start codon[166,170,179,180]. A recent study has seen that the predicted folding energy of the mRNA around the start codon correlated with protein production due to the possibility of the RBS being available for translation initiation[181]. In fact this study has shown that a window covering codons 2-8 can be used to accurately predict production of the monomeric Red Fluorescent Protein (mRFP) and the codons later in the sequence were not important to protein production. Furthermore, most predictive bases were also found 5-10 bases before the start codon[181,182]. This is because the presence of secondary or tertiary structure in the RBS can shield the important SD sequence and the initiation codon. Therefore, it has been shown that masking these regions in the RBS has important regulations in gene expression in bacteria[177,183,184].

A stretch of other nucleotide sequences have shown to enhance the binding affinity of the ribosomes to the mRNA. A ribosomal binding site derived from T7 bacteriophage gene 10 leader sequence (T7-g10L) was identified to aid in overexpression of foreign genes in E. coli[185,186]. The g10L sequence was able to stimulate overexpression of proteins in E.coli for LacZ[186] and Beta-lactamase[187]. The sequence consists of an epsilon motif UUAACUUUA which is a pyrimidine rich sequence, present in the T7-g10L sequence that has been seen to invoke translation initiation even in the absence of the shine Dalgarno sequence[188]. Therefore, the control template plasmid used in this study, initially from the PURExpress kit, contains the T7-g10L sequence consisting of the T7 promoter, epsilon and SD sequence, followed by the start codon respectively. This sequence is derived from the upstream sequence of the native viral T7-g10L capsid protein gene which has shown that the first series of bases from the T7-g10L gene, after the start codon, also increases protein expression[187]. Therefore, we add the first 8 codons from the T7-g10L gene to the N-terminus of mVenus and mCherry genes and

measured its expression level through fluorescence and protein gels. Although this has been shown before by A.Venancio-marques et al[189] and J.Smith et al[144], in this thesis we show other short sequences placed downstream of the start codon, and observe their impact on the production of the fluorescent proteins. These results might provide an understanding of the impact of short sequences at the 5' end of the GOI mRNA sequence and their potential use to increase protein yields.

4.2 Results

The aim of this chapter was to increase the yield of proteins that are produced in IVTT systems which would allow a higher yield of proteins in the SCs. One of the methods identified was by adding short strands of specific sequences at the 5' end of the GOI right after the AUG start codon. Whilst exploring N-terminal CPP sequences for alternative purposes, we noticed that certain CPP sequences at the N-terminus, increased the overall protein yield whilst others decreased protein yield (Figure 4.2). We therefore, decided to use mVenus and mCherry proteins to test this. Two versions of the codons were where the genes were either mammalian codon optimised or E.coli codon optimised. The mammalian codon optimised mVenus had been originally used in various studies by the Booth group[7], but we identified that this same protein could have its yield increased with the presence of certain N-terminus/5' short additional sequences. This was an important revelation as this means that a simple addition of short sequence at the beginning of a gene can be added to increase yield instead of needing to modify multiple locations of a protein or adding specific features or optimising proteins expression and purifications steps in order to ensure a large quantity of proteins were available to use.

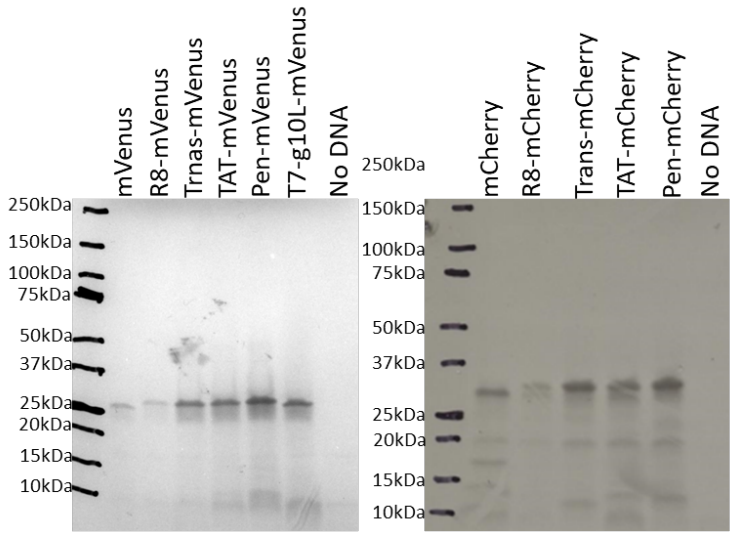

Figure 4.2: Radiolabelled proteins shown on SDS-PAGE gels. CPP sequences, R8, Transportan (Trans), TAT, Penetratin (Pen) and T7-g10L, were cloned into the N-terminus of mammalian codon optimised mVenus and mCherry genes. The genes were expressed in PURExpress IVTT system with radioactive methionine. mV expected size= 26.9 kDa, mC expected size= 28 kDa

4.2.1 Testing mVenus and mCherry Expression

Two versions of mVenus and mCherry were prepared so that the gene sequences were optimised to contain mammalian optimised codons (Mam-mV or Mam-mC) or E.coli optimised codons (Eco-mV or Eco-mC).

In the context of our study, the gene sequences optimized for mammalian expression and E. coli expression were subjected to expression analysis in PURExpress systems over a span of 6 hours. To monitor the progress of the reactions, samples of 0.5 µL from the IVTT mix were collected at hourly intervals. The collected samples were then analysed for fluorescence in a 40 µL Tris Buffer solution using a plate reader (Figure 4.3).

Regarding mVenus expression, a notable observation was made, indicating significantly higher protein expression levels with Eco-mV in comparison to Mam-mV. This distinction was

apparent as early as 2 hours, with the fluorescence level of Eco-mV being approximately 4.4 times higher than the mammalian-optimized mVenus. By the 3-hour mark, the fluorescence of Mam-mV appeared to reach a plateau, while Eco-mV continued to exhibit an upward trend until the 5-hour mark, ultimately reaching a fluorescence level 5 times higher than the mammalian-optimized gene. Subsequently, a similar experiment was conducted with mCherry, resulting in distinct fluorescence behaviour. At 2 hours, Eco-mC seemed to achieve maximum fluorescence, whereas Mam-mC demonstrated a continuous increase until levelling off at the 4-hour mark. It is noteworthy that both mCherry genes eventually reached the same level of maximum fluorescence, despite the slightly higher rate of reaction observed with Eco-mC. Notably, a decline in fluorescence was observed during the final hour, possibly suggesting that the mC protein required more than 1 hour to achieve its maximum fluorescence due to an extended folding time.

In summary, our findings indicate that the mCherry protein exhibits high fluorescence even at the early stages of expression and likely possessed a prolonged folding time, which could significantly impact the overall analysis of results.

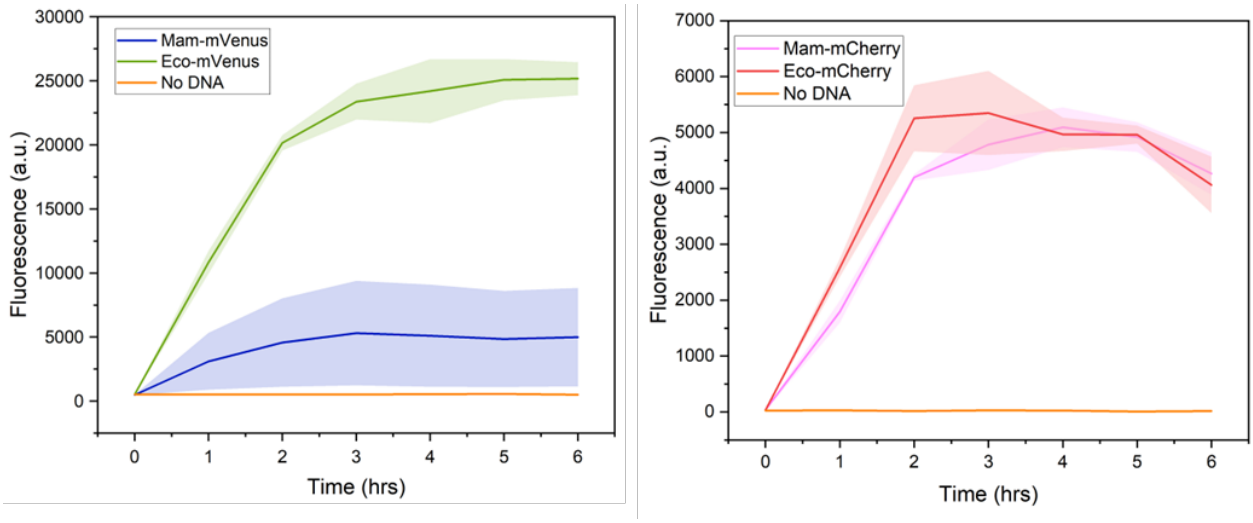

Figure 4.3: Fluorescent proteins mVenus and mCherry genes with mammalian or E.coli optimised codons were expressed in PURExpress IVTT system and the fluorescence was measured over 6 hours.

4.2.2 T7-g10L Ribosome Binding Site

The translation efficiency of recombinant proteins are not always efficient, even with the presence of a SD sequence upstream of a gene. A RBS that was found on the upstream region of the gene 10 of the phage T7 (T7-g10L) has been used to increase protein yield[185]. The g10 gene codes for the coat protein of the highly virulent T7 phage after infection which produces thousands of phages within 15 minutes in E.coli[190]. The mRNA of this protein is highly expressed in E.coli which is important for the T7 phage production which means the expression systems have evolved to have maximum efficiency. Therefore, it is the most abundantly expressed T7 gene and therefore, its RBS is used to express heterologous genes of high quantity[185]. The T7 mRNA transcripts are far more stable than E.coli mRNA, possibly due to the 5' hairpin structure before the SD sequence which has a connection to the degradation rate of the mRNA[191]. Many genes have evolved to contain stabilising elements in the mRNA to counter nuclease attack by 3'-5' exoribonucleases[192] or endoribonucleases[193]. Therefore, there are specific sequences which are able to fold into a stem-loop at the 3' end of the gene which allows protection of the mRNA and decrease in decay[194]. The 5'-end has been shown to stabilise mRNA in eukaryotic systems as well[195] and the homology region where 16s rRNA binds on the mRNA tend to be at a region which lacks a secondary structure. The plasmid construct in the PURExpress kit (pPURE) consists of some parts of the T7-g10L RBS in the 5' UTR upstream of the GOI (Figure 4.4). The T7-g10L sequence contributes to the stem loop region due to its high A/U sequences of the mRNA which has been shown to not be the main factor that contributes to the high translation efficiency.

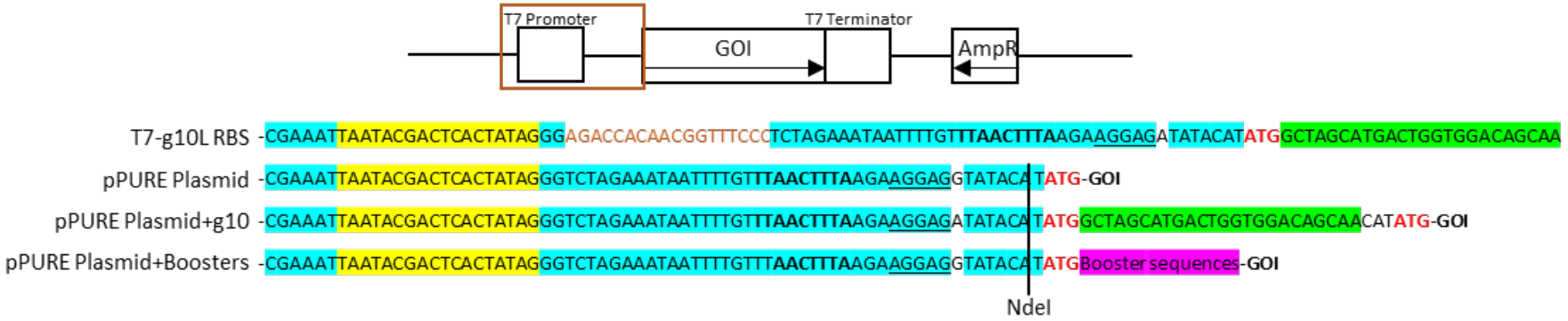

Figure 4.4: Plasmid vector of PURExpress system which has been used to studying the effect of different short sequences around the start codon site on protein expression level of the GOI. Transcription originates from a T7 promoter site (yellow). The expression of the fluorescent proteins mVenus and mCherry is a simple way to measure translation efficiency. The first sequence is found on the RBS of the phage T7-gene 10 which is shown here to compare this sequence with the RBS region of the pPURE plasmid found in the PURExpress system. The blue section shows the sequences that are homologous to the T7-g10L RBS. The third sequence shows the additional short sequence from the T7 phage gene-10 added after the start codon, followed by another start codon before a GOI is added. The fourth sequence shows the location where the additional booster sequences are added which is after the start codon (purple). The NdeI site permitted digestion around the start codon site for rapid homologous recombination to insert short sequences after the start codon. The selection for the correct plasmid was provided by the ampicillin resistant gene (AmpR). The plasmid shown is not to scale and has been linearised for this figure.

Instead the specific sequence of the mRNA was important rather than only the stem-loop. This is because a perfect 9-base homology, an epsilon sequence, with the complementary sequence of the 16S rRNA was present[186] which was important to enhance translation dramatically. It has been also demonstrated that placing the same epsilon sequence early within the coding region of a LacZ gene also increased expression[186] which showed that this sequence can be positioned either upstream or downstream of the start codon.

In this study we used the pPURE plasmid which contained the second sequence on Figure 4.4 before the start codon to express the proteins in this thesis. Another sequence was prepared in the pPURE plasmid which contained additional sequences (3rd sequence in Figure 4.4-green) from the first 8 codons of the T7 phage gene-10 (g10) which was placed after the start codon as designed by A. Venacio-marques et al in 2012[187] to increase expression of β-lactamase enzyme. We were able to show that the addition of this g10 sequence was able to increase the protein expression level of mVenus compared to just using the T7-g10L RBS by a factor of 1.8 for mammalian coded mVenus and a factor 5 in the E.coli encoded mVenus (Table 3). However, different pattern of expression were seen with mCherry where the addition of all short sequences before the mCherry gene decreased the expression of this protein, or remained the same.

4.2.3 Exploring CPPs as "Booster Sequences"

Cell-Penetrating Peptides (CPPs), alternatively known as Protein Transduction Domains (PTDs), are concise amino acid sequences capable of facilitating the passage of various molecular cargos across cellular membranes[196]. This ability positions them as valuable delivery vectors, especially for therapeutic molecules that are inherently unable to traverse cellular membranes due to their size, charge, or hydrophilic nature. The types of CPP

sequences used in this thesis are Penetratin (Pen), TAT, Transportan (Trans), and Polyarginine 8 (R8). Some of these short sequences were observed to produce higher production of the mVenus gene.

Penetratin, a cationic CPP derived from the Antennapedia protein in Drosophila, facilitates cargo delivery by interacting with the negatively charged cell membrane, leading to internalisation of the peptide and its cargo[197]. TAT, another cationic CPP originating from the HIV-1 virus, operates in a similar manner[198]. Transportan, an amphipathic CPP, is a chimera of the neuropeptide galanin and a sequence from the wasp venom peptide mastoparan[199]. It possesses both hydrophilic and hydrophobic regions, forming structures that facilitate interaction with the cellular membrane, leading to peptide internalisation. Polyarginine 8, also a cationic CPP, leverages its positively charged arginine residues to interact with the cell membrane and facilitate the internalisation process[200].

The mechanisms by which these CPPs penetrate cells continue to be an active research area. Current evidence suggests a combination of endocytosis and direct penetration processes[201]. The potential applications of these CPPs span several fields, including drug delivery, gene therapy, and immunotherapy[202]. However, challenges such as potential toxicity, lack of cell specificity, and potential immune responses must be addressed to fully leverage the promise of CPPs in therapeutic delivery systems[203]. Future research should focus on optimising the use of these peptides and overcoming the associated challenges.

For the purpose of this chapter, the short sequences were called “Booster sequences” and were cloned into the pPURE plasmid at the 5’ end of the genes for mammalian optimised mVenus and mCherry, as well as E.coli optimised mVenus and mCherry. The genes were linearised so it contained the section from the T7 promoter site to the terminator site and the

gene was expressed in the PURExpress IVTT system (Figure 4.5). The codons for the booster sequences themselves were optimised using E.coli codon usage tables.

It was decided further that shorter versions of these booster sequences would be produced with the aim to identify which regions or codes in the short sequences gave rise to the higher protein expression level. Therefore, three shorter versions of Pen and three shorter versions of TAT were produced (Table *2*), where the numbers indicate the codon position of the original CPP.

Table 2: CPP RNA sequences and the respected amino acid sequences.

Name	**RNA sequences**	**Amino Acid Sequence**
Penetratin	CGC CAG AUU AAA AUU UGG UUU CAG AAC CGC CGC AUG AAA UGG AAG AAA	R Q I K I W F Q N R R M K W K K
Pen1-8	CGC CAG AUU AAA AUU UGG UUU CAG	R Q I K I W F Q
Pen1-4	CGC CAG AUU AAA	R Q I K I
Pen9-16	AAC CGC CGC AUG AAA UGG AAG AAA	N R R M K W K K
TAT	CGC AAG AAA CGC CGU CAG CGC CGU CGC	R K K R R Q R R R
TAT1-5	CGC AAG AAA CGC CGU	R K K R R
TAT1-3	CGC AAG AAA	R K K
TAT6-9	CAG CGC CGU CGC	Q R R R
Transportan	GGC UGG ACC CUG AAC AGC GCG GGC UAU CUG CUG GGC AAA AUU AAC CUG AAA GCG	G W T L N S A G Y L L G K I N L K A
Polyarginine (R8)	CGC CGU CGA CGU CGC CGG CGC CGC	R R R R R R R R
g10L	GCU AGC AUG ACU GGU GGA CAG CAA CAU AUG	A S M T G G Q Q H M

The proteins were all expressed for 3 hours before their fluorescence was measured. One of the main observations was that some of the booster sequences affected the protein expressions positively for the mVenus gene. However, the mCherry gene expression was affected negatively (Figure 4.5).

For mVenus expression alone, the overall expression was 1.3 factors higher for E.coli codon optimised mV (Eco-mV) compared to the mammalian codon optimised mV (Mam-mV) as expected. It was however interesting to see that the Mam-mV expression can significantly be

higher than even the Eco-mV sequence when certain booster sequences were added at the 5' end of the gene. For example, all the Pen and TAT sequences as well as the g10L sequence gave rise to higher level of protein expression compared to both the Mam-mV and Eco-mV gene sequences. Indicating that when a gene uses poorly optimised codons for a specific expression system, a certain short sequence at the 5' end of the gene can increase its yield without needing to optimise all the codons of the coding sequence.

Furthermore, in the group of Pen sequences, the 9-16Pen sequence showed one of the highest levels of expression in both the Mam-mV and Eco-mV, possibly indicating that this sequence is able to bind and interact with the 16S rRNA more strongly compared to other sequences. Alternatively, it is also possible that the sequence allowed the mRNA structure to open to allow better interaction with the SD sequence.

On the other hand, the mC proteins showed a different pattern of protein expression. For both the mammalian codon optimised mCherry (Mam-mC) and E.coli codon optimised mCherry (Eco-mC), the highest level of expression was seen in the original gene sequence without any of the additional booster sequences. We were uncertain of the reasons but recently there has been a study that has shown that the mC gene sequence has a shorter protein isoform formed from the methionine (M) at position 10 which can interfere as a reporter function[204]. The reason for the shorter isoform is due to the presence of a SD-like sequence ranging from -12 to -6 nucleotides before the M10 codon which contained a mix of G and A bases to code for glycine (G) and two glutamic acid (E). Therefore, when this residue was mutated to leucine or glutamine, the isoform production is abolished whilst conserving the fluorescent properties[204]. The large proportion of the problem relate to the first 7 amino acids (MVSKGEE) being present before an M aa, which is also present in mNG. mV also

contains this sequence but not the M, therefore the reporter functionality of mV can be presumed to be more reliable for this study.

To conclude, it is possible that the rate of protein synthesis is high when the certain booster sequences are present, however, the isoform formation rate would be different as it would not be impacted by the presence of the booster. Therefore, the expression of mC with all the N-terminal booster sequences would need to be repeated with the M10 aa mutated to a G or E.

The interesting thing that was observed from expressing mC with the additional sequences was how the presence of R8 and Trans sequence on the 5' end decreased the expression of both mV and mC. Firstly, for mV, the expression was inhibited (Table 3) as the expression was lower than the Mam-mV without any 5' sequence. In Mam-mC, the expression was also inhibited, indicating that the formation of the mC isoform was low and the expression from the original SD sequence was higher for these sequences. The 1-4Pen sequence also another sequence that decreased the expression level of both Mam-mC and Eco-mC.

To conclude which parts of the CPP sequences resulted in affecting the overall protein expression, shorter versions of the sequences were tested. Using the mVenus sequences, it can be seen that just having certain sequences was not enough to give rise to the higher expressions. But rather, the positioning of specific sequences after the start codon was important. For example, for the full penetratin sequence (Pen-mV), gave rise to lower protein expression than the second half of the sequence (9-16Pen).

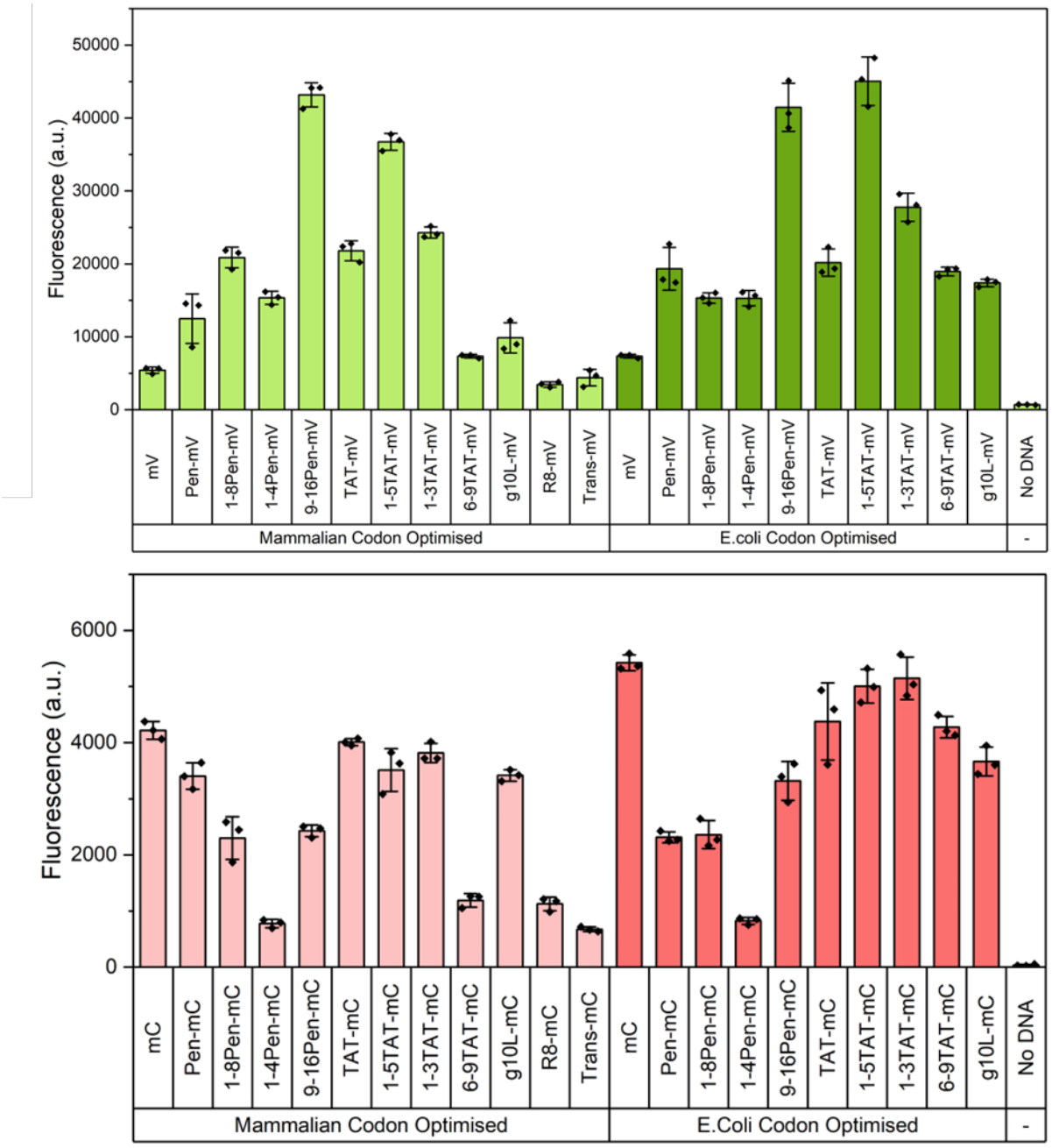

Figure 4.5: Short sequences named as "Booster sequences" were cloned into pPURE plasmids before four different versions of fluorescent proteins: codon optimised mVenus gene for mammalian and E.coli protein expression systems, as well as codon optimised mCherry for mammalian and E.coli protein expression systems. The T7 promoter, including relevant 5' UTR and protein coding region was amplified out by PCR. This was used for IVTT in PURExpress to express the fluorescent proteins above and fluorescence was measured at ex/em at 515nm/527nm and 587nm/610nm for mVenus and mCherry respectively.

Table 3: Effects of various short “booster” sequences at the 5’ end of mVenus and mCherry sequences. The numbers represent the factor by which each gene expressed the respected protein compared to the gene without any t7-g10L or booster sequences, which was given the arbitrary value of 1.0.

	mVenus		mCherry	
Booster sequence	Mamalian Codon Optimised	E.coli Codon Optimised	Mamalian Codon Optimised	E.coli Codon Optimised
g10L	1.8	5.0	0.8	0.7
Pen	2.3	2.6	0.5	0.4
1-8Pen	3.9	2.1	0.5	0.5
1-4Pen	2.8	5.6	0.2	0.2
9-16Pen	8.0	4.9	0.6	0.6
TAT	4.0	2.7	0.9	0.9
1-5TAT	6.8	3.8	0.8	1.0
1-3TAT	4.5	6.1	0.9	1.0
6-9TAT	1.4	2.6	0.3	0.8
R8	0.6	-	0.3	-
Trans	0.8	-	0.2	-

One of the possible reasons that a certain booster sequence was able to allow higher level of protein expression than the others is due to possible stronger interaction between the mRNA and the 16S rRNA around the anti-SD sequence. When observing the sequences around the anti-SD sequence on the rRNA and its potential Watson-Crick forces with the booster sequences right after the start codon (AUG), certain patterns were observed (Table 4). It was seen that there was an obvious set of nucleotides right after the AUG codon in the sequences with 9-16Pen, which can form Watson-Crick bonds with their respected pairs. However, the other booster sequences that gave rise to lower protein expression, had lower number and sparsely spread availability for potential base pairing. For the Trans and R8 sequences, the yield of protein was a lot lower. This could be related to the fact that there is a high portion of C and G bases in these booster sequences which possibly increased the secondary structure within this region, leading to the SD sequence not being easily available for recognition by the 16S rRNA[205].

Table 4: Proposed base pairing around the start codon site between 16S rRNA (top sequences) and mRNA of booster sequences. The bases highlighted in bold are the potential bases that may be able to pair with one another, and increase likelihood of translation initiation.

	Base pairing with 16S rRNA
Penetratin	3'**UAC**G**UUGG**CGUCCAAGGGGAUGCCAAUGGAACAAUGCUGAAGUGGGGUCAGUACUU5' 5'**AUG**C**CC**AG**A**UUAAAAUUUGGUUUCAGAACCGCCGCAUGAAAUGGAAGAAA
1-8Pen	3'**UAC**G**U**U**GG**CG**U**CCAAGGGGAUGCCAAUGGAACAAUGCUGAAGUGGGGUCAGUACUU5' 5'AUG**C**G**CC**AG**A**UUAAAAUUUGGUUUCAG3'
1-4Pen	3'**UAC**G**U**U**GG**CG**U**CCAAGGGGAUGCCAAUGGAACAAUGCUGAAGUGGGGUCAGUACUU5' 5'AUG**C**G**CC**AG**A**TTAAA3'
9-16Pen	3'**UAC**G**UUGGCG**U**C**CAAGGGGAUGCCAAUGGAACAAUGCUGAAGUGGGGUCAGUACUU5' 5'AUG**AACCGC**C**G**CAUGAAAUGGAAGAAA3'

4.3 Conclusion

In conclusion, this chapter has highlighted a significant opportunity to increase the yield of proteins in PURExpress system, thus it has the potential to be used for a higher yield of proteins in SCs. The addition of certain short sequences from CPPs, to the 5' end of the GOI, immediately following the AUG start codon, has been found to effectively influence protein yield. This has been demonstrated through our work with mVenus and mCherry proteins, both in mammalian codon-optimised and E.coli codon-optimised versions. However, as exciting and promising as these initial findings are, it is necessary to proceed with a more comprehensive examination of the applicability of this method. In order to fully validate these results, the effect of these short sequences should be tested on a broader array of genes. This will allow us to confirm if the impact on protein yield is general or specific to certain genes.

Additionally, the structure and yield of the resultant mRNA should be measured. Such measurements are crucial as they will provide deeper insights into the precise changes that these sequences induce in the final mRNA product, thus further elucidating the mechanisms that are used for translation.

What makes this work particularly useful is the simplicity and potential wide-reaching impacts of these short sequence additions. Instead of multiple mutations at various protein locations, or the need to incorporate specific features or optimise protein expression and purification steps, a simple addition at the gene's outset can be used to bolster protein yield. This is expected to significantly ease the process and enhance efficiency of cell-free protein synthesis.

Chapter 5 - Conclusion and Future Directions

The application of synthetic cells (SCs) equipped with a gene expression system could revolutionise multiple fields. One significant area where these could prove vital is in the field of healthcare, particularly in the development of personalised medicine. For instance, the design of synthetic cells with the capability to express certain proteins can enable us to custom-make cells that can interact with unique targets in a patient's body, effectively tailoring treatments to the individual's unique physiological and genetic makeup. This precision, paired with an understanding of the patient's particular condition, could enhance treatment efficacy, minimise side effects, and reduce the chance of treatment failure. Another example where SCs with a gene expression system could excel is in environmental biotechnology. Their ability to express certain enzymes could be harnessed to degrade pollutants or synthesise useful compounds, thereby providing innovative solutions for issues such as waste treatment and the development of sustainable biofuels. In these capacities, synthetic cells can bring about an evolution in our approach to problem-solving, melding the disciplines of engineering, biology, and medicine. Harnessing the potential of synthetic cells for drug delivery has emerged as a particularly promising application, owed to their inherent programmability, which is possible as any DNA template can be used to produce and deliver therapeutic proteins directly in the patient's body.

Synthetic cell-like structures of liposomes have already proven effective as drug delivery vehicles, specifically in tumour targeting. These tiny, biocompatible vehicles can encapsulate drug molecules and selectively deliver them to cancer cells, thereby increasing the drug's therapeutic efficiency while minimising its systemic toxicity. As an evolution of this concept,

thermosensitive liposomes have been developed. These liposomes are designed to release their encapsulated drug when exposed to slightly elevated temperatures, which can be applied externally. By using such a thermosensitive delivery system, clinicians can target tumours more precisely and avoid harming healthy tissues.

This thesis provides a substantial contribution to these evolving concepts by engineering a novel synthetic cell that combines all these key characteristics - high yield, protein synthesis capabilities, and heat sensitivity. The designed synthetic cells serve as a model system, demonstrating how advanced gene expression systems can be incorporated into SCs to yield proteins of interest, illustrating their potential for on-demand therapeutic protein synthesis. The heat sensitivity of these synthetic cells aligns with the concept of thermosensitive liposomes, setting a new foundation for drug delivery systems that can respond to the biological cues of diseased tissues.

In Chapter 2, SCs were assembled using the inverted emulsion method to include a cell-free in-vitro transcription and translation system (IVTT). The SCs included templates of simple linear DNA for fluorescent proteins (mNeonGreen) or a reporter enzyme (DHFR, β-Lactamase, β-Galactosidase). Different parameters of the SC conditions were tested to identify the most appropriate condition for producing the SCs. It was shown that although the IVTT system was able to be encapsulated within the SCs, the level of expression can vary from one SC to another. Therefore, this work can be expanded on by testing other oils, lipids, centrifugation speeds or even different IVTT system to produce SCs, in order to increase encapsulation levels and hence increase yield of protein within individual SCs.

Measuring the total release of the SC contents was important in order to establish a positive control to compare the released contents of heat-responsive SCs. As a result, β-Gal assay was

optimised and tested with SCs to identify the most appropriate assay to measure the release of the synthesised proteins from the SCs. Although this reporter enzyme was better than the DHFR and β-lactase assays which were tested, it would be beneficial to use a reporter enzyme that was smaller in size. For example, a small enzyme such as a lysozyme or pore forming therapeutic proteins could be more beneficial as they could allow its usage to test their therapeutic capability rather than just using them as a reporter protein. A smaller fluorescent protein such as luciferase or HiBit proteins can also be used, as tagged proteins to a therapeutic protein or on their own as reporters.

In Chapter 3 of this thesis, we ventured to create heat-responsive liposome based SCs. The approach adopted for the production of these thermosensitive synthetic cells was novel, utilising the Freeze-Dried Empty Liposomes (FDEL) method. This technique borrows key principles from the hydration method, establishing a unique procedural approach. The challenges we encountered in the process of encapsulating an IVTT system in heat-responsive lipid vesicles were significant. Maintaining a delicate balance with the temperature and timing of the methos was intricate: on one hand, the temperature needed to be high enough to exceed the transition temperature of the thermosensitive lipids, and on the other, care had to be taken to ensure it didn't reach a level that could potentially damage the IVTT system.

The research showed that it was feasible to produce thermosensitive synthetic cells capable of releasing synthesised proteins upon heating. However, the issue of consistent production of the synthetic cells emerged as a serious challenge, highlighting the need for further investigation in this area. Additional work will be needed to address these complexities and enhance the reliability of synthetic cell production that was high yielding, thermosensitive and encapsulating a gene expression system. This research has underscored the need for a

delicate balance between technical requirements and practical feasibility, offering valuable insights for the future development of heat-responsive SCs. To expand on this work, other lipid mixtures and compositions can be studied.

The hurdles encountered during the formation of the TSV were presumed largely due to the small scale at which the optimisation efforts were executed. The incorporation of IVTT systems into lipids, constrained to only 10 µL. However, viable alternatives systems can be explored for the future such as inexpensive, homemade IVTT systems like the ΔDE3 lysate extract or OnePot PURE systems, which can be deployed in greater quantities for TSV production.

Moreover, the intended use of these TSVs for targeted delivery makes it necessary for future research to focus on their interaction with live cells. Subsequent investigations should ensure the osmolarity of the TSVs aligns with the external environment at the delivery site, in order to guarantee stability under physiological conditions. It's also crucial to consider that temperature-sensitive bilayers develop pores when subjected to heat, enabling the vesicles' interior content to be transported out. Consequently, smaller proteins than β-Gal, like lysozymes, should be leveraged to examine controlled release.

Future work could explore ways to bring together light controlled transcription within synthetic cells and heat to release the synthesised proteins. This would allow for dual control of the TSV when applying them in medical therapy. This work brings us one step closer to realising the potential of synthetic cells as programmable, responsive, and precise drug delivery vehicles, setting the stage for future developments that could revolutionise healthcare, biotechnology, and environmental management.

Finally in chapter 4, short sequences were identified which were able to increase the yield of mVenus protein in cell-free proteins synthesis system. In this thesis we show that certain versions of the sequences can increase the yield of mV, but did not yield the same level of increase in mC. To understand their mechanism of action, further research needs to be carried out by testing these sequences on a variety of genes. The impact of the sequences on mRNA expression can be studied as well as their secondary structure and their interaction with the ribosomes.

Chapter 6 - Materials and Methods

6.1 Materials

All solvents and reagents were purchased from Sigma/Merck unless stated otherwise. PURExpress and NEBExpress was purchased from New England Biolabs NEB. All enzymes were purchased from New England Biolabs, unless stated otherwise. Standard DNA oligonucleotides were synthesized by Integrated DNA Technologies. Egg PC, POPC, DPPC, DSPC, MSPC, MPPC, DSPE-mPEG2000 were purchased from Avanti Polar Lipids. Geneframes were 131 purchased from Thermofisher. pMAT-mNeonGreen was synthesised by GeneArt. Components to produce ΔLacZ IVTT system gifted by Dr Fernando FGC Guzman Chavez (University of Cambridge). Microscope slides with 1 mm holes drilled through 25 mm x 75 mm microscope slides to correspond with diagonal corners of 25 µL gene frames were gifted by Dr Jefferson Smith (Oxford).

6.2 General Methods

The following methods were used consistently throughout each of the chapters. They are written in full here and then referred in each respective chapter when used.

6.2.1 Homologous Recombination

Homologous recombination was conducted with two PCR products to insert sections of DNA into a vector DNA. Usually, 2 µL of the insert and 0.5 µL of the vector DNA is mixed together in a 1.5 mL Eppendorf tube. 15 µL E. coli XL10-Gold cells were added and incubated on ice for 20 minutes, heated to 42 ◦C for 30 seconds, then placed back on ice for 30 minute. The cells

were spread onto LB + Ampicillin (100 µg/mL) agar plates with glass beads and the plates were incubated at 37 ◦C for ∼14 hours. Transformants were picked with pipette tips and used to inoculate 5 mL LB media + (100 µg/mL) ampicillin in 50 mL falcon tubes; lids were loosely applied. Cells were incubated at 37 ◦C, 225 rpm for ∼16 hours. All 5 mL of overnight culture was centrifuged at 14,000 x g for 1 minute and plasmids were extracted from the cell pellets using a QIAprep Spin Miniprep Kit. Plasmid sequences were verified by Sanger sequencing.

6.2.2 Colony PCR

Colony PCR was conducted using individual bacterial colonies grown on LB Agar plates. A 10 µL mix of DreamTaq Green PCR Master Mix, 1 µM T7 e.long/Rev CT 2 primers and MQ water was prepared. A small pipette tip was used to collect a single colony from the LB agar plate and mixed in the PCR mix. The picked colony was labelled and the pipette tip was safely discarded. Reactions were cycled according to the following programme: 95 ◦C 3 minutes, 35 cycles of [95 ◦C for 30 s, 50 ◦C for 30 s and 72 ◦C for the time that corresponded to the size of amplifying DNA (1minute/kb)], 72 ◦C for 4 minutes, 4 ◦C HOLD. The samples were run on agarose gel to identify if the size of DNA was as expected. No additional dye was needed as the DreaTaq Green Master mix contained DNA binding dye.

6.2.3 Gel Electrophoresis

1.2% of agarose gel was prepared by mixing 0.72 g of agarose (Sigma Aldrich) with 60 mL of 1X TAE buffer in a microwavable flask and heated in the microwave for 1-3 minutes until the agarose dissolved. The agarose was poured onto a gel tray with well combs, removing any bubbles. The gel was allowed to set at room temperature for ~1 hour. DNA samples were prepared in 12 µL volumes by mixing 2 µL of the DNA sample with, 2 µl of 6x Purple Gel Loading Dye (NEB) and 8 µL of MQ water. The agarose gel was placed in the gel box of the

electrophoresis uni and filled with 1xTAE buffer until it covered the top of the gel surface. A molecular weight ladder was loaded into the first well. DNA samples were then loaded into the gel. The gel was run at 100 V for 1 hour 20 minutes (or until the dye can be seen to have moved to the end of the gel. The TAE buffer was discarded and the gel was placed in 1x GelRed Nucleic Acid Stain for ~30 minutes-1 hour. The gel was imaged using a BioRad Geldox XR+ gel imager.

6.2.4 Restriction Enzyme Digestion

A volume of 10 µL consisting of 15 ng of the plasmid DNA 1x CutSmart Buffer and 0.5 µL of the restriction enzyme was mixed in a PCR tube. The mixture was incubated at 37 ℃ for 1 hour in a thermocycler and then stored at -20 ℃ until needed.

6.2.5 Preparation of linear DNA templates

Linear DNA templates were prepared by PCR from plasmids encoding the desired GOI with the vector originating from the PURExpress kit (pPURE). The plasmid was first cut by restriction enzyme HindIII which cut the plasmid after the T7 terminator. Then PCRs were performed with Phusion DNA polymerase mastermix using 3 ng of the cut plasmid and 500 nM T7 e.long/Rev CT 2 primers. Reactions were cycled according to the following programme: 98 ◦C 30s, 35 cycles of [98 ◦C for 10 s, 55 ◦C for 20 s and 72 ◦C for seconds that corresponded to the size of amplifying DNA (30 sec/kb)], 72 ◦C for 10 minutes, 4 ◦C HOLD. 2x50 µL of PCR samples were produced to produce large amounts of the final product. PCR products were purified using QIAquick PCR purification kits – 2 x 50 µL of deionised water were used to recover as much DNA as possible from the spin columns. Linear DNA templates were then ethanol precipitated and resuspended in TE buffer or Milli-Q H2O to 100 ng/µL.

6.2.6 Ethanol Preparation

DNA samples were mixed with 1:10 (v/v) of 3 M Ammonium acetate (pH 5.2) in a 1.5 mL centrifuge tube by pipetting up and down thoroughly. 3 volumes of ice cold 99% ethanol were added, and the samples were mixed thoroughly. Samples were incubated at -80 ◦C 4 hours to overnight. Tubes were centrifuged at 16,000 x g, 4 ◦C for 30 minutes to pellet the precipitated DNA and the ethanol was carefully removed as to not disturb the DNA pellet. The DNA pellet was washed twice by adding 500 µL of ice cold 70% ethanol to the DNA pellet. The tubes were centrifuged at 16,000 x g, 4 ◦C for 15 minutes. All the ethanol was carefully removed, and tubes containing the DNA pellet were centrifuged under vacuum for 10 minutes using a speed vac to remove residual ethanol. Dry DNA pellets were resuspended in Milli-Q H2O to a final concentration of 100 ng/µL.

6.2.7 DNA Quantification

Double stranded DNA concentrations were determined with the dsDNA setting on a Nanophotometer (Implen). PCB-modified oligonucleotide concentrations were determined using the beerlambert law via its A260 (measured on a Nanophotometer) and its extinction coefficient (371900 L.mol-1.cm-1).

6.3 Chapter 2 Methods

6.3.1 Preparing Lipid Films for Inverted Emulsion SC Preparation

Supelco glass vials were cleaned with isopropanol. Egg PC, POPC, DPPC, MSPC, MPPC and DSPE-mPEG2000 arrived from Avanti Polar Lipids in the form of powder which was dissolved and mixed well in chloroform in 100 mg/mL concentration in the cleaned glass vials which was wrapped with electric tape and stored in -20 ℃. The appropriate amount of the lipid-

chloroform mixture was measured out using a Hamilton syringe and placed in a 1 mL clear glass vial. Nitrogen was blown into the vial gently to evaporate the chloroform out and form a lipid film inside the glass vial. The lipids were then further dried in a desiccator for > 2 hours under vacuum to remove residual chloroform.

6.3.2 Preparing Lipid-Oil Mix

Once the lipids were dry, 700 µL of dodecane, squalene, paraffin oil or mineral oil was added to give a final lipid concentration between 2 mg/mL and 10 mg/mL which was vortexed vigorously for 1 minute. The glass vial was put in a modular heating block for 10 minutes and heated to 80 ℃ without the vial lid to prevent build up of pressure within. The lid was tightened back on and vortexed for another 1 minute. Nitrogen was blown into the vial to remove air from within and the lid was screwed on. The vial was secured using an electric tape to prevent the entry of air. The vial was placed in a sonication bath at 50 ℃ and sonicated for 1 hour. The vial was stored at room temperature and could be used to prepare water in oil emulsion on the same day or the next day.

6.3.3 Preparing Water-in-Oil Emulsion

The inner solution droplets in the in the oil consisted of either of either a buffer with a fluorescent dye or PURExpress system with 10 ng/µL DNA and 200 mM Sucrose (some samples also contained 25 µM Texas Red Dextran). 200 uL of the lipid oil mix was placed in an Eppendorf tube which was left to chill on ice. Total of 2-4 µL of inner solution was pipetted into the lipid oil mix slowly in a circular fashion in batches of 2 µL, forming small droplets. The Eppendorf was then either extruded, vortexed, sonicated with a sonication probe (60% amplitude, 3s pulse, 6 seconds pause, total of 2.5 minutes[206]) or agitated mechanically by drawing the tube across the uneven surface of a tube rack to break up the droplets to smaller

sizes. The droplets were allowed to chill on ice for at least 10 minutes before imaging or using them to produce vesicles using the inverted emulsion method.

6.3.4 Producing Synthetic Cells

250 µL of the outer solution (50 mM HEPES, 400 mM Potassium Glutamate, 200 mM Glucose, pH 7.6) was pipetted into 1.5 mL tubes. 100 µL of the lipid/oil mix was placed gently on top of the outer solution and allowed to stabilise for 5 minutes at room temperature or until the oil-outer solution interface became even. 200 uL of the droplet emulsion was gently pipetted on top of the outer solution column and incubated on ice for 5 to 30 minutes. The column was spun between 120xg to 16,000xg for 30 minutes at 4 ℃ depositing the vesicles at the bottom of the tube. The oil and most of the outer solution was carefully removed with a 200 µL pipette tip, being careful not to remove the last 20 uL of the outer solution where the vesicles would be deposited. A 20 µL pipette was used to take the vesicles off the side of the tube and mix into the outer solution using slight push with air from the pipette. The vesicles were carefully transferred to another tube with 200 µL of chilled outer solution and spun again at the same speed for 10 minutes. Majority of the outer solution was removed using a pipette, leaving about 20 µL with the vesicles which were then transferred to another tube containing 200 µL of the outer solution and spun once more. This repeated transfer and spinning allows the removing of any excess oil. The final 20 µL of the vesicles were transferred to 40 µL of outer solution which was used for imaging or assays.

6.3.5 Preparing Vesicles for Imaging

All slides and coverslips (22 mm x 22 mm) were cleaned with 2% decon, isopronaol and Milli-Q H2O, then sonicated in Milli-Q H2O for at least 10 minutes and dried under N2 flow before use. Coverslips were O2 plasma treated for 5 minutes. 0.1% of Bovine Serum Albumin (BSA)

in PBS was added inside the gene frames and incubated at room temperature for 15 minutes. The BSA was removed and the coverslips were washed with the outer solution, twice. The outer solution was removed and gene frames were applied to the drilled microscope slides using double sided tape. 25 µL of samples were introduced through the drilled holes which was sealed with tape. The samples were incubated with the coverslip side down for the vesicles to rest on the BSA on the coverslip.

6.3.6 Epifluorescence Microscopy and Image Processing

The imaging chambers contained samples that were visualized using a Leica DMi8 inverted epifluorescence microscope equipped with a 100x oil immersion objective lens. The brightfield, TXR, and GFP filter settings were used to capture images of the vesicles. The images were processed in ImageJ.

6.3.7 Preparing PURExpress System SCs made by Inverted Emulsion Method

A specific volume of the IVTT mix includes 40 % of Solution A and 30% of Solution B, 2.5% of RNASe inhibitor, 10 ng/uL of template linear DNA with GOI, and/or Texas-Red Dextran at 25 µM. The volume is made up to the final volume with deionised water. The mixture was incubated at 37 ℃ for minimum 3 hours.

6.3.8 DHFR Assay

The plasmid from the PURExpress kit was used as the source of the DHFR gene. The gene was linearised as explained in subsection 4.2.5. The measurement of enzyme activity was performed using the DHFR Assay kit obtained from Sigma Aldrich. The assay was conducted by preparing 50 µL reaction mixtures containing 0.06 mM NADPH, 0.05 mM dihydrofolic acid, and 1x Assay Buffer. Various reaction conditions were employed, including the recommended DHFR quantity specified in the kit, 3 µL of PURExpress reaction with DHFR DNA, and/or 0.1%

Triton X-100. The reaction mixtures were transferred to transparent 96-well plates, and a kinetic program was executed with readings taken at 15-second intervals for either 3 minutes or 13 minutes, at 340 nm and 25 ℃

6.3.9 Preparing β-Lactamase Plasmid Construct-add in supp.

The construction of the pPURE plasmid with β-Lac gene was conducted by cutting the pPURE plasmid with NdeI (subsection 4.2.4) and using this as the template for PCR as it contains the β-lac gene on the plasmid vector. Then PCR reactions were conducted using Phusion DNA polymerase mastermix mixed with the digested DNA and 500 nM BLctFP2/BLctRP2 for the DNA vector backbone and BLAmpFP/BLAmpRP for the β-Lac insert DNA. Reactions were cycled according to the following programme for the DNA vector backbone: 98 ◦C 30s, 35 cycles of [98 ◦C for 10 s, 60 ◦C for 30 s and 72 ◦C for 1 minute and 9 seconds], 72 ◦C for 10 minutes, 4 ◦C HOLD. For the β-lac gene amplification, the same template was used but the primers were BLAmpFP/BLAmpRP in the following programme: 98 ◦C 30s, 35 cycles of [98 ◦C for 10 s, 65 ◦C for 30 s and 72 ◦C for 25 seconds], 72 ◦C for 10 minutes, 4 ◦C HOLD. The PCR products were used in carry out homologous recombination (subsection 4.2.2) to insert the β-lac enzyme into the vector and the plasmids were then harvested. The DNA was linearised using the steps in subsection 4.2.6.

6.3.10 β-Lactamase Assay

The β-La was synthesised in the PURExpress system, for 3 hours at 37 ℃. The IVTT solution was subsequently diluted to an 18% concentration using a 120 mM sodium phosphate solution. Assay reactions were prepared in 96-well clear plates, consisting of either 20 µL of the diluted IVTT reaction or vesicles, with or without Triton X-100 treatment. The outer solution contained 36 µg/mL of nitrocefin (abcam) in a total volume of 80 µL. Absorbance

readings were recorded at 490 nm every 20 seconds for a total of 58 minutes, maintaining a temperature of 37 ℃.

6.3.11 Chloroform/Phenol Extraction of E.Coli Genome

50 mL Falcon Tubes were prepared with 5 mL of LB media with small number of XL10 Gold cells which were grown overnight at 37 ℃. 200 µL of the cells were pipetted into 1.5 mL tubes and the same volume of phenol:chloroform:isoamylalcohol (25:24:1) was added to the tube. The mixture was vortexed thoroughly and then centrifuged at room temperature for 5 minutes at 16,000 x g. The upper aqueous phase was removed and placed in a clean tube. Then the extracted DNA from the E.coli was cleaned by ethanol precipitation as explained in 4.2.7.

6.3.12 Preparing β-Galactosidase Plasmid Construct

Lac Z gene was amplified from XL10 E.coli cells genome. Gradient set of PCR reactions were set up with different annealing temperatures and two type of DNA polymerase. A mix of 3ng of E.coli genome, 1 µM of LZFP1/LZRP2 primers, with either Phusion Master mix or DreamTaq master mix and sterile deionised water to a total of 10 µL reactions were made up. Reactions were cycled according to the following programme for DreamTaq: 95 ◦C 30s, 40 cycles of [95 ◦C for 10 s, varying temperatures at 54.5 ◦C, 58.6 ℃, 60, 61.1 ℃, 65 ℃, 68 ℃ for 30 s and 72 ◦C for 3 minute and 4 seconds], 72 ◦C for 5 minutes, 4 ◦C HOLD. For Phusion PCR the following programme was used: 98 ◦C for 30s, 35 cycles of [98 ◦C for 10 s, varying temperatures at 54.5 ◦C, 58.6 ℃, 60, 61.1 ℃, 65 ℃, 68 ℃ for 30 s and 72 ◦C for 1 minute and 34 seconds], 72 ◦C for 10 minutes, 4 ◦C HOLD.

The pPURE plasmid backbone was amplified with the Laz Z gene overlap at the ends by mixing 0.5ng of NdeI digested pPURE-mVenus, 250 nM FPLacZCT/RPLacZCT primers and sterile

deionised water to 50 µL. Reactions were cycled according to the following programme: 98 ◦C for 30s, 35 cycles of [98 ◦C for 10 s, 60 ℃ for 3o seconds, 72 ◦C for 1 minute and 10 seconds], 72 ◦C for 10 minutes, 4 ◦C HOLD. The PCR products of the above amplified Lac Z gene and the pPURE plasmid backbone used for homologous recombination and the gene was linearised and cleaned as explained in section 4.2.

6.3.13 β-Galactosidase Assay

The optimisation of the assay was conducted using the outer solution buffer of the synthetic cells: 50 mM HEPES, 400 mM Potassium Glutamate, 200 mM Glucose, pH 7.6. Different conditions were tested including varying concentrations of CUG (abcam) at 50 µM, 200 µM, 500 µM or 1 mM at a volume of 5 µL, 40 µL or 65 µL for 20, 40 or 60 minutes. Once the best conditions were chosen at 1 mM CUG concentration at 40 uL for 20 minutes, this was used for the rest of the CUG assays conducted.

6.4 Chapter 3 Methods

6.4.1 Inverted Emulsion Method to Produce Thermosensitive Vesicles

The inverted emulsion method used to produce DPPC contained vesicles, was the same method as in section 5.3.

6.4.2 Lipid Preparation for Hydration

10 mL glass round-bottom flask was prepared by washing with acetone and then isopropanol. The solvents were removed using a flow of N2 gas. Lipid/lysolipid/PEG in chloroform of the desired ratio was transferred to the round-bottom flask using Hamilton syringe, ensuring the total final lipid mix added to 8.8 mg. A rotoray evaporator was used to remove the chloroform slowly under 474 mbar vacuum whilst maintain the temperature at 40 ℃ in the water bath,

for ~1-2 hours, ensuring that the glass continuously rotated. A thin film of the lipid mix formed at the bottom of the flask. The flask was dessicated further for >1 hour under vacuum to remove remaining chloroform. 1 mL of nuclease-free water was added to the lipids. For POPC lipids, the sample was vortexed until all lipids disconnected from the glass surface and dissolved in the water. For the thermosensitive lipids, the vial was placed in a water bath at 45 ℃ for ~5 minutes before vortexing to dissolve the lipids. The lipids were transferred to 1.5 mL Eppendorf tubes. The lipid mix was placed in a sonication bath and sinicated for 20 minutes at 50 ℃. The lipid mix was then extruded either on a hot a plate heated at 45 ℃ for thermosensitive lipids or at room temperature for POPC lipids. The extrusion membranes used were either 0.2 µm, 1 µm or 12 µm in pore size. The lipids were aliquoted into individual 1.5 mL tubes in 1.2 µL, 2.5 µL, 5 µL, 10 µL, 20 µL, 40 µL which would allow production of vesicles at concentrations 1.5 mM, 3 mM, 6 mM, 12 mM, 23 mM and 46 mM respectively. A hole was created on top of the tube lid. The tubes were gently placed in liquid nitrogen to freeze the samples which was then lyophilised overnight to dehydrate the empty liposomes and remove the water. Tubes were removed from the lyophiliser and the holes were sealed or replaced by another lid which was sealed with electric tape and stored at -20 ℃ until needed.

6.4.3 NEBExpress Preparation

A 10 µL of NEBExpress IVTT system was added to each tube of empty liposomes. Therefore, to prepare 10 µL of the IVTT syste, a mixture of 2.4 µL of NEBExpress S30 Synthesis Extract, 5 µL of Protein Synthesis Buffer, 0.2 µL T7 RNA Polymerase, 0.2 µL of RNAse inhibitor (Murine), NEBExpress GamS Nuclease Inhibitor, 200 mM sucrose and 10 ng/µL of linear DNA with GOI was mixed and made up to 10 µL total volume. The preparations was carried out on ice.

6.4.4 Hydration Method to Produce Thermosensitive Vesicles

10 µL of NEBExpress IVTT system was added to each tube of dried empty liposomes. The tubes were placed in 45 ℃ heated between 1 to 4 minutes, vortexed for ~15 seconds and centrifuged with a short pulse. The tubes were allowed to cool on ice for 2 minutes before repeating the heating, vortexing and centrifuging cycle. The tubes were incubated on ice for 20 minutes. Outer solution buffer was prepared with DNASeI enzyme. 25 µL of the buffer was added to the vesicles and gently mixed by swirling the vesicles, rather than pipetting up and down (vortexing was not used at this stage). The vesicles were allowed to incubate at 37 ℃ for 3 hours before conducting the CUG assay.

6.4.5 Heating Vesicles

To heat up the vesicles for controlled thermosensitive release, the tubes with the vesicles were placed in heated water bath at 43 ℃ for 5 minutes to 15 minutes with intervals of cooling on ice every 5 minutes.

6.4.6 CUG Assay with Vesicles made from Hydration Method

Stock of CUG was prepared in MQ water. For the CUG assay with the vesicles, 5 µL of the vesicle sample, 1 mM of CUG with or without Triton X-100 was made up to total of 40 µL volume with Buffer of the outer solution buffer.

6.4.7 Preparation of ΔLacZ lysate extract

Lysate extract and all components related was produced using the method described by the Haseloff group[207].

6.5 Chapter 4 Methods

The methods in this chapter consisted of conducting PCR as explained in 6.2.1 which uses homologous recombination.

The Flluorescence assays conducted were carried out as following; 3 µL total volume of the PURExpress mix was prepared. This includes 40 % of Solution A and 30% of Solution B, 2.5% of RNASe inhibitor, 10 ng/uL of template linear DNA with GOI. The volume is made up to 3 µL with deionised water. The mixture was incubated at 37 ℃.

For the time series experiments, 0.5 µL of the IVTT mix was collected and diluted into 90 µL of Tris-HCl, pH8 and stored at 4 ℃. The rest of the reactions were allowed to continue with the reaction at 37 ℃. Aliquot of 0.5 µL of each sample was collected every hour for 3 hours. 80 µL of the Tris-HCl with the IVTT was placed in a 384 black-bottom plate and fluorescence was measured at 515nm/527nm for mVenus and 5587nm/610nm for mCherry.

The one rest of the fluorescence readings were taken after 3 hours of incubation at 37 ℃.

Supplementary Information

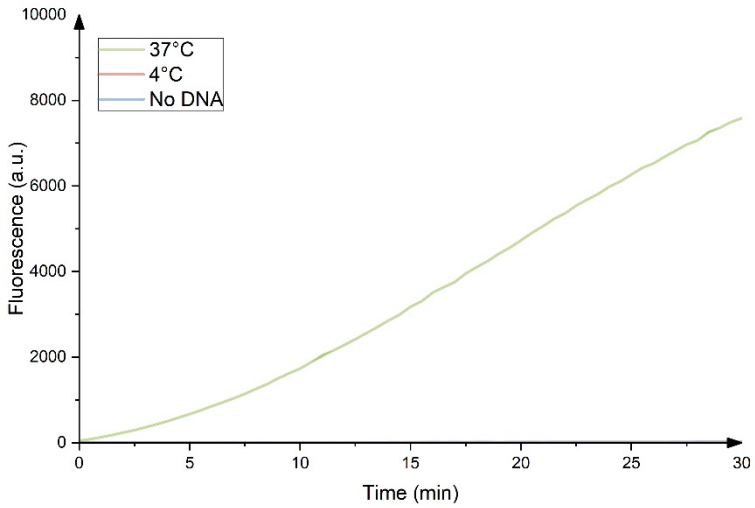

Supplementary Figure 1: β-Gal assay with CUG was conducted and fluorescence was measured over time. The β-Gal enzyme was expressed in the PURExpress IVTT system. The assay reaction was setup with 1mM final concentration of CUG with 0.25 µL of the IVTT expressed β-Gal enzyme. The kinetic cycle was set up to read every 30 seconds for 30 minutes. The assay was conducted at either 37 ℃ or at 4 ℃ in a 384 well plate reader at volume of 80 µL. Excitation=390 nm, emission=460 nm.

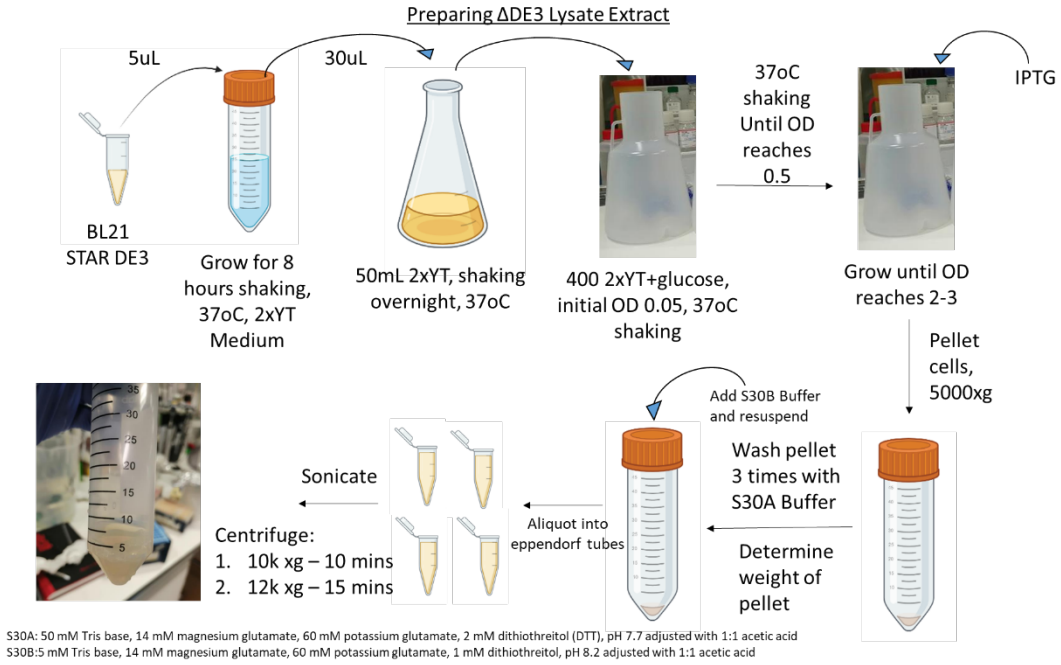

Supplementary Figure 2: Protocol to produce DE3 lysate extract without LacZ gene present in the E.coli genome.

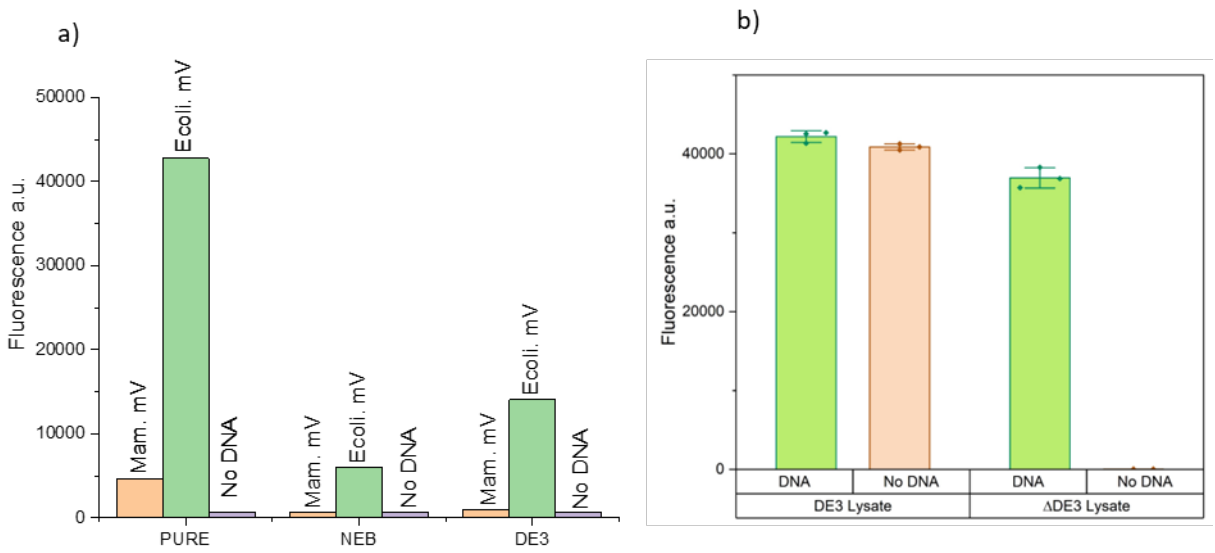

Supplementary Figure 3: Proteins expressed in IVTT systems in-situ; a) Mammalian optimised mVenus (Mam.mV) and E.coli optimised mVenus (Ecoli.mV) were expressed using different IVTT systems- PURExpress (PURE), NEBExpress (NEB) and DE3 lysate extract (DE3). Fluorescence reading was taken after 3 hours. B) β-Gal enzyme synthesised in DE3 lysate extract (with LcZ gene in E.coli genome) and ΔDE3 lysate extract (without LacZ gene in E.coli genome). β-Gal assay with CUG was conducted for 30 minutes which showed that there were no background fluorescence in the ΔDE3 lysate compared to DE3 lysate which had LacZ gene in the E.coli genome.

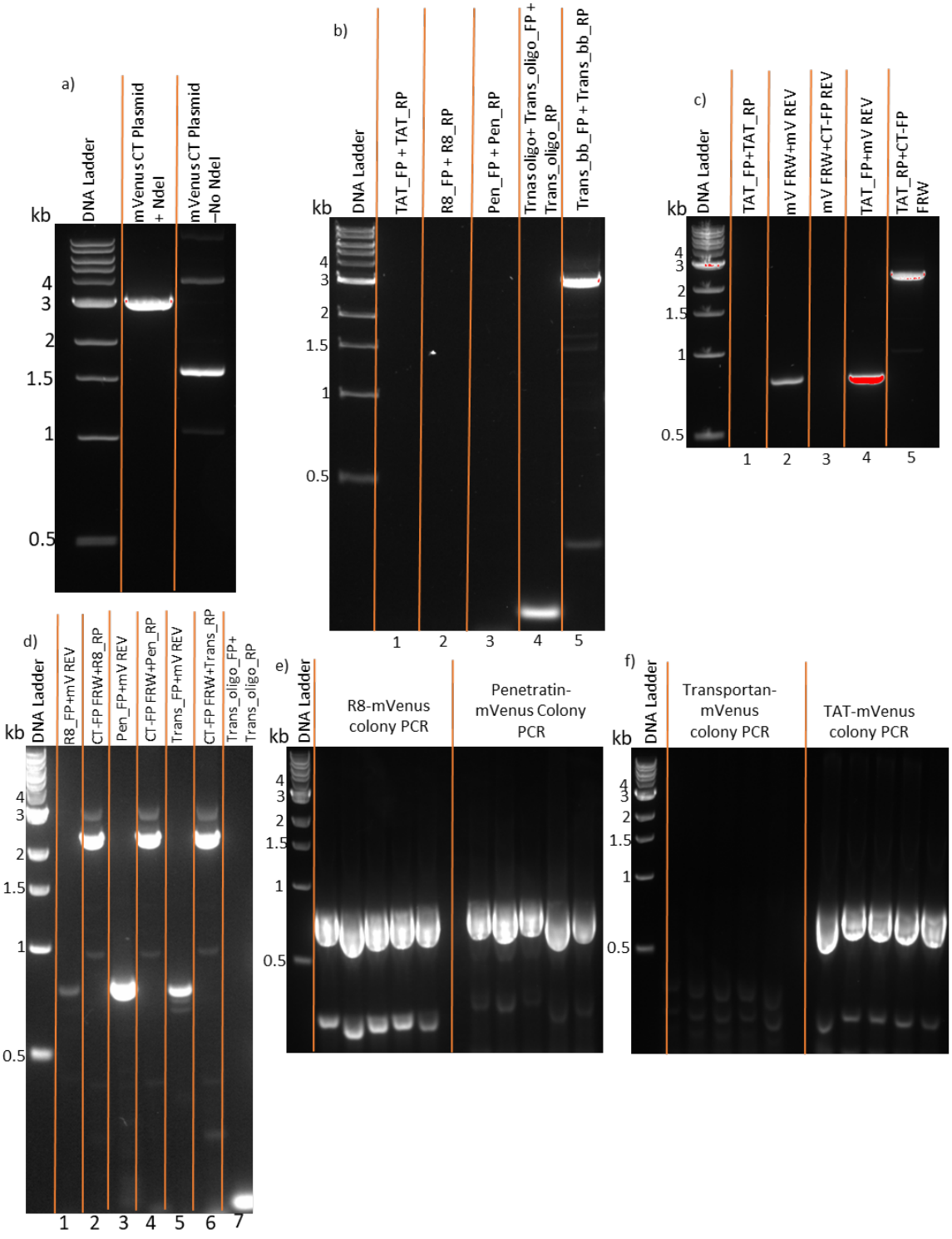

Supplementary Figure 4: DNA gel of PCR products or cut DNA. A) pPURE-mVenus plasmid cut with restriction enzyme NdeI. B, c, d) PCR productsPCR reactions carried out with respected primers. Some reactions were repeated with different conditions. E, f) Colony PCR carried out to test if homologous recombination worked- only transportan did not work.

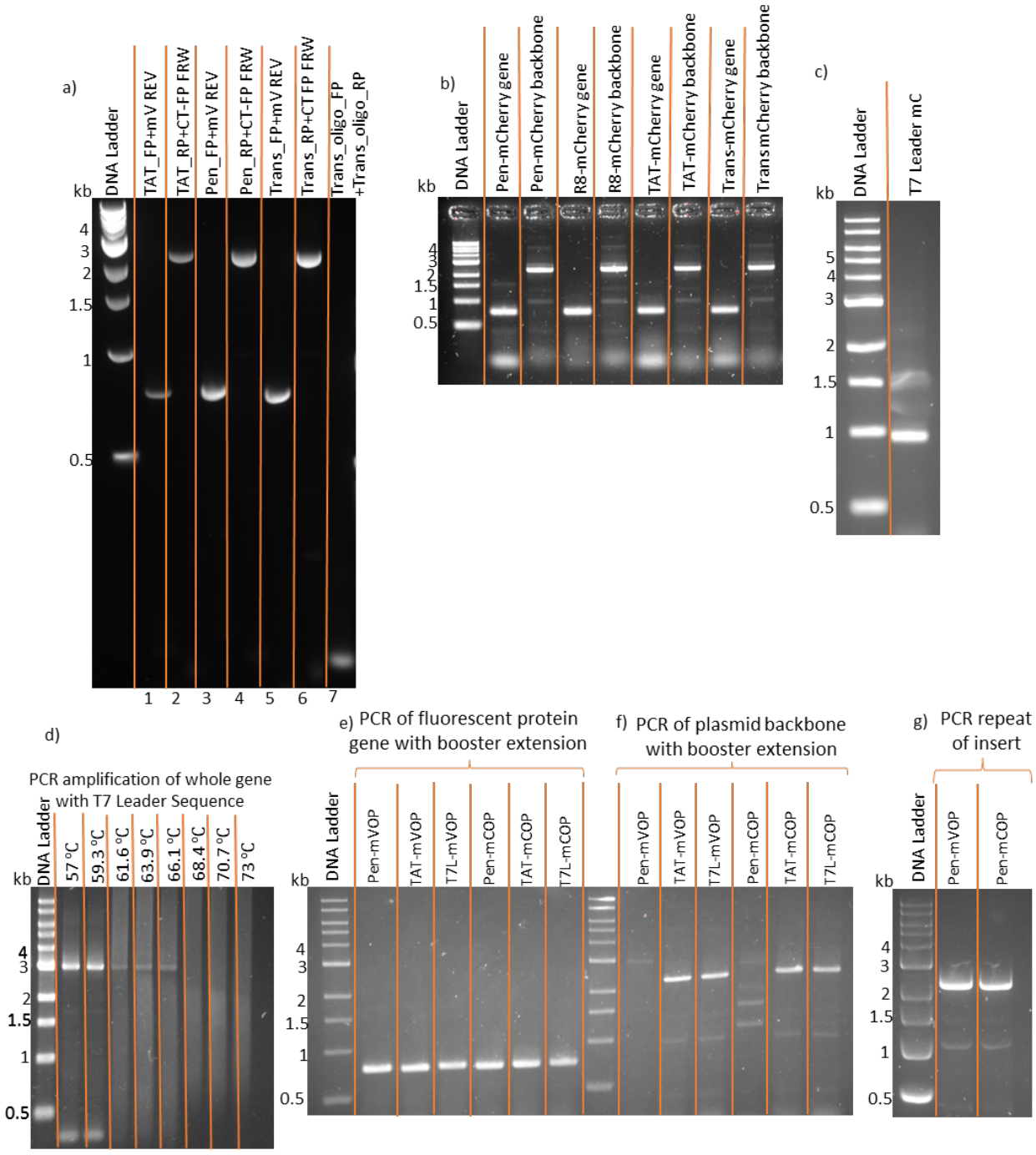

Supplementary Figure 5: DNA gel of PCR products. A) repeat of PCR with respected primers. B, c) PCR of mCherry genes with respected booster sequences. D) optimisation of PCR condition for T7-g10L sequence with mVenus gene. E, g) PCR of E.coli optimised mVenus gene with respected booster sequences.

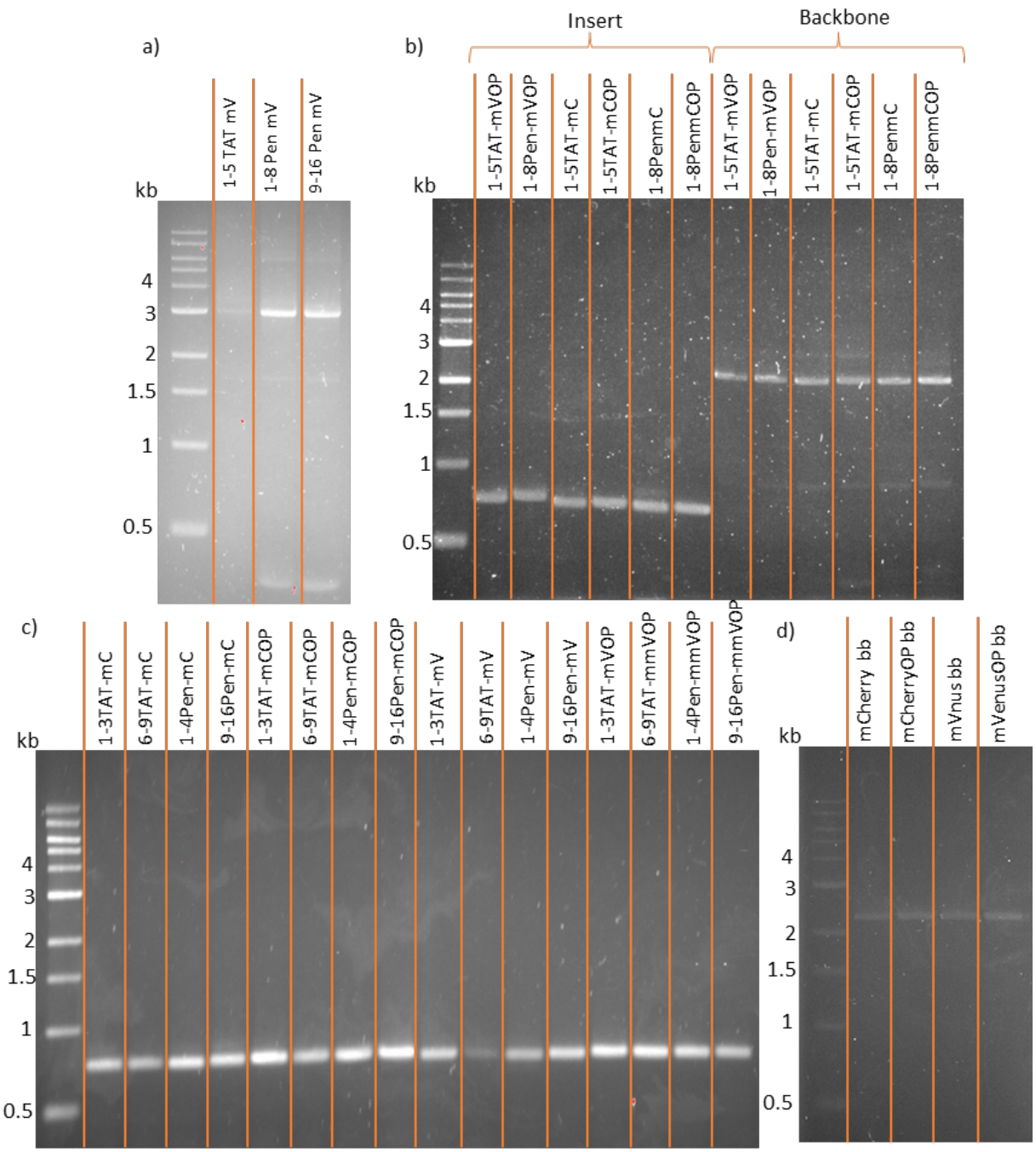

Supplementary Figure 6: DNA gel of PCR products. A) shorter TAT and Pen booster sequences after PCR amplification. B, c) PCR of shorter versions of the booster sequences for E.coli optimised mVenus and mCherry. D) pcr amplification of the pPURE plasmid containing overlaps for homologous recombination.

6.6 Primers Used

Table 5: Primers that were used in this thesis.

Primer Name	DNA Sequence
T7 elong	GAAATTAATACGACTCACTATAGGGTCTAG
CT2_REV	CTGAAAGGAGGAACTATATC
BLctFP	CACTGATTAAGCATTGGTAATGAGGATCCCGGGAATTCTCG
BLAmpRPCOR	CGGAAATGTTGAATACTCATATGTATACCTCCTTCTTAAAG
BLAmpFPCOR	TTTAAGAAGGAGGTATACATATGAGTATTCAACATTTCCGTG
BLAmpRP	CGAGAATTCCCGGGATCCTCATTACCAATGCTTAATCAGTG
LZFP1	CTTTAAGAAGGAGGTATACATATGACCATGATTACGGATTCACTGGC
LZRP2	CGAGAATTCCCGGGATCCTCATTATTTTTGACACCAGACCAAC
FPLacZCT	CCATTACCAGTTGGTCTGGTGTCAAAAATAATGAGGATCCCGGGAATTC
RPLacZCT	GACGGCCAGTGAATCCGTAATCATGGTCATATGTATACCTCCTTC
TAT_FP	ATGCGCAAGAAACGCCGTCAGCGCCGTCGCGTGAGCAAGGGCGAGG
TAT_RP	GCGACGGCGCTGACGGCGTTTCTTGCGCATATGTATACCTCCTTC
Pen_FP	TAAAATTTGGTTTCAGAACCGCCGCATGAAATGGAAGAAAGTGAGCAAG GGC
Pen_RP	TCATGCGGCGGTTCTGAAACCAAATTTTAATCTGGCGCATATGTATACCTC C
R8_FP	ATGCGCCGTCGACGTCGCCGGCGCCGCGTGAGCAAGGGCGAGG
R8_RP	GCGGCGCCGGCGACGTCGACGGCGCATATGTATACCTCCTTC
Transportan oligo	GGCTGGACCCTGAACAGCGCGGGCTATCTGCTGGGCAAAA TTAACCTGAAAGCGCTGGCGGCGCTGGCGAAGAAAATTCTG
Trans_oligo_FP	GAAGGAGGTATACATATGGGCTGGACCCTGAACAGC

Trans_oligo_RP	CCTCGCCCTTGCTCACCAGAATTTTCTTCGCCAG
Trans_bb_FP	CTGGCGAAGAAAATTCTGGTGAGCAAGGGCGAGG
Trans_bb_RP	GCTGTTCAGGGTCCAGCCCATATGTATACCTCCTTC
mV FRW	TTAACTTTAAGAAGGAGGTATACATATGGTGAGCAAGGGCGAGGAGCTG T
mV REV	TACTCGAGAATTCCCGGGATCCTCATTACTTGTACAGCTCGTCCATGCCG
CT-FP FRW	CGGCATGGACGAGCTGTACAAGTAATGAGGATCCCGGGAATTCTCGAGTA
CT-FP REV	ACAGCTCCTCGCCCTTGCTCACCATATGTATACCTCCTTCTTAAAGTTAAAC
T7_elong_FP	GAAATTAATACGACTCACTATAGGGTCTAG
CT2_RP	CTGAAAGGAGGAACTATATC
mVT710Lrp	CCATATGTTGCTGTCCACCAGTCATGCTAGCCATGGTATATCTCCTTCTTAA AGTTAA
Pen1to8mVFP	CATATGCGCCAGATTAAAATTTGGTTTCAGGTGAGCAAGGGCGAGG
Pen1to8mVRP	CACCTGAAACCAAATTTTAATCTGGCGCATATGTATACCTCCTTC
Pen9to16mVFP	CATATGAACCGCCGCATGAAATGGAAGAAAGTGAGCAAGGGCGAGG
Pen9to16mVRP	CACTTTCTTCCATTTCATGCGGCGGTTCATATGTATACCTCCTTC
TAT1to5mVFP	GTATACATATGCGCAAGAAACGCCGTGTGAGCAAGGGCGAG
TAT1to5mVRP	CTTGCTCACACGGCGTTTCTTGCGCATATGTATACCTCCTTC
N-mCTransFP	CTTTAAGAAGGAGGTATACATATGGGCTGGACCCTGAACAGCGC
N-mCTransBBRP	GCGCTGTTCAGGGTCCAGCCCATATGTATACCTCCTTCTTAAAG
mCBBFP	TGGACGAGCTGTACAAGTAATGAGGATCCCGGGAATTCTC
mCRP	GAGAATTCCCGGGATCCTCATTACTTGTACAGCTCGTCCA
mVBBFP	CTCGGCATGGACGAGCTGTACAAGTAATGAGGATCCCGGGAATTC
mVinsertRP	GAGAATTCCCGGGATCCTCATTACTTGTACAGCTCGTCCATG
mCOPctBBfp	CCGGTGGTATGGATGAACTGTATAAATAATGAGGATCCCGGGAATTC

mCOPinsertRP	CGAGAATTCCCGGGATCCTCATTATTTATACAGTTCATCCATACC
mVOPbbFP	GGCATGGACGAGCTGTACAAGTAATGAGGATCCCGGGAATTCTCGAG
mVOPinsertRP	CAGGTTAACCTTACTCGAGAATTCCCGGGATCCTCATTACTTGTACAGC
Pen_mCOPfp	TGGTTTCAGAACCGCCGCATGAAATGGAAGAAAGTGAGCAAAGGTGAAG AGG
TAT_mCOPfp	CATATGCGCAAGAAACGCCGTCAGCGCCGTCGCGTGAGCAAAGGTGAAG AGG
T7L_mCOPfp	ATATACCATGGCTAGCATGACTGGTGGACAGCAACATATGGTGAGCAAAG GTGAAGAGG
TAT_mVOPfp	ATGCGCAAGAAACGCCGTCAGCGCCGTCGCGTGAGTAAAGGTGAAG
T7L_mVOPfp	GATATACCATGGCTAGCATGACTGGTGGACAGCAACATATGGTGAGTAAA GGTGAAG
Pen-mVOPfp	TAAAATTTGGTTTCAGAACCGCCGCATGAAATGGAAGAAAGTGAGTAAAG GTGAAG
N-mCPenRP	GCGGCGGTTCTGAAACCAAATTTTAATCTGGCGCATATGTATACCTCCTTC TT
N-mCTATRP	CGCGACGGCGCTGACGGCGTTTCTTGCGCATATGTATACCTCCTTCTTAAA G
mCT7LinsertRP	TGCTGTCCACCAGTCATGCTAGCCATGGTATATCTCCTTCTTAAAGTTAAAC
N-mCTransFP	CTTTAAGAAGGAGGTATACATATGGGCTGGACCCTGAACAGCGC
N-mCTransBBRP	GCGCTGTTCAGGGTCCAGCCCATATGTATACCTCCTTCTTAAAG
N-mCR8RP	ACGCGGCGCCGGCGACGTCGACGGCGCATATGTATACCTCCTTCTTAAAG
15TAT_mVOPinsertFP	GGTATACATATGCGCAAGAAACGCCGTGTGAGTAAAGGTGA
15TAT_mVOPbbRP	CTTTACTCACACGGCGTTTCTTGCGCATATGTATACCTCCTTC
18Pen_mVOPinsertFP	CATATGCGCCAGATTAAAATTTGGTTTCAGGTGAGTAAAGGTGAAG

18Pen_mVOPbbRP	CACCTGAAACCAAATTTTAATCTGGCGCATATGTATACCTC
15TAT-mCinsertFP	GTATACATATGCGCAAGAAACGCCGTGTGAGCAAGGGCGAG
15TAT_mCBBrp	CTTGCTCACACGGCGTTTCTTGCGCATATGTATACCTCCTTC
15TAT_mCOPinsertFP	GAGGTATACATATGCGCAAGAAACGCCGTGTGAGCAAAGGTG
15TAT_mCOPbbRP	CTTTGCTCACACGGCGTTTCTTGCGCATATGTATACCTCCTTC
18Pen_mCinsertFP	CATATGCGCCAGATTAAAATTTGGTTTCAGGTGAGCAAGGGCGAGG
18Pen_mCbbRP	ACCTGAAACCAAATTTTAATCTGGCGCATATGTATACCTCCTTC
18Pen_mCOPinsertFP	CATATGCGCCAGATTAAAATTTGGTTTCAGGTGAGCAAAGGTG
18Pen_mCOPbbRP	CCTGAAACCAAATTTTAATCTGGCGCATATGTATACCTCCTTC
Trans_mCOPinsertFP	GCGCTGGCGAAGAAAATTCTGGTGAGCAAAGGTGAAGAGG
Trans_mCOPamplifyRP	CCTCTTCACCTTTGCTCACCAGAATTTTCTTCGCCAGCGC
R8_mCOPinsertFP	CATATGCGCCGTCGACGTCGCCGGCGCCGCGTGAGCAAAGGTGAAGAGG
Trans_mVOPinsertFP	GCGCTGGCGAAGAAAATTCTGGTGAGTAAAGGTGAAGAAC
Trans_mVamplifyRP	GTTCTTCACCTTTACTCACCAGAATTTTCTTCGCCAGCGC
R8_mVOPinsertFP	CATATGCGCCGTCGACGTCGCCGGCGCCGCGTGAGTAAAGGTGAAGAAC
ctBBRP	ATGTATACCTCCTTCTTAAAGTTAAACAAAATTATTTCTAG
13TATmCinsertFP	CTTTAAGAAGGAGGTATACATATGCGCAAGAAAGTGAGCAAGGGCGAGG AGG
69TATmCinsertFP	CTTTAAGAAGGAGGTATACATATGCAGCGCCGTCGCGTGAGCAAGGGCG AGGAG
14PenmCinsertFP	GAAGGAGGTATACATATGCGCCAGATTAAAGTGAGCAAGGGCGAGG
9_16PenmCinsertFP	GGAGGTATACATATGAACCGCCGCATGAAATGGAAGAAAGTGAGCAAGG GCGAGG
13TATmCOPinsertFP	CTTTAAGAAGGAGGTATACATATGCGCAAGAAAGTGAGCAAAGGTGAAG

69TATmCOPinsertFP	CTTTAAGAAGGAGGTATACATATGCAGCGCCGTCGCGTGAGCAAAGGTGAAG
14PenmCOPinsertFP	CTTTAAGAAGGAGGTATACATATGCGCCAGATTAAAGTGAGCAAAGGTGAAGAG
916PenOPmCinsertFP	GGAGGTATACATATGAACCGCCGCATGAAATGGAAGAAAGTGAGCAAAGGTGAAG
13TATmVinsertFP	CTTTAAGAAGGAGGTATACATATGCGCAAGAAAGTGAGCAAGGGCGAGG
69TATmVinsertFP	GAAGGAGGTATACATATGCAGCGCCGTCGCGTGAGCAAGGGCGAGGAGC
14PenmVinsertFP	GAAGGAGGTATACATATGCGCCAGATTAAAGTGAGCAAGGGCGAGG
916PenmVinsertFP	GGAGGTATACATATGAACCGCCGCATGAAATGGAAGAAAGTGAGCAAGGGCGAGG
13TATmVOinsertPFP	AGAAGGAGGTATACATATGCGCAAGAAAGTGAGTAAAGGTGAAG
69TATmVOPinsertFP	GAAGGAGGTATACATATGCAGCGCCGTCGCGTGAGTAAAGGTGAAG
14PenOPmVinsertFP	CTTTAAGAAGGAGGTATACATATGCGCCAGATTAAAGTGAGTAAAGGTG
9_16PenmVOPinsertFP	GGAGGTATACATATGAACCGCCGCATGAAATGGAAGAAAGTGAGTAAAGGTGAAG

References

1. Zhao J, Zhang Y, Zhang X, et al. Artificial cells: building bioinspired systems using small-scale biology. *Anal Chem*. 2022;94(9):3811-3818. doi:10.1021/acs.analchem.1c04696

2. Noireaux V, Maeda YT, Libchaber A. Development of an artificial cell, from self-organization to computation and self-reproduction. *Proc Natl Acad Sci U S A*. 2011;108(9):3473-3480. doi:10.1073/pnas.1017075108

3. Smith JM, Chowdhry R, Booth MJ. Controlling Synthetic Cell-Cell Communication. *Front Mol Biosci*. 2022;8(January):1-9. doi:10.3389/fmolb.2021.809945

4. Browning ST, Shuler ML. Towards the development of a minimal cell model by generalization of a model of Escherichia coli: Use of dimensionless rate Parameters. *Biotechnol Bioeng*. 2001;76(3):187-192. doi:10.1002/bit.10007

5. Solé R V. Evolution and self-assembly of protocells. *Int J Biochem Cell Biol*. 2009;41(2):274-284. doi:10.1016/j.biocel.2008.10.004

6. Stano P. Gene Expression Inside Liposomes: From Early Studies to Current Protocols. *Chem - A Eur J*. 2019;25(33):7798-7814. doi:10.1002/chem.201806445

7. Booth MJ, Restrepo Schild V, Box SJ, Bayley H. Light-patterning of synthetic tissues with single droplet resolution. *Sci Rep*. 2017;7(1):1-10. doi:10.1038/s41598-017-09394-9

8. Rideau E, Dimova R, Schwille P, Wurm FR, Landfester K. Liposomes and polymersomes: a comparative review towards cell mimicking. *Chem Soc Rev*. 2018;47(23):8572-8610. doi:10.1039/c8cs00162f

9. Huang X, Li M, Green DC, Williams DS, Patil AJ, Mann S. Interfacial assembly of protein-polymer nano-conjugates into stimulus-responsive biomimetic protocells. *Nat Commun*. 2013;4(May):1-9. doi:10.1038/ncomms3239

10. Branco MC, Schneider JP. Self-assembling materials for therapeutic delivery. *Acta Biomater*. 2009;5(3):817-831. doi:10.1016/J.ACTBIO.2008.09.018

11. Paleos CM, Tsiourvas D, Sideratou Z, Pantos A. Formation of artificial multicompartment vesosome and dendrosome as prospected drug and gene delivery carriers. *J Control Release*. 2013;170(1):141-152. doi:10.1016/j.jconrel.2013.05.011

12. Amidi M, de Raad M, Crommelin DJA, Hennink WE, Mastrobattista E. Antigen-expressing immunostimulatory liposomes as a genetically programmable synthetic vaccine. *Syst Synth Biol*. 2011;5(1):21-31. doi:10.1007/s11693-010-9066-z

13. Mobed M, Chang TMS. Preparation And Surface Characterization Of Carboxymethylchitin-Incorporated Submicron Bilayer-Lipid Membrane Artificial Cells (Liposomes) Encapsulating Hemoglobin. *Biomater Artif Cells Immobil Biotechnol*. 1991;19(4):731-744. doi:10.3109/10731199109117851

14. Jeong S, Nguyen HT, Kim CH, Ly MN, Shin K. Toward Artificial Cells : Novel Advances in Energy Conversion and Cellular Motility. 2020;1907182:1-26. doi:10.1002/adfm.201907182

15. Deshpande PP, Biswas S, Torchilin VP. Current trends in the use of liposomes for tumor targeting. *Nanomedicine*. 2013;8(9):1509-1528. doi:10.2217/nnm.13.118

16. Roeder RG. The role of general initiation factors in transcription by RNA polymerase II. *Trends Biochem Sci*. 1996;21(9):327-335. doi:10.1016/0968-0004(96)10050-5

17. Weake VM, Workman JL. Inducible gene expression: Diverse regulatory mechanisms. *Nat Rev Genet*. 2010;11(6):426-437. doi:10.1038/nrg2781

18. Browning DF, Busby SJW. The regulation of bacterial transcription initiation. *Nat Rev Microbiol*. 2004;2(1):57-65. doi:10.1038/nrmicro787

19. Kohler R, Mooney RA, Mills DJ, Landick R, Cramer P. Architecture of a transcribing-translating expressome. 2017;197(April):194-197.

20. Shine J, Dalgarno L. The 3' terminal sequence of Escherichia coli 16S ribosomal RNA: complementarity to nonsense triplets and ribosome binding sites. *Proc Natl Acad Sci U S A*. 1974;71(4):1342-1346. doi:10.1073/pnas.71.4.1342

21. Rodnina M V. Translation in Prokaryotes. 2018:1-21. doi:10.1101/cshperspect.a032664

22. Xu B, Liu L, Song G. Functions and Regulation of Translation Elongation Factors. *Front Mol Biosci*. 2022;8(January):1-20. doi:10.3389/fmolb.2021.816398

23. Milligan JF, Groebe DR, Whherell GW, Uhlenbeck OC. Oligoribonucleotide synthesis using T7 RNA polymerase and synthetic DNA templates. *Nucleic Acids Res*. 1987;15(21):8783-8798.

24. Garamella J, Marshall R, Rustad M, Noireaux V. The All E. coli TX-TL Toolbox 2.0: A Platform for Cell-Free Synthetic Biology. *ACS Synth Biol*. 2016;5(4):344-355. doi:10.1021/acssynbio.5b00296

25. Garenne D, Noireaux V. Cell-free transcription–translation: engineering biology from the nanometer to the millimeter scale. *Curr Opin Biotechnol*. 2019;58(Figure 1):19-27. doi:10.1016/j.copbio.2018.10.007

26. Silverman AD, Karim AS, Jewett MC. Cell-free gene expression: an expanded repertoire of applications. *Nat Rev Genet*. 2020;21(3):151-170. doi:10.1038/s41576-019-0186-3

27. Wilding KM, Hunt JP, Wilkerson JW, et al. Endotoxin-Free E. coli-Based Cell-Free Protein Synthesis: Pre-Expression Endotoxin Removal Approaches for on-Demand Cancer Therapeutic Production. *Biotechnol J*. 2019;14(3). doi:10.1002/biot.201800271

28. Adiga R, Al-adhami M, Andar A, et al. Point-of-care production of therapeutic proteins of good-manufacturing-practice quality. *Nat Biomed Eng*. 2018;2(9):675-686. doi:10.1038/s41551-018-0259-1

29. Shin J, Jardine P, Noireaux V. Genome replication, synthesis, and assembly of the bacteriophage T7 in a single cell-Free reaction. *ACS Synth Biol*. 2012;1(9):408-413. doi:10.1021/sb300049p

30. Rustad M, Eastlund A, Jardine P, Noireaux V. Cell-free TXTL synthesis of infectious bacteriophage T4 in a single test tube reaction. *Synth Biol*. 2018;3(1):1-7. doi:10.1093/synbio/ysy002

31. Shimizu Y, Inoue A, Tomari Y, et al. Cell-free translation reconstituted with purified components. *Nat Biotechnol*. 2001;19(8):751-755. doi:10.1038/90802

32. Szakács G, Paterson JK, Ludwig JA, Booth-Genthe C, Gottesman MM. Targeting multidrug resistance in cancer. *Nat Rev Drug Discov*. 2006;5(3):219-234. doi:10.1038/nrd1984

33. Kunjachan S, Ehling J, Storm G, Kiessling F, Lammers T. Noninvasive Imaging of Nanomedicines and Nanotheranostics: Principles, Progress, and Prospects. *Chem Rev*. 2015;115(19):10907-10937. doi:10.1021/cr500314d

34. Wu J. The enhanced permeability and retention (Epr) effect: The significance of the concept and methods to enhance its application. *J Pers Med*. 2021;11(8). doi:10.3390/jpm11080771

35. Maeda H. The enhanced permeability and retention (EPR) effect in tumor vasculature: The key role of tumor-selective macromolecular drug targeting. *Adv Enzyme Regul*. 2001;41(1):189-207. doi:10.1016/S0065-2571(00)00013-3

36. Dymek M, Sikora E. Liposomes as biocompatible and smart delivery systems – the current state. *Adv Colloid Interface Sci*. 2022;309(February). doi:10.1016/j.cis.2022.102757

37. Akbarzadeh A, Rezaei-Sadabady R, Davaran S, et al. Liposome: Classification, preparation, and applications. *Nanoscale Res Lett*. 2013;8(1):1. doi:10.1186/1556-276X-8-102

38. Inglut CT, Sorrin AJ, Kuruppu T, et al. Immunological and toxicological considerations for the design of liposomes. *Nanomaterials*. 2020;10(2). doi:10.3390/nano10020190

39. Ta T, Porter TM. Thermosensitive liposomes for localized delivery and triggered release of chemotherapy. *J Control Release*. 2013;169(1-2):112-125. doi:10.1016/j.jconrel.2013.03.036

40. Barenholz Y. Doxil® - The first FDA-approved nano-drug: Lessons learned. *J Control Release*. 2012;160(2):117-134. doi:10.1016/j.jconrel.2012.03.020

41. Safra T. Cardiac Safety of Liposomal Anthracyclines. *Oncologist*. 2003;8(S2):17-24. doi:10.1634/theoncologist.8-suppl_2-17

42. Laginha KM, Verwoert S, Charrois GJR, Allen TM. Determination of doxorubicin levels

in whole tumor and tumor nuclei in murine breast cancer tumors. *Clin Cancer Res*. 2005;11(19 I):6944-6949. doi:10.1158/1078-0432.CCR-05-0343

43. Dellapasqua S, Aliaga PT, Munzone E, et al. Pegylated liposomal doxorubicin (Caelyx®) as adjuvant treatment in early-stage luminal b-like breast cancer: A feasibility phase II trial. *Curr Oncol*. 2021;28(6):5167-5178. doi:10.3390/curroncol28060433

44. Collier MA, Bachelder EM, Ainslie KM. Electrosprayed Myocet-like Liposomes: An Alternative to Traditional Liposome Production. *Pharm Res*. 2017;34(2):419-426. doi:10.1007/s11095-016-2072-4

45. Fulton MD, Najahi-missaoui W. Liposomes in Cancer Therapy : How Did We Start and Where Are We Now. 2023.

46. Tomanin R, Scarpa M. Why Do We Need New Gene Therapy Viral Vectors? Characteristics, Limitations and Future Perspectives of Viral Vector Transduction. *Curr Gene Ther*. 2004;4(4):357-372. doi:http://dx.doi.org/10.2174/1566523043346011

47. Sung YK, Kim SW. Recent advances in the development of gene delivery systems. *Biomater Res*. 2019;23(1):1-7. doi:10.1186/s40824-019-0156-z

48. Rampioni G, D'Angelo F, Messina M, et al. Synthetic cells produce a quorum sensing chemical signal perceived by: Pseudomonas aeruginosa. *Chem Commun*. 2018;54(17):2090-2093. doi:10.1039/c7cc09678j

49. Kaczmarek JC, Kowalski PS, Anderson DG. Advances in the delivery of RNA therapeutics: From concept to clinical reality. *Genome Med*. 2017;9(1):1-17. doi:10.1186/s13073-017-0450-0

50. Yoo J, Park C, Yi G, Lee D, Koo H. Active targeting strategies using biological ligands for

nanoparticle drug delivery systems. *Cancers (Basel)*. 2019;11(5). doi:10.3390/cancers11050640

51. Taléns-Visconti R, Díez-Sales O, de Julián-Ortiz JV, Nácher A. Nanoliposomes in Cancer Therapy: Marketed Products and Current Clinical Trials. *Int J Mol Sci*. 2022;23(8). doi:10.3390/ijms23084249

52. Gabizon AA, Shmeeda H, Zalipsky S. Pros and cons of the liposome platform in cancer drug targeting. *J Liposome Res*. 2006;16(3):175-183. doi:10.1080/08982100600848769

53. Koning GA, Eggermont AMM, Lindner LH, Ten Hagen TLM. Hyperthermia and thermosensitive liposomes for improved delivery of chemotherapeutic drugs to solid tumors. *Pharm Res*. 2010;27(8):1750-1754. doi:10.1007/s11095-010-0154-2

54. Carreño F, Paese K, Silva CM, Guterres SS, Dalla Costa T. Pre-clinical investigation of the modulation of quetiapine plasma pharmacokinetics and tissues biodistribution by lipid-core nanocapsules. *J Pharm Biomed Anal*. 2016;119:152-158. doi:10.1016/j.jpba.2015.11.027

55. Mura S, Nicolas J, Couvreur P. Stimuli-responsive nanocarriers for drug delivery. *Nat Mater*. 2013;12(11):991-1003. doi:10.1038/nmat3776

56. Ponce A, Wright A, Dewhirst M, Needham D. Targeted bioavailability of drugs by triggered release from liposomes. *Future Lipidol*. 2006;1(1):25-34. doi:10.2217/17460875.1.1.25

57. Bibi S, Lattmann E, Mohammed AR, Perrie Y. Trigger release liposome systems: Local and remote controlled delivery? *J Microencapsul*. 2012;29(3):262-276. doi:10.3109/02652048.2011.646330

58. Kaasgaard T, Andresen TL. Liposomal cancer therapy: Exploiting tumor characteristics. *Expert Opin Drug Deliv*. 2010;7(2):225-243. doi:10.1517/17425240903427940

59. Silva R, Ferreira H, Cavaco-Paulo A. Sonoproduction of liposomes and protein particles as templates for delivery purposes. *Biomacromolecules*. 2011;12(10):3353-3368. doi:10.1021/bm200658b

60. Torchilin VP. Multifunctional, stimuli-sensitive nanoparticulate systems for drug delivery. *Nat Rev Drug Discov*. 2014;13(11):813-827. doi:10.1038/nrd4333

61. Farooque F, Wasi M, Mughees MM. Liposomes as Drug Delivery System: An Updated Review. *J Drug Deliv Ther*. 2021;11(5-S):149-158. doi:10.22270/jddt.v11i5-s.5063

62. GREGORIADIS G, NEERUNJUN DE. Control of the Rate of Hepatic Uptake and Catabolism of Liposome-Entrapped Proteins Injected into Rats. Possible Therapeutic Applications. *Eur J Biochem*. 1974;47(1):179-185. doi:10.1111/j.1432-1033.1974.tb03681.x

63. Kamps JAAM, Morselt HWM, Swart PJ, Meijer DKF, Scherphof GL. Massive targeting of liposomes, surface-modified with anionized albumins, to hepatic endothelial cells. *Proc Natl Acad Sci U S A*. 1997;94(21):11681-11685. doi:10.1073/pnas.94.21.11681

64. Sercombe L, Veerati T, Moheimani F, Wu SY, Hua S. Advances and Challenges of Liposome Assisted Drug Delivery. 2015;6(December):1-13. doi:10.3389/fphar.2015.00286

65. Gheibi Hayat SM, Jaafari MR, Hatamipour M, Jamialahmadi T, Sahebkar A. *Harnessing CD47 Mimicry to Inhibit Phagocytic Clearance and Enhance Anti-Tumor Efficacy of Nanoliposomal Doxorubicin*. Vol 17. Taylor & Francis; 2020.

doi:10.1080/17425247.2020.1772749

66. Solomon R, Gabizon AA. Clinical pharmacology of liposomal anthracyclines: Focus on pegylated liposomal doxorubicin. *Clin Lymphoma Myeloma*. 2008;8(1):21-32. doi:10.3816/CLM.2008.n.001

67. Cumming EE, Diamond AW. The cellular and molecular basis of hyperthermia Bert. *Can Field-Naturalist*. 2002;116(1):69-75.

68. Colombo R, Da Pozzo LF, Salonia A, et al. Multicentric study comparing intravesical chemotherapy alone and with local microwave hyperthermia for prophylaxis of recurrence of superficial transitional cell carcinoma. *J Clin Oncol*. 2003;21(23):4270-4276. doi:10.1200/JCO.2003.01.089

69. Kneidl B, Peller M, Winter G, Lindner LH, Hossann M. Thermosensitive liposomal drug delivery systems: state of the art review. *Int J Nanomedicine*. 2014;9:4387-4398. doi:10.2147/IJN.S49297

70. Hauck ML, La Rue SM, Petros WP, et al. Phase I trial of doxorubicin-containing low temperature sensitive liposomes in spontaneous canine tumors. *Clin Cancer Res*. 2006;12(13):4004-4010. doi:10.1158/1078-0432.CCR-06-0226

71. Wust P, Hildebrandt B, Sreenivasa G, et al. Hyperthermia in combined treatment of cancer. *Lancet Oncol*. 2002;3(8):487-497. doi:10.1016/S1470-2045(02)00818-5

72. De Smet M, Heijman E, Langereis S, Hijnen NM, Grüll H. Magnetic resonance imaging of high intensity focused ultrasound mediated drug delivery from temperature-sensitive liposomes: An in vivo proof-of-concept study. *J Control Release*. 2011;150(1):102-110. doi:10.1016/j.jconrel.2010.10.036

73. Kelsey C. Martin Mhatre V. Ho J-AL, Ruben Martin and Stephen L. Buchwald, Mhatre V. Ho and Kelsey C. Martin J-AL, Craik C, Manuscript A, Kantrowitz. Image-guided drug delivery with magnetic resonance guided high intensity focused ultrasound and temperature sensitive liposomes in a rabbit Vx2 tumor model. *Bone*. 2008;23(1):1-7. doi:10.1016/j.jconrel.2011.12.011.Image-guided

74. Gomes IP, Duarte JA, Maia ALC, et al. Thermosensitive nanosystems associated with hyperthermia for cancer treatment. *Pharmaceuticals*. 2019;12(4). doi:10.3390/ph12040171

75. Al-Ahmady Z, Kostarelos K. Chemical Components for the Design of Temperature-Responsive Vesicles as Cancer Therapeutics. *Chem Rev*. 2016;116(6):3883-3918. doi:10.1021/acs.chemrev.5b00578

76. Needham D, Anyarambhatla G, Kong G, Dewhirst MW. A new temperature-sensitive liposome for use with mild hyperthermia: Characterization and testing in a human tumor xenograft model. *Cancer Res*. 2000;60(5):1197-1201.

77. Kono K. Thermosensitive polymer-modified liposomes. *Adv Drug Deliv Rev*. 2001;53(3):307-319. doi:10.1016/S0169-409X(01)00204-6

78. Preiss MR, Bothun GD. Stimuli-responsive liposome-nanoparticle assemblies. *Expert Opin Drug Deliv*. 2011;8(8):1025-1040. doi:10.1517/17425247.2011.584868

79. Volodkin D V., Skirtach AG, Möhwald H. Near-IR remote release from assemblies of liposomes and nanoparticles. *Angew Chemie - Int Ed*. 2009;48(10):1807-1809. doi:10.1002/anie.200805572

80. Torchilin V. Antibody-modified liposomes for cancer chemotherapy. *Expert Opin Drug*

Deliv. 2008;5(9):1003-1025. doi:10.1517/17425247.5.9.1003

81. Mamot C, Drummond DC, Noble CO, et al. Epidermal growth factor receptor-targeted immunoliposomes significantly enhance the efficacy of multiple anticancer drugs in vivo. *Cancer Res*. 2005;65(24):11631-11638. doi:10.1158/0008-5472.CAN-05-1093

82. Yatvin M, Weinstein J, Dennis W, Blumenthal R. Design of liposomes for enhanced local release of drugs by hyperthermia. *Science (80-)*. 1978;202(4374):1290-1293. doi:10.1126/science.364652

83. Nibu Y, Inoue T, Motoda I. Effect of headgroup type on the miscibility of homologous phospholipids with different acyl chain lengths in hydrated bilayer. *Biophys Chem*. 1995;56(3):273-280. doi:10.1016/0301-4622(95)00041-U

84. Dou Y, Hynynen K, Allen C. To heat or not to heat: Challenges with clinical translation of thermosensitive liposomes. *J Control Release*. 2017;249:63-73. doi:10.1016/j.jconrel.2017.01.025

85. Li L, ten Hagen TLM, Schipper D, et al. Triggered content release from optimized stealth thermosensitive liposomes using mild hyperthermia. *J Control Release*. 2010;143(2):274-279. doi:10.1016/j.jconrel.2010.01.006

86. Anyarambhatla GR, Needham D. Enhancement of the phase transition permeability of DPPC liposomes by incorporation of MPPC: A new temperature-sensitive liposome for use with mild hyperthermia. *J Liposome Res*. 1999;9(4):491-506. doi:10.3109/08982109909035549

87. Chung AH, Jolesz FA, Hynynen K. Thermal dosimetry of a focused ultrasound beam in vivo by magnetic resonance imaging. *Med Phys*. 1999;26(9):2017-2026.

doi:10.1118/1.598707

88. McDannold N, Hynynen K, Wolf D, Wolf G, Jolesz F. MRI evaluation of thermal ablation of tumors with focused ultrasound. *J Magn Reson Imaging*. 1998;8(1):91-100. doi:10.1002/jmri.1880080119

89. Kong G, Anyarambhatla G, Petros WP, et al. Efficacy of liposomes and hyperthermia in a human tumor xenograft model: Importance of triggered drug release. *Cancer Res*. 2000;60(24):6950-6957.

90. Needham D, Park JY, Wright AM, Tong J. Materials characterization of the low temperature sensitive liposome (LTSL): Effects of the lipid composition (lysolipid and DSPE-PEG2000) on the thermal transition and release of doxorubicin. *Faraday Discuss*. 2012;161:515-534. doi:10.1039/c2fd20111a

91. Landon CD, Park JY, Needham D, Dewhirst MW. Nanoscale drug delivery and hyperthermia: The materials design and preclinical and clinical testing of low temperature-sensitive liposomes used in combination with mild hyperthermia in the treatment of local cancer. *Open Nanomed J*. 2011;3(SPEC. ISSUE):38-64. doi:10.2174/1875933501103010038

92. Tristram-Nagle S, Wiener MC, Yang CP, Nagle JF. Kinetics of the Subtransition in Dipalmitoylphosphatidylcholine. *Biochemistry*. 1987;26(14):4288-4294. doi:10.1021/bi00388a016

93. Haest CWM, De Gier J, Van Es GA, Verkleij AJ, Van Deenen LLM. Fragility of the permeability barrier of Escherichia coli. *BBA - Biomembr*. 1972;288(1):43-53. doi:10.1016/0005-2736(72)90221-0

94. Goudsmit SA. Model of interfacial melting. *Phys Rev Lett*. 1967;18(9):301. doi:10.1103/PhysRevLett.18.301

95. Winter ND, Murphy RKJ, O'Halloran T V., Schatz GC. Development and modeling of arsenic-trioxide-loaded thermosensitive liposomes for anticancer drug delivery. *J Liposome Res*. 2011;21(2):106-115. doi:10.3109/08982104.2010.483597

96. López-Noriega A, Ruiz-Hernández E, Quinlan E, Storm G, Hennink WE, O'Brien FJ. Thermally triggered release of a pro-osteogenic peptide from a functionalized collagen-based scaffold using thermosensitive liposomes. *J Control Release*. 2014;187:158-166. doi:10.1016/j.jconrel.2014.05.043

97. Bangham AD, Horne RW. Negative staining of phospholipids and their structural modification by surface-active agents as observed in the electron microscope. *J Mol Biol*. 1964;8(5):660-668. doi:10.1016/S0022-2836(64)80115-7

98. Hope MJ, Bally MB, Webb G, Cullis PR. Production of large unilamellar vesicles by a rapid extrusion procedure. Characterization of size distribution, trapped volume and ability to maintain a membrane potential. *BBA - Biomembr*. 1985;812(1):55-65. doi:10.1016/0005-2736(85)90521-8

99. Pautot S, Frisken BJ, Weitz DA. Production of unilamellar vesicles using an inverted emulsion. *Langmuir*. 2003;19(7):2870-2879. doi:10.1021/la026100v

100. Lombardo D, Kiselev MA. Methods of Liposomes Preparation: Formation and Control Factors of Versatile Nanocarriers for Biomedical and Nanomedicine Application. *Pharmaceutics*. 2022;14(3). doi:10.3390/pharmaceutics14030543

101. Stein H, Spindler S, Bonakdar N, Wang C. Production of Isolated Giant Unilamellar

Vesicles under High Salt Concentrations. 2017;8(February):1-16. doi:10.3389/fphys.2017.00063

102. Oberholzer T, Nierhaus KH, Luisi PL. Protein expression in liposomes. *Biochem Biophys Res Commun*. 1999;261(2):238-241. doi:10.1006/bbrc.1999.0404

103. Yu W, Sato K, Wakabayashi M, et al. Synthesis of functional protein in liposome. *J Biosci Bioeng*. 2001;92(6):590-593. doi:10.1016/S1389-1723(01)80322-4

104. Nomura SIM, Tsumoto K, Hamada T, Akiyoshi K, Nakatani Y, Yoshikawa K. Gene Expression within Cell-Sized Lipid Vesicles. *ChemBioChem*. 2003;4(11):1172-1175. doi:10.1002/cbic.200300630

105. Lu Y, Allegri G, Huskens J. Vesicle-based artificial cells: materials, construction methods and applications. *Mater horizons*. 2022;9(3):892-907. doi:10.1039/d1mh01431e

106. Dimitrov DS. Liposome Electro formation. 1986:303-311.

107. Rodriguez N, Pincet F, Cribier S. Giant vesicles formed by gentle hydration and electroformation: A comparison by fluorescence microscopy. *Colloids Surfaces B Biointerfaces*. 2005;42(2):125-130. doi:10.1016/j.colsurfb.2005.01.010

108. Doeven MK, Folgering JHA, Krasnikov V, Geertsma ER, Van Den Bogaart G, Poolman B. Distribution, lateral mobility and function of membrane proteins incorporated into giant unilamellar vesicles. *Biophys J*. 2005;88(2):1134-1142. doi:10.1529/biophysj.104.053413

109. Deng N-N, Yelleswarapu M, Zheng L, Huck WTS. Microfluidic Assembly of Monodisperse Vesosomes as Artificial Cell Models. *J Am Chem Soc*. 2017;139(2):587-590. doi:10.1021/jacs.6b10977

110. Abkarian M, Loiseau E, Massiera G. Continuous droplet interface crossing encapsulation (cDICE) for high throughput monodisperse vesicle design. *Soft Matter*. 2011;7(10):4610-4614. doi:10.1039/c1sm05239j

111. Funakoshi K, Suzuki H, Takeuchi S. Formation of giant lipid vesiclelike compartments from a planar lipid membrane by a pulsed jet flow. *J Am Chem Soc*. 2007;129(42):12608-12609. doi:10.1021/ja074029f

112. Abate AR, Hung T, Marya P, Agresti JJ, Weitz DA. High-throughput injection with microfluidics using picoinjectors using picoinjectors. *Proc Natl Acad Sci U S A*. 2010;107(45):19163-19166. doi:10.1073/pnas.1006888107

113. Caschera F, Lee JW, Ho KKY, Liu AP, Jewett MC. Cell-free compartmentalized protein synthesis inside double emulsion templated liposomes with: In vitro synthesized and assembled ribosomes. *Chem Commun*. 2016;52(31):5467-5469. doi:10.1039/c6cc00223d

114. Van Swaay D, Demello A. Microfluidic methods for forming liposomes. *Lab Chip*. 2013;13(5):752-767. doi:10.1039/c2lc41121k

115. de Matos MBC, Miranda BS, Rizky Nuari Y, et al. Liposomes with asymmetric bilayers produced from inverse emulsions for nucleic acid delivery. *J Drug Target*. 2019;27(5-6):681-689. doi:10.1080/1061186X.2019.1579819

116. Chiba M, Miyazaki M, Ishiwata S. Quantitative analysis of the lamellarity of giant liposomes prepared by the inverted emulsion method. *Biophys J*. 2014;107(2):346-354. doi:10.1016/j.bpj.2014.05.039

117. Terasawa H, Nishimura K, Suzuki H, Matsuura T, Yomo T. Coupling of the fusion and

budding of giant phospholipid vesicles containing macromolecules. *Proc Natl Acad Sci U S A*. 2012;109(16):5942-5947. doi:10.1073/pnas.1120327109

118. Kikuchi H, Suzuki N, Ebihara K, et al. Gene delivery using liposome technology. *J Control Release*. 1999;62(1-2):269-277. doi:10.1016/S0168-3659(99)00047-4

119. Ishikawa K, Sato K, Shima Y, Urabe I, Yomo T. Expression of a cascading genetic network within liposomes. *FEBS Lett*. 2004;576(3):387-390. doi:10.1016/j.febslet.2004.09.046

120. Spencer AC, Torre P, Mansy SS. The Encapsulation of Cell-free Transcription and Translation Machinery in Vesicles for the Construction of Cellular Mimics. *J Vis Exp*. 2013;(80):1-7. doi:10.3791/51304

121. Kita H, Matsuura T, Sunami T, et al. Replication of genetic information with self-encoded replicase in liposomes. *ChemBioChem*. 2008;9(15):2403-2410. doi:10.1002/cbic.200800360

122. Hosoda K, Sunami T, Kazuta Y, Matsuura T, Suzuki H, Yomo T. Quantitative study of the structure of multilamellar giant liposomes as a container of protein synthesis reaction. *Langmuir*. 2008;24(23):13540-13548. doi:10.1021/la802432f

123. Lee KY, Park SJ, Lee KA, et al. Photosynthetic artificial organelles sustain and control ATP-dependent reactions in a protocellular system. *Nat Biotechnol*. 2018;36(6):530-535. doi:10.1038/nbt.4140

124. Zhu TF, Szostak JW. Coupled growth and division of model protocell membranes. *J Am Chem Soc*. 2009;131(15):5705-5713. doi:10.1021/ja900919c

125. Lentini R, Santero SP, Chizzolini F, et al. Integrating artificial with natural cells to translate chemical messages that direct E. coli behaviour. *Nat Commun*.

2014;5(May):1-6. doi:10.1038/ncomms5012

126. Moga A, Yandrapalli N, Dimova R, Robinson T. Optimization of the inverted emulsion method for high-yield production of biomimetic giant unilamellar vesicles. *ChemBioChem*. 2019:2674-2682. doi:10.1002/cbic.201900529

127. Robinson T, Verboket PE, Eyer K, Dittrich PS. Controllable electrofusion of lipid vesicles: Initiation and analysis of reactions within biomimetic containers. *Lab Chip*. 2014;14(15):2852-2859. doi:10.1039/c4lc00460d

128. Nishimura K, Suzuki H, Toyota T, Yomo T. Size control of giant unilamellar vesicles prepared from inverted emulsion droplets. *J Colloid Interface Sci*. 2012;376(1):119-125. doi:10.1016/j.jcis.2012.02.029

129. Tsugane M, Suzuki H. Reverse Transcription Polymerase Chain Reaction in Giant Unilamellar Vesicles. 2018;(June):1-11. doi:10.1038/s41598-018-27547-2

130. Litschel T, Ganzinger KA, Movinkel T, et al. Freeze-thaw cycles induce content exchange between cell-sized lipid vesicles. *New J Phys*. 2018;20(5). doi:10.1088/1367-2630/aabb96

131. Okano T, Inoue K, Koseki K, Suzuki H. Deformation Modes of Giant Unilamellar Vesicles Encapsulating Biopolymers. *ACS Synth Biol*. 2018;7(2):739-747. doi:10.1021/acssynbio.7b00460

132. Trantidou T, Dekker L, Polizzi K, Ces O, Elani Y. Functionalizing cell-mimetic giant vesicles with encapsulated bacterial biosensors. *Interface Focus*. 2018;8(5). doi:10.1098/rsfs.2018.0024

133. Natsume Y, Toyota T. Asymmetrical polyhedral configuration of giant vesicles induced

by orderly array of encapsulated colloidal particles. *PLoS One*. 2016;11(1):1-16. doi:10.1371/journal.pone.0146683

134. Toparlak D, Zasso J, Bridi S, et al. Artificial cells drive neural differentiation. *Sci Adv*. 2020;6(38):1-13. doi:10.1126/sciadv.abb4920

135. Adir O, Albalak MR, Abel R, et al. Synthetic cells with self-activating optogenetic proteins communicate with natural cells. *Nat Commun*. 2022;13(1). doi:10.1038/s41467-022-29871-8

136. Chen G, Levin R, Landau S, et al. Implanted synthetic cells trigger tissue angiogenesis through de novo production of recombinant growth factors. *Proc Natl Acad Sci U S A*. 2022;119(38). doi:10.1073/pnas.2207525119

137. Whittenton J, Harendra S, Pitchumani R, Mohanty K, Vipulanandan C, Thevananther S. Evaluation of asymmetric liposomal nanoparticles for encapsulation of polynucleotides. *Langmuir*. 2008;24(16):8533-8540. doi:10.1021/la801133j

138. Levine RM, Pearce TR, Adil M, Kokkoli E. Preparation and characterization of liposome-encapsulated plasmid DNA for gene delivery. *Langmuir*. 2013;29(29):9208-9215. doi:10.1021/la400859e

139. Osawa M, Erickson HP. Liposome division by a simple bacterial division machinery. *Proc Natl Acad Sci U S A*. 2013;110(27):11000-11004. doi:10.1073/pnas.1222254110

140. Noireaux V, Libchaber A. A vesicle bioreactor as a step toward an artificial cell assembly. *Proc Natl Acad Sci*. 2004;101(51):17669-17674. doi:10.1073/pnas.0408236101

141. Natsume Y, Wen HI, Zhu T, Itoh K, Sheng L, Kurihara K. Preparation of giant vesicles encapsulating microspheres by centrifugation of a water-in-oil emulsion. *J Vis Exp*.

2017;2017(119):1-8. doi:10.3791/55282

142. Booth MJ, Schild VR, Graham AD, Olof SN, Bayley H. Light-activated communication in synthetic tissues. *Sci Adv*. 2016;2(4):1-12. doi:10.1126/sciadv.1600056

143. Hartmann D, Chowdhry R, Smith JM, Booth MJ. Orthogonal Light-Activated DNA for Patterned Biocomputing within Synthetic Cells. 2023. doi:10.1021/jacs.3c02350

144. Smith JM, Hartmann D, Booth MJ. Engineering cellular communication between light-activated synthetic cells and bacteria. *bioRxiv*. 2022:2022.07.22.500923. https://www.biorxiv.org/content/10.1101/2022.07.22.500923v1%0Ahttps://www.biorxiv.org/content/10.1101/2022.07.22.500923v1.abstract.

145. Aiso K, Nozaki T, Shimoda M, Kokue E. Assay of dihydrofolate reductase activity by monitoring tetrahydrofolate using high-performance liquid chromatography with electrochemical detection. *Anal Biochem*. 1999;272(2):143-148. doi:10.1006/abio.1999.4174

146. Raimondi MV, Randazzo O, Franca M La, et al. DHFR inhibitors: Reading the past for discovering novel anticancer agents. *Molecules*. 2019;24(6):1-19. doi:10.3390/molecules24061140

147. Lee J, Yennawar NH, Gam J, Benkovic SJ. Kinetic and structural characterization of dihydrofolate reductase from Streptococcus pneumoniae. *Biochemistry*. 2010;49(1):195-206. doi:10.1021/bi901614m

148. abcam. Dihydrofolate Reductase Assay Kit (Colorimetric) (ab239705). https://www.abcam.com/products/assay-kits/dihydrofolate-reductase-assay-kit-colorimetric-ab239705.html.

149. Hooff GP, Van Kampen JJA, Meesters RJW, Van Belkum A, Goessens WHF, Luider TM. Characterization of β-lactamase enzyme activity in bacterial lysates using MALDI-mass spectrometry. *J Proteome Res*. 2012;11(1):79-84. doi:10.1021/pr200858r

150. Eiamphungporn W, Schaduangrat N, Malik AA, Nantasenamat C. Tackling the antibiotic resistance caused by class a β-lactamases through the use of β-lactamase inhibitory protein. *Int J Mol Sci*. 2018;19(8). doi:10.3390/ijms19082222

151. Sharma S, Ramnani P, Virdi JS. Detection and assay of β-lactamases in clinical and non-clinical strains of Yersinia enterocolitica biovar 1A. *J Antimicrob Chemother*. 2004;54(2):401-405. doi:10.1093/jac/dkh365

152. abcam. Beta Lactamase Activity Assay Kit (Colorimetric) (ab197008). https://www.abcam.com/products/assay-kits/beta-lactamase-activity-assay-kit-colorimetric-ab197008.html.

153. Juers DH, Matthews BW, Huber RE. LacZ b -galactosidase : Structure and function of an enzyme of historical and molecular biological importance. 2012;21. doi:10.1002/pro.2165

154. Garavito RM, Ferguson-Miller S. Detergents as Tools in Membrane Biochemistry. *J Biol Chem*. 2001;276(35):32403-32406. doi:10.1074/jbc.R100031200

155. Lichtenberg D, Ahyayauch H, Goñi FM. The mechanism of detergent solubilization of lipid bilayers. *Biophys J*. 2013;105(2):289-299. doi:10.1016/j.bpj.2013.06.007

156. Henriksen JR, Andresen TL, Feldborg LN, Duelund L, Ipsen JH. Understanding detergent effects on lipid membranes: A model study of lysolipids. *Biophys J*. 2010;98(10):2199-2205. doi:10.1016/j.bpj.2010.01.037

157. Düzgüneş N, Straubinger RM, Baldwin PA, Friend DS, Papahadjopoulos D. Proton-Induced Fusion of Oleic Acid-Phosphatidylethanolamine Liposomes. *Biochemistry*. 1985;24(13):3091-3098. doi:10.1021/bi00334a004

158. Protocols S. *Synthesis of Functional Proteins Within Liposomes*.

159. Lavickova B, Maerkl SJ. A Simple, Robust, and Low-Cost Method to Produce the PURE Cell-Free System. *ACS Synth Biol*. 2019;8:455-462. doi:10.1021/acssynbio.8b00427

160. Torchilin VP. Cell penetrating peptide-modified pharmaceutical nanocarriers for intracellular drug and gene delivery. *Biopolym - Pept Sci Sect*. 2008;90(5):604-610. doi:10.1002/bip.20989

161. Buhr F, Jha S, Thommen M, et al. Synonymous Codons Direct Cotranslational Folding toward Different Protein Conformations. *Mol Cell*. 2016;61(3):341-351. doi:10.1016/j.molcel.2016.01.008

162. Zhou M, Guo J, Cha J, et al. Non-optimal codon usage affects expression, structure and function of clock protein FRQ. *Nature*. 2013;494(7439):111-115. doi:10.1038/nature11833

163. Ikemura T. Codon usage and tRNA content in unicellular and multicellular organisms. *Mol Biol Evol*. 1985;2(1):13-34. doi:10.1093/oxfordjournals.molbev.a040335

164. Sharp PM, Li W-H. The codon adaptation index-a measure of directional synonymous codon usage bias, and its potential applications. *Nucleic Acids Res*. 1987;15(3):1281-1295. doi:10.1093/nar/15.3.1281

165. Kudla G, Murray AW, Tollervey D PJ. Coding-Sequence Determinants of Gene Expression in Escherichia coli. *Science (80-)*. 2009;324(5924)(April):255-258.

doi:10.1126/science.1170160

166. Cambray G, Guimaraes JC, Arkin AP. Evaluation of 244,000 synthetic sequences reveals design principles to optimize translation in escherichia coli. *Nat Biotechnol*. 2018;36(10):1005. doi:10.1038/nbt.4238

167. Welch M, Govindarajan S, Ness JE, et al. Design parameters to control synthetic gene expression in Eschorichia coli. *PLoS One*. 2009;4(9). doi:10.1371/journal.pone.0007002

168. Quax TEF, Claassens NJ, Söll D, van der Oost J. Codon Bias as a Means to Fine-Tune Gene Expression. *Mol Cell*. 2015;59(2):149-161. doi:10.1016/j.molcel.2015.05.035

169. Hanson G, Coller J. Codon optimality, bias and usage in translation and mRNA decay. *Nat Rev Mol Cell Biol*. 2018;19(1):20-30. doi:10.1038/nrm.2017.91

170. Goodman DB, Church GM, Kosuri S. Causes and effects of N-terminal codon bias in bacterial genes. *Science (80-)*. 2013;342(6157):475-479. doi:10.1126/science.1241934

171. Chang B, Halgamuge S, Tang SL. Analysis of SD sequences in completed microbial genomes: Non-SD-led genes are as common as SD-led genes. *Gene*. 2006;373(1-2):90-99. doi:10.1016/j.gene.2006.01.033

172. Nieuwkoop T, Finger-Bou M, van der Oost J, Claassens NJ. The Ongoing Quest to Crack the Genetic Code for Protein Production. *Mol Cell*. 2020;80(2):193-209. doi:10.1016/j.molcel.2020.09.014

173. Gold L, Pribnow D, Schneider T, Shinedling S, Singer BS, Stormo G. Translational initiation in prokaryotes. *Annu Rev Microbiol*. 1981;35:365-403. doi:10.1146/annurev.mi.35.100181.002053

174. Schneider TD, Stormo GD, Gold L, Ehrenfeucht A. Information content of binding sites on nucleotide sequences. *J Mol Biol*. 1986;188(3):415-431. doi:10.1016/0022-2836(86)90165-8

175. Lenstra TL, Rodriguez J, Chen H, Larson DR. Transcription Dynamics in Living Cells. *Annu Rev Biophys*. 2016;45:25-47. doi:10.1146/annurev-biophys-062215-010838

176. Lee J, Borukhov S. Bacterial RNA polymerase-DNA interaction-The driving force of gene expression and the target for drug action. *Front Mol Biosci*. 2016;3(NOV). doi:10.3389/fmolb.2016.00073

177. Looman AC, Bodlaender J, Comstock LJ, et al. Influence of the codon following the AUG initiation codon on the expression of a modified lacZ gene in Escherichia coli. *EMBO J*. 1987;6(8):2489-2492. doi:10.1002/j.1460-2075.1987.tb02530.x

178. Isacchis A, Sarmientos P, Lorenzettia R, Soria M, Isacchi A. Mature apolipoprotein AI and its precursor proApoA1: influence of the sequence at the 5' end of the gene on the efficiency of expression in Escherichia coli. *Carlo Erba Viale Bezzi*. 1989;81(3912):54587.

179. Kelsic ED, Chung H, Cohen N, Park J, Wang HH, Kishony R. RNA Structural Determinants of Optimal Codons Revealed by MAGE-Seq. *Cell Syst*. 2016;3(6):563-571.e6. doi:10.1016/j.cels.2016.11.004

180. Frumkin I, Schirman D, Rotman A, et al. Gene Architectures that Minimize Cost of Gene Expression. *Mol Cell*. 2017;65(1):142-153. doi:10.1016/j.molcel.2016.11.007

181. Nieuwkoop T, Terlouw BR, Stevens KG, et al. Revealing determinants of translation efficiency via whole-gene codon randomization and machine learning. *Nucleic Acids*

Res. 2023;51(5):2363-2376. doi:10.1093/nar/gkad035

182. Gary D. Stormo, Thomas D. Schneider LMG. Characterization of translational initiation sites in E. coli. *Mucleic Acid Res*. 1982;10(9):2971–2996.

183. Iserentant D, Fiers W. Secondary structure of mRNA and efficiency of translation initiation. *Gene*. 1980;9(1-2):1-12. doi:10.1016/0378-1119(80)90163-8

184. Horinouchi S, Weisblum B. Posttranscriptional modification of mRNA conformation: Mechanism that regulates erythromycin-induced resistance. *Proc Natl Acad Sci U S A*. 1980;77(12 II):7079-7083. doi:10.1073/pnas.77.12.7079

185. Olins PO, Devine CS, Rangwala SH, Kavka KS. The T7 phage gene 10 leader RNA, a ribosome-binding site that dramatically enhances the expression of foreign genes in Escherichia coli. *Gene*. 1988;73:227-235.

186. Olins PO, Rangwala SH. A novel sequence element derived from bacteriophage T7 mRNA acts as an enhancer of translation of the lacZ gene in Escherichia coli. *J Biol Chem*. 1989;264(29):16973-16976. doi:10.1016/s0021-9258(18)71444-0

187. Venancio-Marques A, Liu YJ, Diguet A, Di Maio T, Gautier A, Baigl D. Modification-free photocontrol of β-lactam conversion with spatiotemporal resolution. *ACS Synth Biol*. 2012;1(11):526-531. doi:10.1021/sb300010a

188. O'Connor M, Dahlberg AE. Enhancement of translation by the epsilon element is independent of the sequence of the 460 region of 16S rRNA. *Nucleic Acids Res*. 2001;29(7):1420-1425. doi:10.1093/nar/29.7.1420

189. Venancio-marques A, Liu Y, Diguet A, Gautier A, Baigl D. Modification-Free Photocontrol of β -Lactam Conversion with Spatiotemporal Resolution. 2012.

doi:10.1021/sb300010a

190. Dunn JJ, Studier FW, Gottesman M. Complete nucleotide sequence of bacteriophage T7 DNA and the locations of T7 genetic elements. *J Mol Biol*. 1983;166(4):477-535. doi:10.1016/S0022-2836(83)80282-4

191. Mertens N, Remaut E, Fiers W. Increased stability of Phage T7g10 mRNA is Mediated by either a 5'- or a 3'-Terminal Stem-Loop structure. *Biol Chem Hoppe Seyler*. 1996;377(12):811-818. doi:10.1515/bchm3.1996.377.12.811

192. Deutscher MP, Reuven NB. Enzymatic basis for hydrolytic versus phosphorolytic mRNA degradation in Escherichia coli and Bacillus subtilis. *Proc Natl Acad Sci U S A*. 1991;88(8):3277-3280. doi:10.1073/pnas.88.8.3277

193. Deutscher MP, Enzymes T. E . coli RNases : Making Sense of Alphabet Minireview Soup. *Cell*. 1985;40(April):731-732.

194. Garneau NL, Wilusz J, Wilusz CJ. The highways and byways of mRNA decay. *Nat Rev Mol Cell Biol*. 2007;8(2):113-126. doi:10.1038/nrm2104

195. Jurado AR, Tan D, Jiao X, Kiledjian M, Tong L. Structure and function of pre-mRNA 5'-end capping quality control and 3'-end processing. *Biochemistry*. 2014;53(12):1882-1898. doi:10.1021/bi401715v

196. Derakhshankhah H, Jafari S. Cell penetrating peptides: A concise review with emphasis on biomedical applications. *Biomed Pharmacother*. 2018;108(September):1090-1096. doi:10.1016/j.biopha.2018.09.097

197. Derossi D, Joliot AH, Chassaing G, Prochiantz A. The third helix of the Antennapedia homeodomain translocates through biological membranes. *J Biol Chem*.

1994;269(14):10444-10450. doi:10444-50

198. Frankel AD, Pabo CO. Cellular uptake of the tat protein from human immunodeficiency virus. *Cell*. 1988;55(6):1189-1193. doi:10.1016/0092-8674(88)90263-2

199. Pooga M, Soomets U, Hällbrink M, et al. Cell penetrating PNA constructs regulate galanin receptor levels and modify pain transmission in vivo. *Nat Biotechnol*. 1998;16:857. http://dx.doi.org/10.1038/nbt0998-857.

200. Wender PA, Mitchell DJ, Pattabiraman K, Pelkey ET, Steinman L, Rothbard JB. The design, synthesis, and evaluation of molecules that enable or enhance cellular uptake: Peptoid molecular transporters. *Proc Natl Acad Sci*. 2000;97(24):13003-13008. doi:10.1073/pnas.97.24.13003

201. Ruseska I, Zimmer A. Internalization mechanisms of cell-penetrating peptides. *Beilstein J Nanotechnol*. 2020;11:101-123. doi:10.3762/bjnano.11.10

202. Xie J, Bi Y, Zhang H, et al. Cell-Penetrating Peptides in Diagnosis and Treatment of Human Diseases: From Preclinical Research to Clinical Application. *Front Pharmacol*. 2020;11(May):1-23. doi:10.3389/fphar.2020.00697

203. Reissmann S. Cell penetration: Scope and limitations by the application of cell-penetrating peptides. *J Pept Sci*. 2014;20(10):760-784. doi:10.1002/psc.2672

204. Fages-Lartaud M, Tietze L, Elie F, Lale R, Hohmann-Marriott MF. mCherry contains a fluorescent protein isoform that interferes with its reporter function. *Front Bioeng Biotechnol*. 2022;10(August):1-11. doi:10.3389/fbioe.2022.892138

205. Kudla G, Lipinski L, Caffin F, Helwak A, Zylicz M. High guanine and cytosine content increases mRNA levels in mammalian cells. *PLoS Biol*. 2006;4(6):0933-0942.

doi:10.1371/journal.pbio.0040180

206. Chorev DS, Tang H, Rouse SL, et al. The use of sonicated lipid vesicles for mass spectrometry of membrane protein complexes. *Nat Protoc*. 2020;15(5):1690-1706. doi:10.1038/s41596-020-0303-y

207. Guzman-Chavez F, Arce A, Adhikari A, et al. Constructing Cell-Free Expression Systems for Low-Cost Access. *ACS Synth Biol*. 2022;11(3):1114-1128. doi:10.1021/acssynbio.1c00342